Responses to the review of Dr. Bair

In "Intercomparison of photogrammetric platforms for spatially continuous snow depth mapping" several different photogrammetric approaches are tested in a sparsely vegetated study area in Switzerland. This manuscript is a thorough and useful comparison of state of the art photogrammetric tools for snow depth mapping. It does somewhat read like a commercial for the eBee+ UAS, however the authors have stated no conflicting interests and have demonstrated the eBee's advantages over the other platforms. I would recommend this manuscript for publication subject to a few minor changes.

Dear Dr. Bair

We thank you very much for your review. We absolutely have no conflict of interest concerning the eBee+ UAS. The institute from which most authors are affiliated uses from a range of manufactures. After testing multiple platforms for operational use in alpine environments and for mapping snow depth we determined the eBee+ had the best performance. However, we will change the text in such a way that the name eBee+ is mentioned less.

1) The vegetation issues are discussed, but a solution is not presented. I suggest identification of these regions and spatial interpolation may be the best approach, but there are other solutions. Note that negative snow depths can occur in glacierized areas or areas with persistent snow cover as well with snow on/off differencing approaches.

   Vegetation errors are not easy to eliminate, especially when generated by grassland with various length and uncertain compaction between snow-free and snow-covered conditions during mapping. We agree with the related comment added directly to our manuscript that this limitation of the photogrammetric method maybe insurmountable. In principle, we also agree that a DTM may produce a small improvement for some vegetation, but not for all vegetation. LIDAR in particular is more capable to mitigate this effect thanks to penetration through vegetation as we stressed in Section 6.5. Nonetheless, we disagree that interpolation from open areas onto regions classified as vegetated are the best approach in general. While it may be true on relatively uniform terrain, we believe that in mountainous regions the variability in topography maybe too great to be accurately captured by interpolation from remote open areas. In our opinion, it is of rather minor importance for this specific publication as the investigation is focused primarily above tree line. But we will take this point into consideration and add a comment in section 6.5 of the paper.

2) There are numerous grammatical and stylistic errors. I suggest an English language service be used prior to publication.

   The paper will be proof-read by a native English speaker.

3) The manual validation effort is impressive in scope but seems unnecessary. It seems to me that the resources used could have been better used on snow-covered and snowfree lidar flights, perhaps along with the Ultracam. And why weren't any forested areas sampled manually?

   We thank the reviewer for his appreciation of our efforts towards validation, although we respectfully disagree with the comment that it was unnecessary. We agree that in principle,

repeated lidar flight would have been desirable for validation. However and despite what the reviewer may assume, the associated cost remains very high and would have exceeded the project funding, especially given that an additional manned flight in summer would have been required. We did attempt a winter TLS scan, but due to various recording problems including suboptimal viewing angles, we could not georeference the TLS scan correctly. Therefore, the manual measurements are an important and necessary independent control for the snow depth maps. The large area comparison is there to further assess the Pleiades data, recognizing that the Ultracam is significantly better on the small scale test area, and hence can be used as reference. If "ground truth" is really what bothers the reviewer, then you could propose to rephrase with "reference" and adding the above element as justification.

We did not sample any forest areas manually due to lack of time and manpower. We wanted to concentrate on the Schürlialp area with manual sampling.

4) I don't agree that the Ultracam showed robust enough performance, especially inforested areas, to be called ground truth.

   We agree with you when specifically considering forested terrain. However, when considering the Ultracam DSM in non-forested terrain the RMSE was 0.17 m and the NMAD was of 0.12 m (raw data), which, we believe is sufficiently accurate to be compared with the Pleiades snow depth map over a larger area. The large area comparison is there to further assess the Pleiades data, recognizing that the Ultracam is significantly better on the small scale test area, and hence can be used as reference. We agree that ground-truth is not the right word here and will replace it with reference.

Responses to questions in the paper:

Page 6:
Figure 2:
What type of automated sensors were used, how often were the mesurements recorded, and most importantly, how were the depths filtered? Snow depths from acoustic sensors never look that flat. I'm guessing a single time is shown from each day?

For each day and each station one value is displayed. 5DF, 5MA and 5WJ are SLF observers reading the snow depth from a snow pole manually on a measurement field every day. The time for manual measurements is between 07:00 and 07:30. For the automatic stations, the newest value whose measurement falls within the time window 06:30 to 08:15 is displayed. The snow depth at the automatic stations is measured with ultrasound every 30 minutes. We will add this to the caption.

Page 8:
3: That's unusually accurate for a drone. Are there other UAS with similar geolocational accuracy?

Yes, current RTK UAS can attain such accuracies. Other systems with comparable accuracies are the WingtraOne or the Trimble UX HP.

Page 11:
7: Why wasn't the ALS company hired for winter acquisitions. That would have avoided the bent/missing poles and likely would have produced more accurate snow depths.

We agree with you that an ALS flight would have been useful for the comparison but unfortunately it was not feasible for the project as explained in our response to an earlier comment.

Page 14:
26: Any speculation as to why the RMSE in the vertical direction of the summer flight was half that of the winter flight?

At the time of the summer flight we had a better DGNSS (Stonex S800) available with an accuracy in position of 0.014 to 0.022 m and in altitude of 0.02 m. This of course affected the error calculation. We will specify this change of DGNSS in the revised paper.

Page 20:
These images are pixelated and I cannot see the violet stars in (d)

We will improve the image quality. The purple stars were unfortunately forgotten during the reproduction of the image.

Page 21:
10: Negative snow depths are errors. In addition to vegetation, glacierized areas or those with permanent snow can show the same effect. The vegetation problems are a significant limitation of the photogrammetric methods vs lidar. It deserves to be mentioned that the photogrammetric methods have sometimes insurmountable problems in vegetation. No well-versed reader expects one method to work well everywhere.

In many cases we agree with you, but dense vegetation (e.g. *Alnus alnobetula*) present in the study area can also pose a problem to LIDAR. Reutebuch et al., 2003 for example examined the accuracy of a lidar terrain model under a conifer forest canopy and found poorer accuracy for dense canopy. We are currently investigating this topic further by deploying LiDAR on a UAS platform, but this analysis will not be included in this study. But it is a fact that with photogrammetric techniques in dense vegetation you are at the limit at some point and you can never make a DTM like with a LIDAR. We will mention this in the discussion.

Reutebuch, S. E., Mc Gaughey, R. J., Andersen, H. E., & Carson, W. W. (2003). Accuracy of a high-resolution lidar terrain model under a conifer forest canopy. *Canadian Journal of Remote Sensing, 29*(5), 527-535. doi:10.5589/m03-022

Page 24:
Panels a-d need to be captioned explicitly: Ultracam (a), Ebee +(b),....

We will add this to the caption.

Page 29:
5: I don't agree that the Ultracam was tested thoroughly enough to be used as ground truth, specifically its performance in forests

Please see the comment below.

9: All of this underscores the fact that photogrammetric methods are not suitable for estimating snow depth in forested areas, especially not as a ground truth. Without an accurate and independent validation datasets to compare to, e.g. snow on/off TLS or ALS, I suggest simply comparing the snow depths from the different sensors rather than claiming the Ultracam can be used as ground truth.

We agree with you on this to a certain extent and will reformulate this statement. However, the comparison of Pléiades and Ultracam is nevertheless a reasonable comparison when considering the accuracy of the Pléiades data over a large geographic area and in particular within non-forested regions, which makes up > 80% of the comparison.

Page 30:

Table: The average snow depth, based on the Schürlialp measurements is ~ 1.3 m. Thus, the uncertainty exceeds or is close to the average snow depth

Yes, good point. We will add this to the discussion of the results.

Page 34:

18: Vegetation is a problem for all remote sensing techniques in snow. Sometimes the best method is interpolation from open areas where you have more confidence in your measurements. Perhaps that is the best solution for filling these negative values?

We do not agree in this situation. We believe interpolation would give valid results in some areas and not others since snow depth is highly variable, even over short distances, and dependent on underlying topography.

Page 36:

10: And as you say, the snowpack needs to be deep. For example, the eBEE might be great for tundra snowpacks, except for the high windows and depths that are < 0.5 m.

Yes, good point. We will add a comment in the Conclusion.

Response to the review of Prof. Shean

https://tc.copernicus.org/preprints/tc-2020-93/#discussion

David Shean

July 29, 2020

This paper considers several photogrammetric approaches that can be used to produce gridded surface elevation products (satellite stereo, aerial, UAS and terrestrial), which can in turn be differenced to provide snow depth estimates. These methods and products are evaluated over one test site in the Swiss Alps, using photogrammetric data collected within a short time period, contemporaneous ground-truth observations and several external datasets. The authors provide some analysis of their snow depth map quality, and qualitative comparisons of the strengths and weaknesses of the different methods.

In general, this is a nice methods paper. The amount of work presented is substantial. The campaign planning was excellent, the photogrammetry processing and methods are sound, the resulting datasets are impressive, and the writing is generally good. There are many DSM processing challenges involved with precise snow depth mapping, especially when surfaces in the “snow-on” DSM are almost entirely snow-covered. The authors use more traditional, labor-intensive approaches to integrate control data early in the process, rather than alternative approaches involving point-cloud or DSM co-registration later in the process. Some decisions about data processing and presentation should be revisited, as they will impact the quantitative results, though they may not have a substantial impact on the qualitative conclusions. The writing in the results and discussion requires some improvement and I recommend that the more senior authors on the paper dedicate time to help refine these sections.

As a fellow photogrammetry enthusiast/evangelist, I enjoyed reading this paper, and had a lot to say, offering many general and specific comments. I realize that not all of these changes will be possible, but I hope that the authors will consider these suggestions to improve this paper and their future work. I look forward to reading the response and seeing this nice study published!

Dear Prof. Shean

Thank you very much for your valuable and extensive review. We have addressed each of your comments below.

General Comments

● There is ambiguity with the term “ground-based”, as many readers may interpret this to be “ground-truth” (I made this mistake a few times). I would suggest using “terrestrial photogrammetry” or “close-range photogrammetry” throughout the text to avoid issues.

We will use “terrestrial photogrammetry”.

● I would offer that snow depth on glaciers and ice sheets is critical for properly measuring glacier mass balance, beyond the applications you list.

We will add the application for properly measuring the glacier mass balance. We will cite Gascoin et al., 2011 and McGrath et al., 2015.

Gascoin, S., Kinnard, C., Ponce, R., Lhermitte, S., MacDonell, S., and Rabatel, A.: Glacier contribution to streamflow in two headwaters of the Huasco River, Dry Andes of Chile, The Cryosphere, 5, 1099-1113, 10.5194/tc-5-1099-2011, 2011.

McGrath, D., Sass, L., O'Neel, S., Arendt, A., Wolken, G., Gusmeroli, A., Kienholz, C., and McNeil, C.: End-of-winter snow depth variability on glaciers in Alaska, Journal of Geophysical Research: Earth Surface, 120, 1530-1550, 10.1002/2015jf003539, 2015.

● The summer reference data sets were acquired on June 27, 2018 and August 5-6, 2018. Were all surfaces completely snow-free during both periods? For some mountain sites with similar elevation here in Pacific Northwest, we see considerable snow in late June. Do you expect differences in the vegetation during these periods? How do you account for errors introduced by these issues?

All areas were free of snow during both summer flights. We will clarify this accordingly in the revised manuscript. There are indeed differences in the vegetation between the two summer DSMs. Nevertheless, when comparing two snow depth maps, we always resample the winter DSMs to align to the same summer DSM (i.e., either the UAS or the LiDAR). Therefore, the differences between both summer DSMs does not play any part in the comparative outcome of Comparison 2 and Comparison 3.

● I wasn't clear on the strategy used for blending of the independent Pleiades DSMs to create a final triplet DSM product. If the bundle block adjustment was successful, and both P12 and P13 are usable, shouldn't P23 also be usable, even with more limited convergence angle? The text cites Sirguey and Lewis (2019), which is listed as "Sirguey, P., and Lewis, C.: Topographic mapping of Franz Josef glacier region with Pléiades satellite imagery, University of Otago, 2019." - I can't find a published version of this reference, which I think is a technical paper? Need to describe the method in this text if it is not yet published elsewhere. The last sentence of this section mentions a filter to remove triangulation error >0.5 m on the blended DSM. Why not apply this filter to the individual DSMs before blending?

The reference cited is indeed a technical report. Our approach to blending surfaces is a simple weighted arithmetic mean between elevations from each bi-stereo surface, with the weight being the ray-intersection error, which is an output of *point2dem*.

In order to clarify this, we will modify the manuscript as follows: *"~~In tri-stereo configuration, maps of intersection errors are used to weight the contribution of pairwise DSMs into a blended DSM with GDAL (Sirguey and Lewis, 2019).~~ In tri-stereo configuration, we generate a DSM and map of ray intersection error for each stereo-pair. We blend DSMs with GDAL using a weighted arithmetic mean, whereby the elevation from each constituent DSM is weighted by its corresponding ray intersection error (Sirguey and Lewis, 2019). A map of standard error of the weighted mean is generated by uncertainty propagation."*

The bundle adjustment was successful and all pairs are usable. When producing the surface however, it became apparent from hillshades that P23 with the lowest B/H ratio resulted in a substantially more noise in areas of poor contrast. We illustrate this below with subset hillshades of the surfaces

produced form our triangulated triplet, namely the three bi-stereo (a, b, c), our blending of the three bi-stereo (e), the blending of only P12 and P23 (f). The ortho image (d) also illustrates the challenging contrast of our snowpack.

It is clear that decreasing B/H corresponds to increasing amount of noise from the restitution on smooth, undisturbed areas of our snowpack (see a, b, c). This is expected since the lower contrast promotes variability in stereo-matching, which then compounds with lower parallactic angles when B/H decreases, resulting in more dispersion in the triangulated height on poorly textured areas of our snowpack. It appears in our case that restitution with P23 in such poorly textured areas (c) generated a variability that propagated too much in the blended surfaces despite the reduced weight from larger intersection error (e). Note however that with more contrast/texture (e.g., several avalanches are visible on the northern slopes in the ortho), then stereo matching dispersion in P23 compares to other pairs which demonstrates that the issue is not from the triangulation, but rather support our hypothesis that contrast and B/H combine to dictate the dispersion of the restitution. While an in-depth study may be desirable to characterize this further, including testing more stereo-matching options and satellite geometry in such environment, for the purpose of our comparison with other platforms, we only needed to test what we considered to be the best Pleiades surface, and it was obvious that the blending only P12 and P23 was more suitable (e) vs (f).

We do not remove points from individual DSM before the blending because the rationale of the blending is to statistically leverage (with the weighted mean) several estimates of elevation while considering their initial quality, with their contribution weighted by the uncertainty measured by the ray intersection error. We don't believe that applying such a threshold individually to each DSM beforehand finds better justification. On the contrary, we think it is more appropriate to complete the blending initially without prejudice, compute the propagated standard error of the weighted mean, and then apply the binary filtering only once to the latter only. This has the additional advantage of applying the threshold on a single map of standard error (analogous to the ray intersection error but applying to the weighted mean) representative of the statistical leveraging effect.

In order to further clarify our manuscript, we will modify: ***"Finally, the ~~ray-intersection error~~ map of standard error for the blended DSM was used to set all cells of the DSM to no data where the ray intersection error is greater than one panchromatic pixel or 0.5 m as larger errors were found to be often indicative of erroneous stereo-matching".***

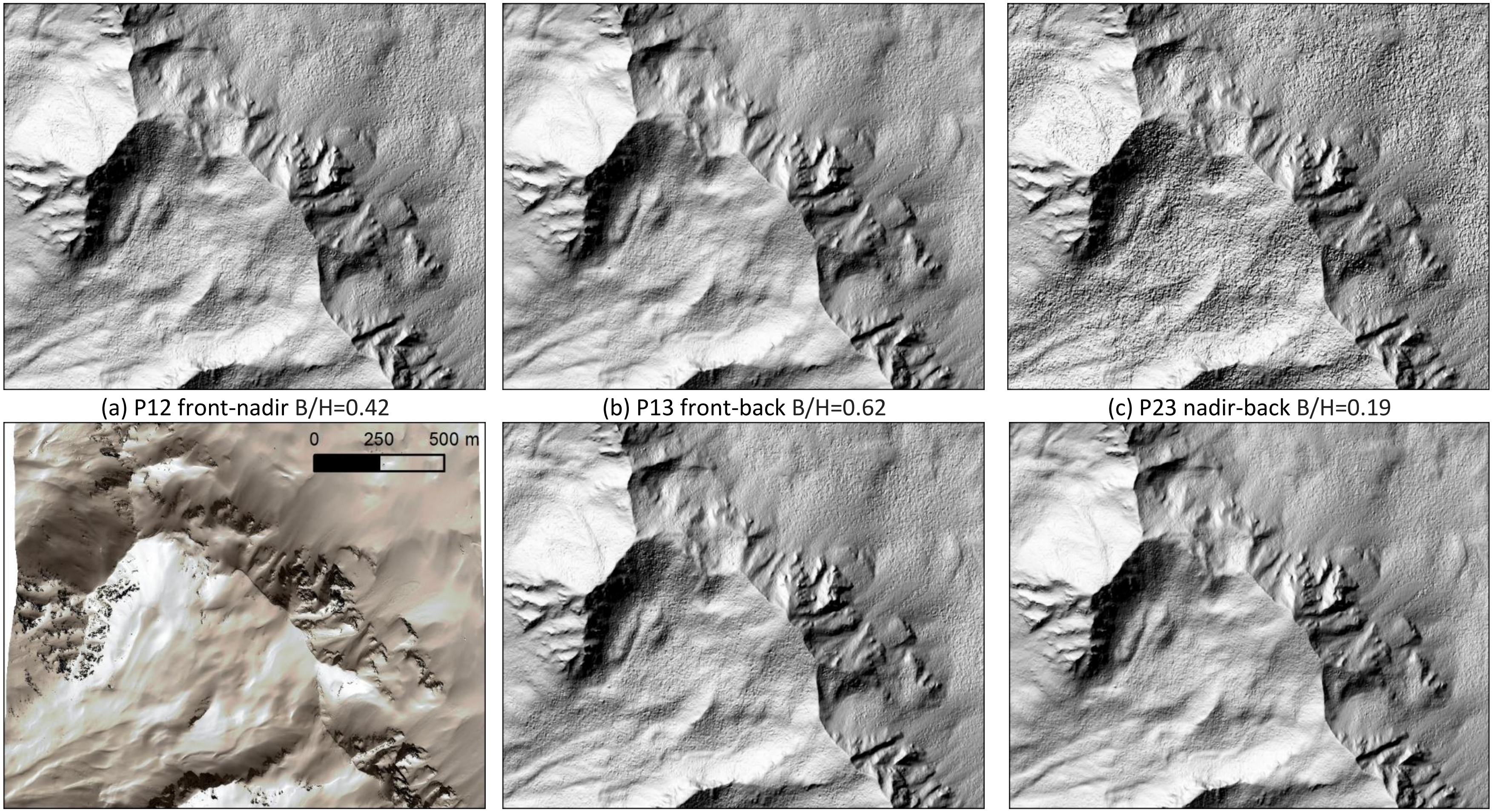

(a) P12 front-nadir B/H=0.42
(b) P13 front-back B/H=0.62
(c) P23 nadir-back B/H=0.19
(d) ortho
(e) Blend P12 & P13 & P23
(f) Blend P12 & P13 (best)

● The +/-1 m (total of 2 m magnitude) over 15 km "tilt" of blended Pleiades DSM is a concern, and seems to indicate that the bundle adjustment was unsuccessful, or the GCPs used are inaccurate or poorly distributed. It's not clear why a more rigorous co-registration approach was not used here rather than a hyperplane fit (presumably least-squares? Need to provide more details on this correction) through residual values at sparse points along roads. I would think a 3D rotation would be more suitable. How does the reader know that this grid correction did not introduce additional error over snow-covered surfaces at greater distances from the points on the roads in valley bottoms?

First, it is important to realize that the process of bundle block adjustment (BBA) will always and inevitably produce some amount of spatial bias with respect to another independent surface. The nature of the adjustment makes it virtually impossible to attain a perfect coherence independently. One challenge of 3D change detection is to detect, characterize, and mitigate/correct systematic biases to improve the signal of change, regardless of the technique used to makes surfaces spatially coherent to each other.

Our winter and summer DSMs (ASL and Pleiades DSM, respectively) are such independent products, and the amount of snow and sparsity of stable ground in our image makes an automatic approach to align surfaces (e.g., Iterative Closest Point on stable ground) untenable. Therefore, we must rely on achieving consistent absolute accuracy for each dataset to ensure the coherence.

It is reasonable to assume that the summer ALS is more accurate than the Pleiades DSM. The magnitude and spatial structure of the bias (e.g., linear vs nonlinear drift) would then be governed by the quality of the BBA, and in turn, indeed related to the quality in the placement and distribution of GCPs. We show in the additional figure below the distribution of the 14 GCPs we used in the BBA, which we believe are well distributed given the complexity of our terrain.

As indicated in our section 3, GCPs have been collected both in winter and summer which complicated the interpretation of some points in the winter image triplet. The visual interpretation of GCPs must also be put into perspective with the 50cm spatial resolution of the imagery. Some variability in GCP placement may have contributed to generate the residual systematic tilt relative to the ALS surface, again assuming that the latter does not or marginally contribute to the tilt. Nonetheless, our Leave-one-out cross-validation (LOOCV) assessment provided a satisfying quality assurance for this step of the process to be valid in view of the 50 cm pixel.

One must then keep in mind that systematic spatial errors can generally be revealed and assessed only in retrospect once surfaces are produced. The process by which we determine the remaining tilt is arguably similar to Deschamps-Berger et al. (2020) identifying, characterizing, and mitigating unmodelled residual jitter from evaluation of the snow depth map *a posteriori* because the rigid body transform associated with their alignment strategy could not capture nor correct it.

In view of this, we do not agree that a tilt of ±1m over 15km in these conditions can be qualified as an unsuccessful triangulation, nor a cause for concern. On the contrary, we argue that the lack of planimetric offset when differencing surfaces processed independently as we did (which is unforgiving

in such steep topography when computing 3D changes) is rather a confirmation of the general quality of the BBA. This leaves most systematic bias in the elevation (which again is inevitable), the magnitude of which is believed to be consistent with what an independent photogrammetric process can achieve at this resolution given our constraints.

Our final assessment of the co-registration to detect remaining (and expected) systematic effect once the surface was produced could only be done from critical evaluation of spatial pattern in the difference with ALS, with the roads being the only suitable surfaces free of snow in this image. As shown in our figures below, the distribution of offsets along roads in the city and inside the valley revealed enough linearity to justify the fitting of a plane in 3D space as a correction grid. This is the definition of a best fit hyperplane, which is solved via least squares. We will clarify this in the revised manuscript.

Considering a vertical offset of 1m over a 7500m distance, the difference between this simple grid correction and a rotation involves a difference of less than 0.1mm on the planimetry which is negligible when working with 0.5/2m resolution. We are therefore not sure of what "rigorous approach" the reviewer think could apply better to our case. One option could have been to revisit the BBA in view of the tilt, potentially revisiting the placement of some GCPs. We argue that, while this could mitigate the problem at the expense of time and reprocessing, the effect is not expected to be significantly different to the debiasing we propose *a posteriori*.

We appreciate the reviewer point about the risk for over-correction away from the road. Nevertheless, the correction we apply is a first order linear offset consistent with the residual trend captured from the only suitable locations where such assessment can be done. The locations of the spot points along the roads and inside the city are shown in the figure below (a) and (b). Their distribution along two nearly orthogonal axes effectively constrains the corrective hyperplane as shown in (c) and (d). (a) and (b) also reveal the difference in snow depth mapped before and after correction and does not suggest such problem exist. Finally, snow depth in our test area has also been assessed and validated well away from the roads.

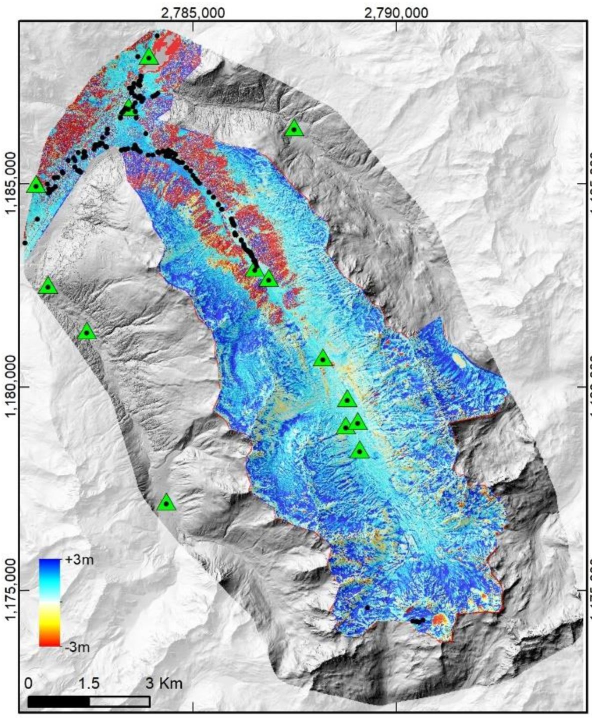

(a) DoD Before tilt correction. Spot points along roads are shown in black and GCPs as triangle.

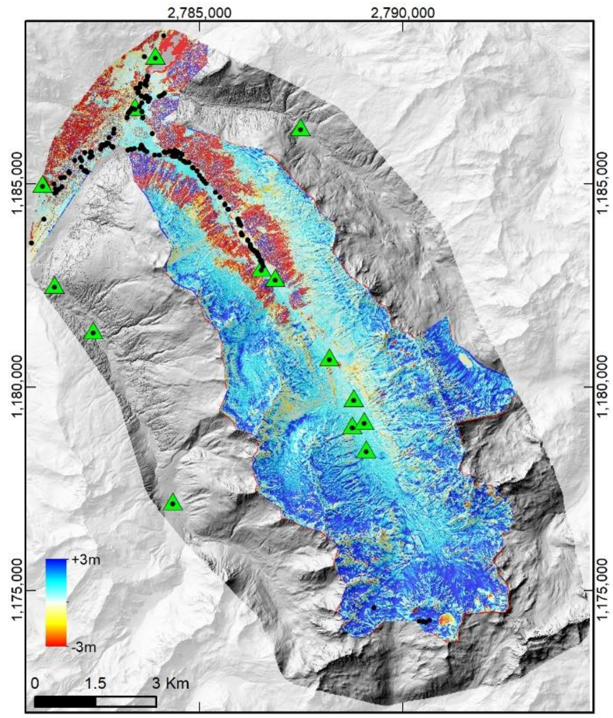

(b) DoD After tilt correction. Spot points along roads are shown in black and GCPs as triangle.

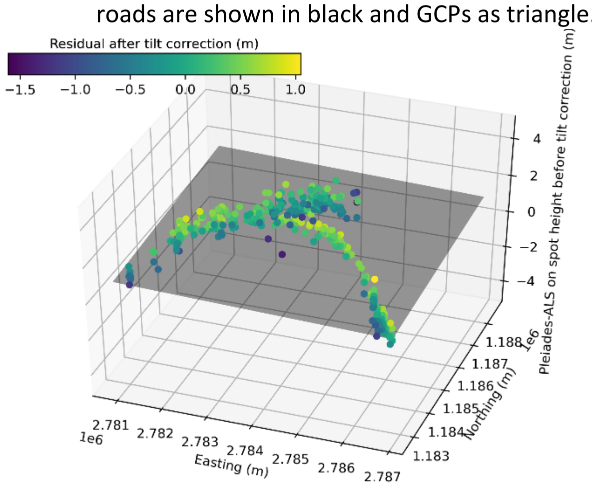

(c) Hyperplane fitting to residual on spot points.

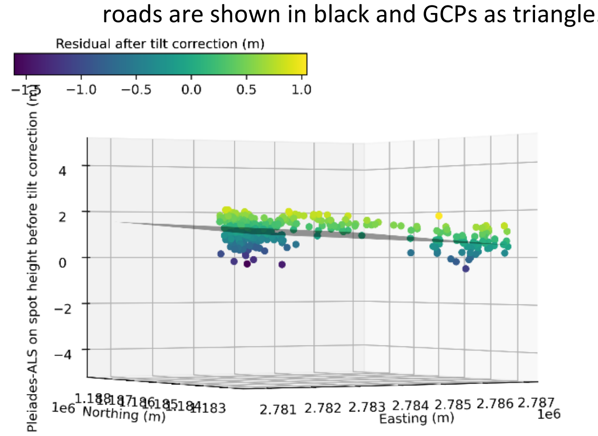

(d) Hyperplane fitting to residual on spot points.

● Figures 5 and 12 show a clipped version of the Pleaides orthomosaic and snow depth products, with data only shown for the polygon defining the Dischma valley study area. It seems like it might be valuable to show the full unclipped extent of these products, maybe in a supplementary figure. The unclipped products should cover a larger area, adjacent valleys/peaks, and hopefully several of the AWS stations identified in Figure 1.

Figure 5 (a) shows the whole Pléiades orthoimage, while Figure 12 (a) shows the full map of snow depth derived from Pleiades minus summer ALS; the latter is limited to the area covered by ALS. In Figure 6 the snow depth map calculated with the eBee+ summer flight is shown. Therefore, snow depths exist only for the red polygon. In Figure 12 the snow depth maps calculated with the ALS scan

are shown. The summer ALS scan is unfortunately still smaller than the footprints of the Pléiades/Ultracam.

● The 0.1 m accuracy (is this both horizontal and vertical? Why don't we see expected ~2x higher error in vertical?) for GCP and CP is relatively high for modern GNSS systems, and this will propagate to all of the photogrammetric solutions. Does the 0.1 m value represent RMSE? How was the differential GNSS processing performed? I don't remember seeing any mention of this, so perhaps a real-time correction was used. In the future, I recommend using a survey-grade GNSS for your positions, or longer occupation times with static occupations at each if RTK accuracy is poor.

Section 4.1 specifies that all GCPs were collected in RTK mode based on a swipos-GIS/GEO correction stream (VRS network). The Trimble Geo XH 6000 is a dual frequency GNSS receiver and was the best equipment available for us at the time of the winter field work. It delivers 10cm accuracy (68 % confidence level) in real time in horizontal and vertical position when connected to a VRS network. We will clarify this in the revised manuscript.

● For validation, several different reference datasets were used. In the snow depth error analysis, it's unclear whether you can isolate the error from the HS_platform from the error in the "spatial ground truth". Do you assume that HS_ALS(Summer) has 0 error? The lidar vendor documentation/metadata should include some assessment of product error (likely ~1-10 cm). This needs to be accounted for. I think what we really care about here is the accuracy for each HS_platform and whether we can, for example, combine two Pleiades DSMs to independently measure snow depth. If you can isolate platform-specific error (not integrating an external reference DSM), that would be really valuable, though I realize this is challenging.

We do not assume that the UAS summer flight or the ALS scan are error free. However, these errors cancel each other out within the different comparisons (2+3) since we always compare snow depth maps derived with the same underlying summer reference. We do not believe that it is possible with these data to explicitly limit the platform-specific error when estimating snow depths. Because the quality and the errors of a winter DSM depends on many factors which are not platform specific as the lightning conditions, the experience of the operator, etc. Also, we only have a summer DSM for the UAS. Therefore, we cannot calculate platform specific snow depth maps.

● Using a 2*STD filter is not necessarily more rigorous. More aggressive, yes. With this filter, you're inevitably classifying many "valid" points as outliers and removing. This filter will always reduce your apparent error, and some might perceive this "cleaning" followed by lower reported error as a bit dishonest. Since you're also defining robust metrics of error - median for bias, NMAD for spread, and using quantile/percentile values (25, 50, 75%) for the boxplots, you should be able to rely on those, rather than these "cleaned" values. I would avoid calling them "cleaned" - you can use "filtered". There is value in presenting and working with "filtered" maps in figures, but try to use the robust descriptive stats in the text/tables.

We will replace the word "cleaned" with "filtered". While it is true that the 2*STD filter can remove "valid" points, we believe the principle of removing outliers and blunders is legitimate, in particular when comparing with manual snow depth since the number of samples reduces the robustness of

metrics to outliers. The reviewer himself is a co-author in Deschamps-Berger et al. (2020) where all snow depth less <1m and >30m are simply set to nodata, and not taken into account in the resulting statistics. We also present results before and after filtering for completeness, and therefore do not accept the comment that our approach and results may be associated with any form of dishonesty. As the reviewer notes, some of our metrics are robust but the 2*STD filter which is supported by little changes before and after filtering. Nonetheless, the filter allows the mean, RMSE and STD to be more indicative of the performance of the majority of data when stereo-matching would have performed satisfactorily.

● Using Agisoft's "aggressive" filtering will remove many of the largest outliers. ASP also uses an outlier-removal filter during gridding of triangulated points to produce a DSM (point2dem utility removes points with triangulation error > 3*75th-percentile). If you had used different filter settings during DSM generation, your 2*STD filter would produce different results.

The inherent variability of stereo-matching makes photogrammetric restitution exposed and sensitive to large outliers, and some form of point cloud filtering is a necessity. Agisoft proposes several options but recommends the aggressive filter in normal cases when there is little vegetation. We have tested the different filtering methods and have found that aggressive filtering was more suitable for snow on steep terrain due to the challenging contrast and parallax, which makes it more prone to erroneous stereo-matches. We will clarify this in the revised manuscript.

We are aware of the filtering by point2dem but as indicated in Section 4.2, our filtering of the blended DEM is based on removing all points whereby the standard error of the blended elevation is less than 0.5 m (one pixel). We agree that any pre-processing choices designed to eliminate bad stereo matches will propagate to the final performance assessment, but not only to the 2*STD filter as the reviewer seems to suggest. Therefore, those choices do not negate the merit of reporting metrics about snow depth with and without the 2*STD on HS.

● Do your errors actually have a normal distribution? Looking at box plots in figure 9, I would say no. So some of these assumptions about 2*STD and percentiles may not hold. Showing histograms (with some transparency) of delta_HS from the different sources on a single plot might be more informative than the box plots.

We think that the boxplot is a useful graph to see the dispersion of the errors, which we calculated for all three comparisons. The histograms show us that the errors are normally distributed except for comparison 1. For comparison 1 there are too few measurements, so we will add a single value plot instead of the histogram to the paper. For comparison 2+3 we will add the histograms. The new figures for comparison 1, 2 and 3 are displayed below.

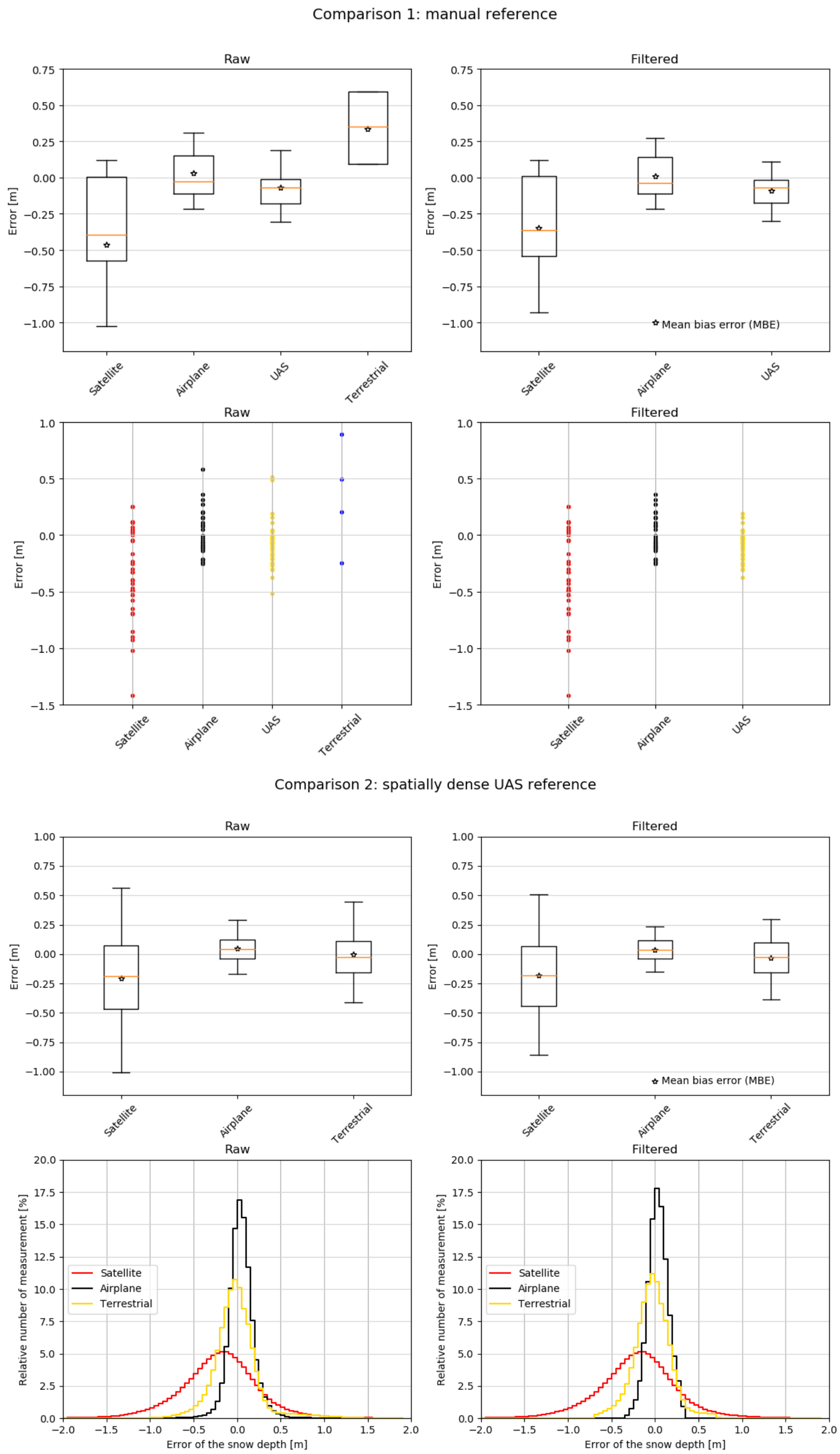
Comparison 1: manual reference
Raw
Filtered
Error [m]
Satellite
Airplane
UAS
Terrestrial
Mean bias error (MBE)
Comparison 2: spatially dense UAS reference
Relative number of measurement [%]
Error of the snow depth [m]
Satellite
Airplane
Terrestrial

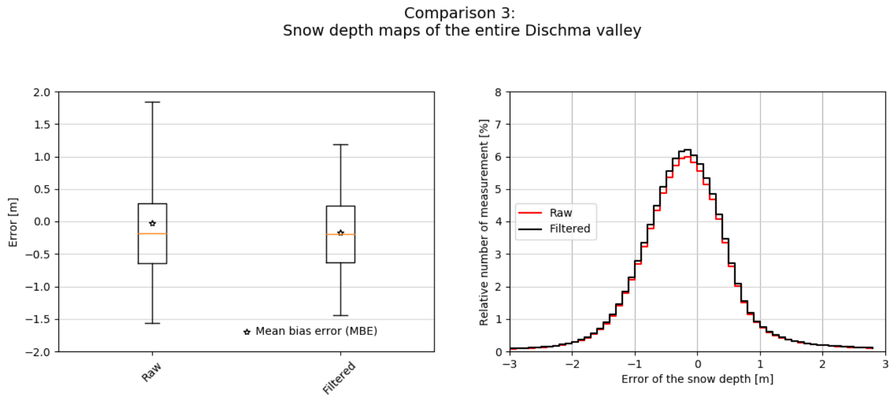

● I don’t think the variable “HS” was ever defined in the text or captions, though it is used in several figures and tables.

Thanks for pointing this out. We will define HS in the introduction when we define snow depth.

● The results section was a bit hard to follow at times - dense presentation of numbers and statistics. The writing could use some additional proofreading as well - hopefully one of the more senior authors can help with this. There was a lot of interpretation and discussion presented in the results section. Some of the more speculative interpretations should probably be moved to the discussion section.

We will improve the result section and move the speculative interpretations to the discussion section. A native English speaker will review the manuscript again carefully before final submission.

● Rather than computing a snow depth for 4 DSM inputs against the same summer reference DEM (with it’s own spatially variable error), and then doing an accuracy analysis of the snow depth rasters, you might perform your analysis directly on the DSMs. If you trust the DSM_eBee (winter), that can be your reference. Differencing each input DSM against this reference will allow you to characterize the error of the input DSM, without any additional error introduced by the summer reference or the resampling process. Alternatively, you could compute a per-pixel median grid from the input DSM values, and then difference each input against that median, though this works better with n >> 4

Snow depth maps are the relevant end product for us. Clearly, resampling distorts the snow depth maps. But in order to compare two DSMs we still have to resample at least one DSM. So, technically it makes only a small difference whether you adapt two DSMs to the same other DSM or one DSM to the other. Therefore, the way we make the comparisons, the summer reference does not introduce any errors. Thank you very much for your idea with the median grid. Since the paper is already very extensive and we also find our comparison strategy important, we will keep this idea in mind for a future comparison.

● I’m not used to seeing the “mean bias error” (MBE) and “median of the bias errors” (MABE). You are calculating these as the mean and median of the signed (not absolute) error values, right? Both will capture any bias in the data. Also, should be definition of MABE be “median absolute bias error”? The equation in Table 3 does not indicate that absolute values were used. You're missing a "model" superscript on m_BE in the NMAD definition in Table 3.

The reviewer is right that MBE and MABE are calculated from the signed error. We use the mean bias error (MBE) and the median of the bias errors to measure the bias of the DSM or snow depth against a reference. We will change the abbreviation MABE for the median of the bias errors into MdBE to avoid confusion with mean absolute bias error or median absolute bias error.

We will add the missing model superscript.

● I'm not sure that the "comparison 1" is representative of true accuracy of the snow depth products, as the sample size of the reference manual/pole measurements is pretty limited with n=4-37, and the spatial distribution of the "ground-truth" is not ideal, with manual samples clustered along the valley bottom, where gridded snow depth values show stronger spatial autocorrelation. The ~11 usable pole samples on valley walls have good spatial distribution. I expect that if you isolated the two "ground-truth" sources (manual vs pole), the resulting accuracy statistics would differ considerably. My guess is the apparent error for manual points will be small, but you'll see much larger errors for the ~11 pole samples.

We thank you very much for the hint. An error has crept into the figure and there are only 10 visible snow poles as described in the text. We will adapt the figure accordingly.

We agree that a more scattered meshed network of manual measurements would have been desirable but probing snow in such environment and limited time across a large area is extremely challenging and often dictated by practical consideration that constrain the spatial distribution. In future campaigns we could try to organize a much larger team for manual measurements. We could also try to either make an ALS flight or to make additional reference measurements with an ALS drone. This was not possible for this study. However, Comparison 1 is important and allows for the comparison with independent non-photogrammetric measurements. It confirms that the eBee+ measurements can be used as reference measurements for further comparisons.

Below you will find an extended version of Table 4 where the accuracy measures are also calculated for the manual measurements and the snow poles measurements separately. We will add this table to the supplements. The table shows that the snow pole measurements are generally better except for the Pleiades data. Despite the small sample size, we find that calculating the accuracy measures of the manual and snow poles measurements is meaningful.

	Satellite				**Airplane**			
	Manual	**Snow poles**	**All data**	**Filtered**	**Manual**	**Snow poles**	**All data**	**Filtered**
RMSE [m]	0.5	1.51	0.90	0.52	0.21	0.18	0.20	0.17
MBE [m]	-0.34	-0.79	-0.46	-0.35	0.04	0.0	0.03	0.01
STD [m]	0.37	1.29	0.77	0.39	0.2	0.18	0.20	0.17
MdBE [m]	-0.33	-0.44	-0.40	-0.36	0.01	-0.07	-0.03	-0.04
NMAD [m]	0.41	0.71	0.44	0.47	0.21	0.09	0.17	0.17

Number of measurements	27	10	37	36	20	7	27	26

	UAS				**Terrestrial**
	Manual	**Snow poles**	**All data**	**Filtered**	**Snow poles**
RMSE [m]	0.23	0.13	0.21	0.16	0.54
MBE [m]	-0.09	-0.03	-0.07	-0.09	0.34
STD [m]	0.21	0.13	0.20	0.13	0.42
MdBE [m]	-0.1	-0.03	-0.07	-0.07	0.35
NMAD [m]	0.14	0.08	0.14	0.12	0.51
Number of measurements	27	10	37	34	4

● If you have maps of vegetation (perhaps from differencing a lidar DSM and DTM, though I think your lidar was unclassified?), you could produce a vegetation mask. This could be used to analyze your HS product accuracy only over pixels that are snow, which will allow you to test whether most of your negative snow depth values are from vegetation (primary hypothesis presented), or due to some other issue (bias, noise in DSM, etc). This is important b/c your HS maps don't cover the same extent, so some are preferentially sampling vegetated areas, and may appear to have more error as a result.

We agree that this is a good approach to classify vegetation errors in snow depth maps, however, extends beyond the scope of this paper. Also, as mentioned above, we indirectly compare winter DSMs in these comparisons and not snow depth maps except for comparison 1. Vegetation induces negative errors in snow depth maps but these negative values are the same in every snow depth map. Nevertheless, we are also convinced that a pure vegetation mask does not solve the vegetation error problem of a photogrammetric DSM.

● Figure 7 shows some of the detailed snow depth products, which is really valuable. It shows the noise in the Pleaides HS product compared to the ultracam and eBee HS products. But the focus is on artifacts in all HS maps due to vegetation. It is clear that the source for these artifacts is the summer ALS DSM product that was subtracted from each of the 4 photogrammetry DSMs provided. It might be valuable to show a panel with a color shaded relief map of your summer ALS DSM and a snow-free orthoimage showing this vegetation. Could also show similar panels for a snow-on DSM and orthoimage. This is tied to the suggestion of providing an evaluation of the DSM products, rather than the derivative HS products.

We thank you for the input. In Figure 7, the snow depth maps were calculated using the eBee+ flight. We will clarify this in the figure caption (see the comment above). We will adapt the figure as shown below.

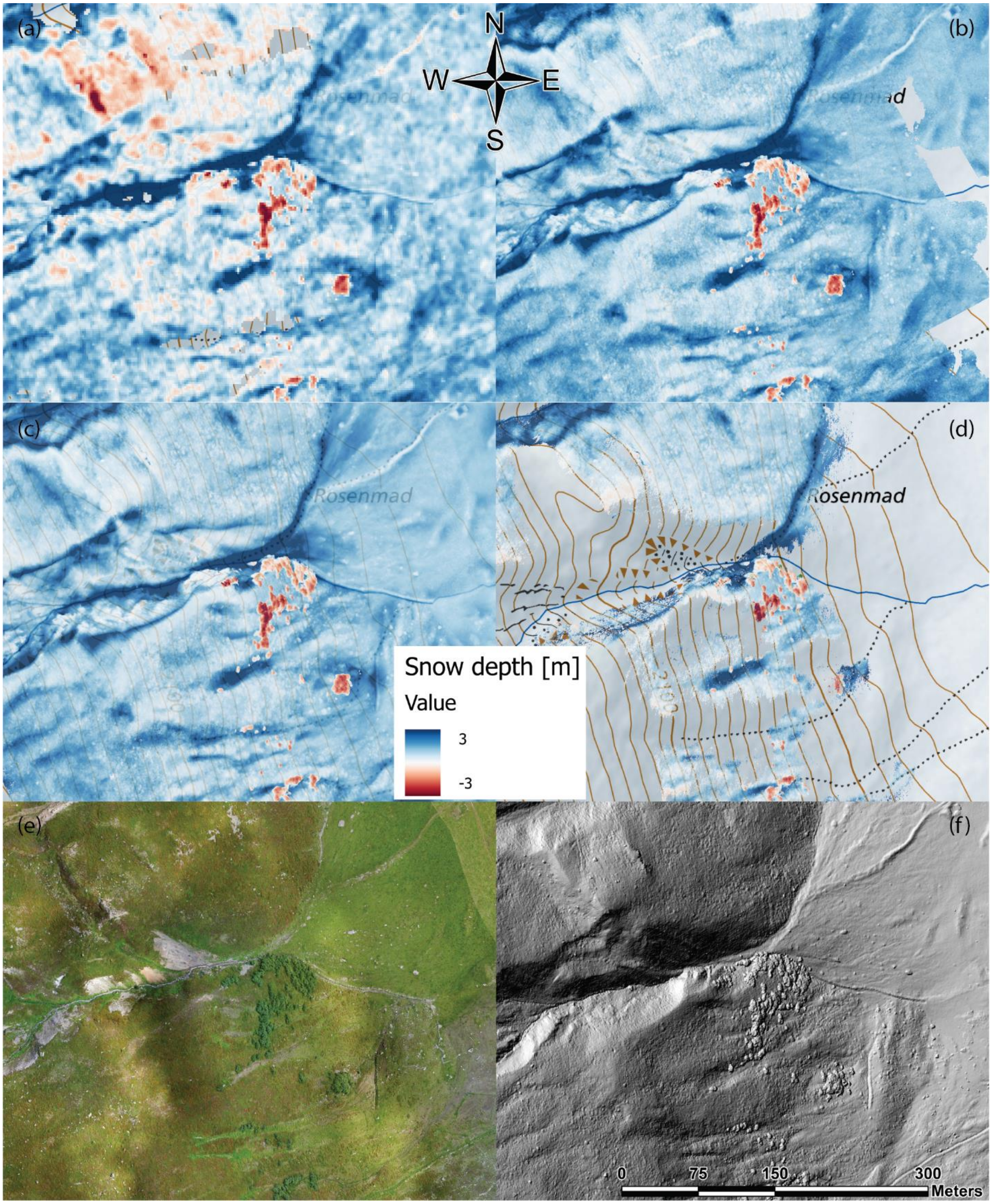

Figure 1: Extract of the Schürlialp snow depth maps shown in Fehler! Verweisquelle konnte nicht gefunden werden. **with the scale ranging from -3 m to 3 m to illustrate the negative snow depths caused by the vegetation. In this extract the dark red spots are mainly bushes of the species *alnus alnobetula* compressed by the snow. Alnus Alnobetula is visible on every snow depth map and on the summer orthophoto and the hillshade of the ALS scan (panel (a) satellite, panel (b) airplane, panel (c) UAS, panel (d) terrestrial, panel (e) orthophoto of the UAS summer flight, panel (f) the hillhsade of the ALS scan). This extract also shows how detailed a photogrammetric snow depth map can be. In the gullies the snow depths reach up to 5m. (Swiss Map Raster© 2019 swisstopo (5 704 000 000), reproduced by permission of swisstopo (JA100118))**

● Can you add some discussion of the maximum snow depths that you're seeing in the gullies? The scales are cut off at 3 m, and I expect that you could have real snow depth of >5 m locally. Your products capture this detail really well, which is a major selling point!

Yes, we will add a discussion point about the maximum snow depth in the gullies and outline it as important point of our products. We will include the values of the gullies in the caption of figure 7 and in the result section of comparison 2.

● It's important to remember (and state) that snow depth maps are just a specific application of a DEM difference map. There are many studies out there offering accuracy analysis of the latter, and it's important to consider these. Photogrammetric DEMs can also suffer from elevation- and/or slope-dependent errors (e.g., Shean et al., 2016). It may be worth considering how this affects your results.

Yes, we agree with you there. We will extend the discussion to clarify this point.

● There are several figures/tables that could be moved to a supplement, which would help reduce length and improve flow

Yes, that is a good point. We will evaluate this and move everything we can into the supplements.

● In your Table 7, you present some qualitative advantages and disadvantages. You might consider breaking out into columns for coverage, acquisition time, cost, accuracy, resolution, repeat, and other. One thing that is missing from this is the "processing time," in addition to acquisition time. It might be useful to mention somewhere the time required to process each dataset (manual interaction and compute), software costs, equipment costs, etc. At the end of the day, these are often the deciding factors...

We agree with you that coverage, acquisition time, costs, accuracy, resolution, repetition are important criteria. But these are very difficult to capture in concrete terms. For example, we have not achieved the maximum possible coverage. Also, the processing time is very difficult to capture, because it depends very much on the computer used and this can change very quickly. Costs are also difficult to define, as they can vary greatly depending on location/market and are in constant development. So, the aim of this table is to summarize what each sensor can be used for.

Specific Comments

Page 1

Rather than "RMSEs" and "NMADs", I recommend "RMSE and NMAD values are…"

We will adapt this.

25: "too few"

We will correct this.

25: Based on abstract, unclear why ground-based obs were used with eBee but not with snow pits; I think the issue is that the ground-based obs don't intersect with "manual and snow pole measurements".

We will clarify this in the abstract. Indeed, the issue is that the terrestrial measurements don't intersect with the manual measurements, only with 4 snow pole measurements.

29: specify "more than two photogrammetry platforms"

We will add "photogrammetry" in the sentence.

30: replace "the specific advantages and disadvantages of them" with "their specific advantages and disadvantages"

We will replace this.

Page 2

18: Specify the sensors or methods used for "manual" or "AWS" - e.g., probing, GPR, sonic ranging, etc.; Also, point measurements themselves are not the problem - the issue is their sparse spatial density, especially over large regions. One can probe every 10 cm on a relatively small grid and get lots of valuable information about the local spatial distribution of snow depth.

We will specify the sensors and methods used for "manual" or "AWS". We will also update the text to be more precise on the issue of point measurements and their sparse spatial density over large regions.

27: Should include Painter et al reference for ASO: https://doi.org/10.1016/j.rse.2016.06.018

We will include Painter et al., 2016.

Painter, T. H., Berisford, D. F., Boardman, J. W., Bormann, K. J., Deems, J. S., Gehrke, F., Hedrick, A., Joyce, M., Laidlaw, R., Marks, D., Mattmann, C., McGurk, B., Ramirez, P., Richardson, M., Skiles, S. M., Seidel, F. C., and Winstral, A.: The Airborne Snow Observatory: Fusion of scanning lidar, imaging spectrometer, and physically-based modeling for mapping snow water equivalent and snow albedo, Remote Sensing of Environment, 184, 139-152, 10.1016/j.rse.2016.06.018, 2016.

31: What kind of accuracy? Is this position accuracy, and 0.1 in horizontal and vertical? Or snow depth? Several important factors for TLS, so careful with a blanket statement like this. See also study by Currier et al (2019): https://dx.doi.org/10.1029/2018WR024533

We will specify this with a sentence as the following one: "Terrestrial laser scanning (TLS) can measure the distance between scanner position and snow surface with accuracies below 0.10 m beyond 1000 m."

Page 3

8: Would be valuable to mention other VHR satellite image options for snow depth mapping. See our preliminary publication on WorldView stereo snow depth: "Spatially extensive ground-penetrating radar snow depth observations during NASA's 2017 SnowEx campaign: Comparison with In situ, airborne, and satellite observations D McGrath, R Webb, D Shean, R Bonnell, HP Marshall… - Water Resources Research, 2019"

We will add "WorldView-3 satellite-derived snow depths were calculated by McGrath et al., 2019 yielding RMSE value of 0.24 m in comparison to GPR measurements."

McGrath, D., Webb, R., Shean, D., Bonnell, R., Marshall, H. P., Painter, T. H., Molotch, N. P., Elder, K., Hiemstra, C., and Brucker, L.: Spatially Extensive Ground-Penetrating Radar Snow Depth Observations During NASA's 2017 SnowEx Campaign: Comparison With In Situ, Airborne, and Satellite Observations, Water Resources Research, 55, 10026-10036, 10.1029/2019wr024907, 2019.

9: Should include medium-format (Phase One) camera SfM mapping: "Assessing the Ability of Structure From Motion to Map High-Resolution Snow Surface Elevations in Complex Terrain: A Case Study From Senator Beck Basin, CO J Meyer, SMK Skiles - Water Resources Research, 2019" Chris Larson's work in Alaska?

We will add "Meyer and Skiles, 2019 produced DSMs from snow covered surfaces with the RGB camera installed on the lidar-based Airborne Snow Observatory and compared them to simultaneously collected lidar data. They found a NMAD of 0.17 m and a mean relative elevation difference of 0.014 m for a spatial resolution of 1 m."

Meyer, J., and Skiles, S. M.: Assessing the Ability of Structure From Motion to Map High-Resolution Snow Surface Elevations in Complex Terrain: A Case Study From Senator Beck Basin, CO, Water Resources Research, 55, 6596-6605, 10.1029/2018wr024518, 2019.

23-24: Consider rewording to emphasize that few studies have evaluated these platforms for the specific application of snow depth mapping. Many past studies have done this for other surface types and scientific/mapping applications.

We will reword this sentence as: *Many studies have investigated the performance of photogrammetry for different surface types and mapping applications. However, few studies have examined the available photogrammetric platforms for their performance on snow (e.g., Bühler et al., 2017, Deschamps-Berger et al., 2020). Therefore, a comprehensive assessment is necessary to compare the snow depth products of terrestrial, UAS, aircraft and satellite platforms.*

Bühler, Y., Adams, M. S., Stoffel, A., and Boesch, R.: Photogrammetric reconstruction of homogenous snow surfaces in alpine terrain applying near- infrared UAS imagery, International Journal of Remote Sensing, 38, 3135-3158, 10.1080/01431161.2016.1275060, 2017.

Deschamps-Berger, C., Gascoin, S., Berthier, E., Deems, J., Gutmann, E., Dehecq, A., Shean, D., and Dumont, M.: Snow depth mapping from stereo satellite imagery in mountainous terrain: evaluation using airborne laser-scanning data, The Cryosphere, 14, 2925-2940, 10.5194/tc-14-2925-2020, 2020b.

26: Mention high-albedo surfaces (sensor saturation), limited surface texture for fresh snow (poor stereo correlation results)

We will mention it: ***Each platform has its advantages and disadvantages, but each must be able to cope with the challenges of imaging alpine environments, including steep terrain and rapidly changing weather conditions, high-albedo surfaces (sensor saturation) and limited surface texture for fresh snow (poor stereo-correlation).***

28: UAS can offer cm-scale products; all depends on altitude

We will add a comment: ***Also, depending on the flying altitude and camera resolution, UAS allow for decimeter-scale to cm-scale snow depth maps even when the accessibility of terrain is restricted i.e. because of avalanche danger and perform well in a winter alpine environment*.**

31: Other issues beyond ownership can prevent flying whenever required - regulations, certified pilot availability, weather

We will add: ***However, factors that may prevent UAS from flying are regulations, availability of certified pilots, harsh alpine weather, etc...***

35: “scales”

We corrected this spelling mistake.

Page 4

19: “surface slope”

We will replace “slope angle” by “surface slope”.

20: “contrasted snow depth distribution” is a bit unclear - I think you’re saying that downslope winds from gullies lead to snow deposition at the base of the gullies?

We will adapt the sentence to be clearer: ***Interesting features of the Schürlialp area are gullies that channel downslope winds and produce snow deposits on the bottom of the gullies.***

24: “Data… provide” (singular, not plural)

We will correct this.

24: not just “snowfall” though, as you have wind redistribution and melt, I think “snow depth evolution” might be better term

Indeed, “snow depth evolution” is better suited and we will change this.

25: “it” - I think you mean the snow stations?

We clarified “it”. We mean the data of the snow measurement stations.

28-29: I agree that things didn't change much, but if you consider the observed change as a percentage, then 20 cm of a ~65-70 cm snowpack is pretty substantial! You might consider framing these observed changes as a percentage of your expected measurement error. For example, 20 cm is well within the Pleiades snow depth accuracy, but much larger than the UAS snow depth accuracy.

We agree with your objections. However, these 20 cm are only to be found in the lower snow measuring stations which are lower than the lowest altitude of the Schürlialp test site (5DF: 1560 m a.s.l. and 5MA: 1655 m a.s.l.). Also, these are point measurements which are very local and also have errors (2-3 cm for well-maintained automatic stations and 2-4 cm for manual observer measurements). We think that here the real measured values are more useful than percentages.

Page 6

10: eBee+ RTK is a "fixed-wing" - should mention this, as many readers may think "drone =quadcopter"

We will add the term "fixed-wing" in the sentence.

13: "triangulation" is not the word I would use here, as it could be confused with stereo triangulation to produce a point cloud. I think you mean consistent geolocation.

We mean triangulation as in the process of block triangulation or aerial triangulation. This refers to the bundle bloc adjustment, the process that needs ground control. Before computer vision used this term to refer to refer to the process of intersection and restitution, it was defined and unambiguous in photogrammetric science (see Granshaw, S. 2016. Photogrammetric Terminology: Third Edition, The Photogrammetric Record 31(154):210-252 DOI: 10.1111/phor.12146).

17: OK, so these are visible in the Ultracam and eBee imagery, but probably not visible in Pleiades?

Yes, the additional points are not visible on the Pleiades imagery.

19: "positioned" to "The positions of all GCPs were determined using…"

We will change the wording of the sentence as suggested.

Page 7

2: "Pleaides-1B stereo image triplet"

We will add "stereo".

7-9: I would also recommend providing the combined off-nadir angles for each image, rather than the signed across and along-track components. I think your B/H numbers are just accounting for along-track off-nadir angles? If possible, good to provide convergence angle for each pair in addition to B/H.

We will add "Along-track incidence angles of -16.3°, 7.6° and 17.9° resulted in combined incidence angles of 23.2°, 14.2° and 20.1°, and three stereo pairs with Base-over-Height ratio…"

Our B/H ratio account for both along and across track angles.

10: Given your scene relief, this is probably acceptable

Here we are echoing the specifications provided by ASTRIUM. The hypothesis that it is acceptable is unspecific as it would need to define "acceptable". In fact, our result show that in our study, this B/H combines with low contrast to challenge stereo matching and yield significantly more noise in the restitution of poorly textured snow surfaces.

15: Provide time zone for times (and all other instances in paper)

We will provide that.

16: Could delete sentence about not acquiring on same day, as we don't know what the technical issues were

Since the flight was planned for the same day, but actually could not be carried out due to technical problems on the plane, we think this is important to mention. But we will evaluate if we can delete it.

20 and Table 1: would be nice to provide sensor dimensions in addition to total pixel count

We will add the sensor dimensions.

21: "Large-format CCD"

We will add this.

22: focal length in Table 1 is 122.7.

Yes, that's the exact focal length and we adapted it. For promoting purposes vexcel is using 120mm that's why there was this value in the text first.

24: "I" is near-infrared? Recommend consistency with terminology used for Pleiades section

RBGI is the short term which Vexcel Imaging GmbH uses to tag the images. I is NIR infrared. We will be consistent with the terminology and use NIR.

28-29: OK, so three flights total? Better to state that, rather than changing the battery twice.

Good point, we will change this.

Page 8:

7: time format 10.37 vs. 10:37, and time zone

We will correct this.

7: What is imaging interval? 1 second, 1 minute? Ah, it wasn't clear that this was a terrestrial photogrammetry survey! I thought you had installed time-lapse stereo cameras. Maybe state this earlier in the section, before you get into details on variable GSD. Could move lines 16-22 or at least 16-19 here.

We will be more precise with our description and move the lines 16-19.

11: That sounds really large for a convergence angle, and earlier you said B/H of 0.25-0.42 is acceptable? Why different here?

A parallactic angle of 90 degrees is optimum to minimize error propagation in ray intersection. This would correspond to a B/H=2. In practice, such B/H requires practical considerations such as potential for obstruction and overlap. For example, vertical aerial photogrammetry (not converging) could not achieve this unless by using relatively short focal (large view angle) at the cost of potential distortion and increased GSD. Tradeoffs are made and B/H ratio of 0.6 have long been the gold standard as it still provided good intersection accuracy, while maintaining optimal overlap. We mentioned B/H of 0.25 to 0.4 as the recommendation from ASTRIUM with respect to stereo acquisition by Pleiades. Again, those refer to practical considerations of acquisition and expected general accuracy of the products.

19: Really cool to see this setup! :) I used a similar rig for terrestrial and oblique aerial surveys in Greenland and Pacific NW: https://dshean.github.io/technology/sfm/ (Fig 4), back before consumer UAS and integrated cameras were up to the task

Thank you!

Page 10

12: Hmm. I think you can do better than 5 cm on the pole shown in fig 3b. Probably down to 1-2 cm precision. Is the inaccurate reading issue also related to the depression in the snow surface immediately around the pole? If so, state this. For future work, you might consider a small quadcopter that you can fly to “inspect” the poles from closer range to make more precise readings.

The idea of the quadcopter is interesting and we thank you for the idea. Also, it was rather difficult to quickly locate the snow poles with binoculars or a camera. If one had a quadcopter, one could program the positions and could record more accurate measurements given the proximity to the snow poles.

The 5cm are on the one hand because of the small depression or accumulation around the snow pole and on the other hand because of the possible skew of the snow pole. It is possible that the snow pole is slightly inclined because of the pressure of the snow. We will make a corresponding comment.

Page 11

4-6: provide date range for ALS survey. I see August 5-6, 2015?

Exactly, the date range was 5-6 August 2015 and we will add it in the text.

9: Provide citation for LAStools. Martin is pretty clear about this, especially if you’re using an unlicensed version :)

We will add the citation as Martin is requesting (https://groups.google.com/g/lastools/c/ximEoUEbIl4?pli=1).

16: “NASA Ames Stereo Pipeline (ASP, Shean et al., 2016, Beyer et al., 2018) version 2.6.2 (corresponding Zenodo DOI)” - please follow latest citation instructions https://github.com/NeoGeographyToolkit/StereoPipeline#citation . Please include Shean et al. 2016, as you are using core ASP functionality for processing Earth observation imagery that was implemented during that effort.

We will modify accordingly and add those citations.

Beyer, Ross A., Oleg Alexandrov, and Scott McMichael. 2018. The Ames Stereo Pipeline: NASA's open source software for deriving and processing terrain data, Earth and Space Science, 5. https://doi.org/10.1029/2018EA000409.

Shean, D. E., O. Alexandrov, Z. Moratto, B. E. Smith, I. R. Joughin, C. C. Porter, Morin, P. J. 2016. An automated, open-source pipeline for mass production of digital elevation models (DEMs) from very high-resolution commercial stereo satellite imagery. ISPRS Journal of Photogrammetry and Remote Sensing, 116. https://doi.org/10.1016/j.isprsjprs.2016.03.012.

Ross Beyer, Oleg Alexandrov, & ScottMcMichael. (2019, June 17). NeoGeographyToolkit/StereoPipeline: ASP 2.6.2 (Version v2.6.2). Zenodo. http://doi.org/10.5281/zenodo.3247734

16: not clear what you mean by “GDAL (for satellite data)” - for orthorectification? Resampling?

We use GDAL in many steps of our processing before and after ASP. That includes resampling, orthorectification, reprojection, grid calculation.

17: For reference, you can also use the ASP geodiff command or generic gdal_calc.py for simple raster operations outside of ArcGIS.

We are aware of those and often rely on gdal_calc.py for this. In this study, most of the analysis was performed in ArcGIS Pro.

17: No mention of co-registration before subtraction here? I assume this will be discussed elsewhere…

Yes, this is addressed in the description of workflows to achieve consistent geo-referencing between products

Page 12:

2: Suggest “analyzing” rather than “using”

We will change the word to “Analyzing”.

9-16: I didn’t completely follow all of this, but it sounds like something you clearly thought about carefully :). Any coordinate system transformation of raster data will require some resampling/interpolation, it’s a question of error introduced by the transformation. If you can provide some sense of this error, that would be valuable. It’s likely several cm. I initially thought the LV03/LN02 were from 2003/2002, but just checked and it was 1903/1902! Good call to convert to LHN95. I would think the lidar vendor should update their products…

Working with various and independent data products in Switzerland coordinate systems is indeed very interesting and potentially a source of errors if not handled carefully. It is true that resampling and height adjustments can add errors. We handle all datum and height transformation using the latest official grids (REFRAME library from swisstopo). Schlatter and Marti, 2005 indicate that the difference between LN02 and LHN95 is modelled with an accuracy of 1 to 10 cm. We will add this in the revised manuscript.

Schlatter, A., and Marti, U.: Höhentransformation zwischen LHN95 und den Gebrauchshöhen LN02, Geomatik Schweiz: Geoinformation und Landmanagement = Géomatique Suisse: géoinformation et gestion du territoire = Geomatica Svizzera : geoinformazione e gestione del territorio, 103, 10.5169/seals-236251, 2005.

20: Already mentioned version number and citation earlier, don't need to repeat here.

We will delete version number and citation.

21: Should state you're using the RPC camera model first, then talk about updating during bundle adjustment

We will add at the start of the sentence: *Processing of Pléiades satellite images involved triangulation and refinement of Rational Polynomial Coefficient (RPC) in ERDAS …*

22/30: Should avoid starting sentence with "14" and acronyms "DSMs"

We will spell out "Fourteen" and "Digital Surface Models" at the start of sentence.

27: Is it expected that the CE90 and LE90 are identical? I would expect a factor of ~2 degradation in LE90.

We doubled checked our LOOCV and those values are correct and indeed identical. Airbus specifies its Elevation1 DSM product with GCPs achieving CE90 = LE90 = 1.50 m (see https://www.intelligence-airbusds.com/files/pmedia/public/r49249_9_elevation1_dsm.pdf).

Page 13:

2: See general comment about the citation here and question about blending. I wouldn't say "with GDAL". This is not a standard GDAL command line utility or API function. I think you created a custom script that would weight values from your 3 input DSMs based on the ASP triangulation error map? I recommend you consider the ASP dem_mosaic weighted average blending approach.

We answered the general comment and clarified the arithmetic used to do this. We use a single gdal_calc.py instance to implement the weighted mean, indeed fed by DSM and error maps, so our statement is factually correct. As far as we know, dem_mosaic in ASP does not allow the weighting of input DEMs in such a way.

9-15: This “tilt” is a bit troubling, and potentially indicates issues with the GCPs, either their spatial distribution and/or recorded position errors. See general comment.

We answered this comment in details earlier.

13-15: The last sentence should be moved to the end of the above paragraph (line 7).

We will move the sentence.

19: Note that Agisoft can process grayscale images, and RPC models these days.

We appreciate the suggestion and will certainly consider it in the future.

29: OK, so refining interior camera parameters is not desirable, so you explicitly disabled from the initial alignment solution? Did you add calibrated lens distortion coefficients, or did you allow Agisoft to solve for these? If so, which coefficients? Provide more detail here.

The Ultracam Eagle M3 is a metric camera precalibrated with no detectable lens distortion as per its calibration report. We believe it would be wrong in such case to use any form of self-calibration (+ subsequent optimization in agisoft), as this would only involve a mathematical optimization on top of the BBA, that would push any departure from the true calibrated values into geometrical distortions of the DSM. So, indeed we set the focal length to calibrated value as well as the principal point coordinates and all lens distortion parameters to 0.

29: Careful about interchanging GCP and CP here. I don’t think you have 29 GCPs, and if you’re using points to control geolocation, they are GCPs, not check points.

We really have 29 GCPs and 15 additional CPs. We are not reusing GCPs.

Page 14

2: I’m really glad that you used a factor of 2x here, and did not export an oversampled DSM at the native image GSD! This is a common issue.

Thank you.

5: I think this was done using the SenseFly eMotion software? This first paragraph is a bit confusing, as you’re already talking about the accuracy of the DSM but you haven’t told us how the DSM was produced. I recommend you move this paragraph later, and integrate with the last sentence of paragraph 2 (lines 21-22), where you actually report the observed RMSE.

We used SenseFly eMotion software only for flight planning and downloading the images from the eBee+. Here we refer to the processing strategy in Agisoft (Integrated Sensor Orientation) with corresponding citations for context, including what sort of accuracy can be achieved with ISO processing. We will move the paragraph as you suggest.

If your base station position is accurate (I think you used NTRIP caster for real-time corrections, not a local base), then you should be able to achieve the accuracy you report without GCPs.

This is correct, we used a NTRIP caster for real-time corrections and did not use GCP to process eBee data. Therefore it is true that we expect to achieve the accuracy we report in the context paragraph starting this section.

15: “EXIF metadata”

We will change this.

32: dGNSS - check for consistency in terminology used elsewhere

We will check for consistency and use DGNSS.

Page 15

1-2: I think you mean it was not possible to determine the precise offset of the GNSS antenna phase center relative to the center of the camera detector. Could probably estimate vertical offset and constrain a bit better than 0.2 m horizontal and vertical, but not a huge issue.

Exactly, that’s what we meant. We will clarify the sentence.

Page 17

3-5: What you did here should work. Technically, you want to use a consistent grid for all output products, with same grid cell size, projection and origin. If the spatial extent of the two rasters varies significantly, then you can use something like GDAL’s -tap option to force output grid extent to use whole integer multiples of the output grid cell size. Can also do this manually in Agisoft when specifying output extent - round left, top, right and bottom bounds to nearest multiple of the cell size. A shared raster origin (upper left coordinates) or this -tap approach avoids the need for a second resampling step, which is going to further degrade resolving power of your products and can introduce additional error.

Thank you for the input!

7-9: I like this approach. Approximately how many pixels were sampled within this circle?

We sampled around 190 pixel for the eBee, around 126 for the ultracam and the ground-based imagery.

10: So this sounds like nearest neighbor sampling for Pleiades snow depth grid. I recommend bilinear or cubic for point sampling like this, esp if you see relatively large pixel-to-pixel variability in snow depth grid values near the sites.

We used the ArcGIS Pro function “Extract Values to points”. We didn’t interpolate because we are interested in the real value of the cells. The product of the Pleiades is already an interpolated product with a much larger cell size than the buffer. We are aware that the nearest neighbor can cause obvious errors in large pixel differences, but when interpolated, the trueness of the values is not guaranteed either. For this reason, we prefer this method.

Page 18:

12: See general comment about the 2*STD filter

We responded to this comment earlier.

12-13: Do your errors actually have a normal distribution? Looking at box plots in figure 9, I would say no. So some of these assumptions may not hold. Overlapping histograms of delta_HS from the 3 sources might be more informative than the box plot.

We will add histograms to the boxplot figures which show that it's nearly normally distributed. The updated figure was provided in the general comment above.

Page 19:

3-5: recommend using "area" for all instances instead of "surface"

We will change all instances to "area".

6: already said ultracam only covers northern part of valley due to clouds elsewhere (which is really too bad, data quality over cloud-free areas looks great). Does "Dischma valley" = "Dischmatal"?

We will remove unnecessary repetitions. Yes, "Dischma valley" is "Dischmatal". We changed it to "Dischma valley" as this is the term we use here.

6-7: what does "good quality of eBee+ flight" mean, and how does an orthoimage illustrate this?

We agree, "good quality of eBee+ flight" can mean different things. We will change the sentence to be more meaningful.

Page 21:

3: "graphically" sounds strange to me, I think you mean "qualitatively"

We will change the word to "qualitatively".

7-8: "errors introduced during photogrammetric processing" - the processing itself is not responsible for the negative values

We will change the wording of the sentence.

9: OK, yes, using a DSM is a problem, but the acquisition date of your summer reference DSM will also be very important in terms of the vegetation growth cycle, leaf-out, etc. Also, you are assuming that your photogrametrically derived DSM is capturing the true top of canopy, which is not necessarily the case (esp with "aggressive" filtering that will remove isolated shrubs/trees)

We agree with you that the acquisition of the summer DSM adds uncertainties. We will investigate how to correct a photogrammetric summer DSM for photogrammetric snow depth maps depending on vegetation and recording date in further studies.

9 and 14: recommend "depressed" or "compressed" rather than "pressed down"

We will change the word to “compressed”.

17-22: What is the total sample size for manual and snow pole measurements again? I would argue that some of your larger apparent error is due to limited sample size, and likely the nearest neighbor sampling approach for the coarser Pleaides snow depth grid.

The total size of the manual and snow pole measurements is 37. Yes, we agree some error is due to the limited sample size and the coarser Pleiades snow depth grid. We will a comment in the discussion.

21-23: Careful with this kind of statement, as it sounds like subjective error reporting…

We will change the wording of the sentence.

23: “decreased” instead of “deteriorated”

We will change the word to decreased.

23: The NMAD and median should not be strongly influenced to one outlier, unless your sample size is an issue.

Yes, the sample size is an issue in comparison 1 and that’s why the NMAD and the median is strongly influenced by the large outlier. We will improve this point as mentioned above in the discussion.

25: Again, triangulation here is a bit ambiguous, as it could be confused with the triangulation to produce the point cloud. I think you’re talking about the integration of GCPs during the bundle adjustment routine.

As explained above, this is what we mean as per the general terminology in photogrammetric science, not in computer vision.

27-29: This information (about the roads used to correct Pleaides DSM) should be moved to the methods section.

This was indicated clearly in section 4.2, only restated here.

29: I think you’re trying to say that one sample Pleaides triplet is not necessarily representative of the capabilities of the sensor.

Not really, and we think your interpretation may be influenced by your definition of “triangulation”. We are discussing the fact that the tilt and its effect on determining snow depth is a limitation having to go through independent block adjustment (triangulation), not a limitation of the sensor and its inherent performance.

30: “...approach for snow-covered images” - this problem will be mitigated with snow-free conditions

We will add “for snow-covered images”.

30-31: Not sure this last sentence is necessary

We think it's important to remind the readers that Pléiades images were recorded from space because this level of detail is quite an achievement. But we will include this point into the discussion and remove it from the result section.

Page 26:

10: recommend changing "data analysis" to "accuracy analysis of comparison 1 is potentially not representative of the true accuracy of the snow depth products" or something along those lines. See general comment on this issue.

We will change the wording of this sentence.

Page 27:

1: Note that this is correlation of per-pixel values, and should not be confused with spatial correlation

We will specify this in the paper.

6-7: Might be useful to report the percentage of data removed with your 0-5 m filter here. Based on Figure 8, this should be minimal for ultracam, but you're removing a nontrivial sample of the Pleiades HS values.

We will report the percentage of the removed values. Yes, it's a nontrivial part of the Pleiades HS values and we will discuss that in the discussion.

8: Don't start sentence with "0 m…"

We will change the sentence.

11: "R^2 values"

Page 29:

3: "imagery" should be "DSMs"

We will change the word.

4: You can only use the ultracam HS as ground truth to evaluate the Pleiades HS, right? The way it is stated, it sounds like you're using to evaluate both.

We will change the sentence.

Page 32:

8: There are also studies by Shaw et al. (2019?). Please review Simon Gascoin and Etienne Berthier's recent publications, as they are listed on other recent papers using Pleiades for accuracy of DEM difference maps, including snow depth

We will review the recent publications identified and adapt them to this section.

12: I don’t think it’s fair to present your “cleaned” values here

We will change this.

12: Again, rather than comparing DSM accuracy, you’re comparing snow depth accuracy, which includes error from the reference dataset.

We will adapt this in the paper so that it’s clear that is an indirect comparison of the winter DSMs.

13: “This is higher” here is a bit confusing, as your numbers are lower. Consider rephrasing. Also “this” is ambiguous.

We will rephrase.

14: Why is one pixel considered the maximum??? Sub-pixel correlation should be capable of 0.1-0.2 px accuracy. Is the issue with your manual GCP identification? Still should be able to achieve sub-pixel with this, esp with modern GCP markers.

We agree with you. We will rephrase this sentence to account for sub-pixel accuracy.

18-19: I don’t follow the last sentence, but I may just be getting tired :) Consider rewording. What is “they”

We will reword the sentence. With “they” we mean “The RMSE and the NMAD”.

21: Need to qualify this with “from Pleiades, without further correction”. We have demonstrated better accuracy with WorldView-3 DEM difference (same as snow depth) products (see McGrath et al, 2019; Shean et al., 2016). And there are several systematic errors in the individual DSM products (e.g., CCD offsets, unmodeled attitude error [“jitter”], parallax issues in L1B camera models) that can be corrected to further improve accuracy. We are actively working on this, so hopefully Pleiades DSM accuracy can be improved!

We will qualify this and add more information about accuracies of satellite products and errors, including in the most recent studies involving snow depth mapping.

25: I would avoid using the world “profit” to avoid confusion with commercial applications, “benefit” would be better

We will use the word “benefit”.

28-30: I disagree. ICP co-registration approaches can work very well, even when only sparse exposed surfaces are available. Co-registration using methods like Nuth and Kaab (2011) can also be used to take advantage of the slope and aspect-dependent dh - can then use limited snow-free surfaces for final vertical correction. I think you may be referring to cases when the entire scene is 100% snow-covered (rare for mountains).

Thank you very much for the input and we agree with you. We will reword this accordingly.

Page 33:

14: Issues of contrast can also be problematic in satellite imagery. In my experience, it is more about fresh snowfall and whether image GSD is fine enough to capture relevant length scales of surface roughness.

We will add a sentence in the discussion section for the satellites (6.1).

18: An aircraft outfitted with high-end GNSS and IMU should be able to provide very accurate camera position and orientation data, eliminating the need for GCPs (as with your eBee RTK results)

At first glance, this should indeed be the case. But the accuracy of the Ultracam positions (0.2 m) is worse than the accuracy of the eBee+ (0.02 m for the position and 0.03 m for the height).

19: Again “higher GSD” - careful here, as lower numeric value means better resolution

We will adapt the sentence.

24-25: This is consistent with my experience using eBee RTK platform. But careful about generalizing to all “UAS photogrammetry” - a DJI Phantom with no GCPs is not nearly as capable

Thanks for this comment and we will consider how we phrase.

Page 34:

8: This is where using a 3-4 m pole can be beneficial.

Yes, but it’s difficult to have a setup with a 3-4 m pole which is also mobile.

14: “non-negligible”

We will adapt the word.

20: Careful with this - using a DTM may help in some areas, but not others; “bushes” is pretty generic, and a bush with leaves appears very different than a leaf-free bush to a laser or camera

Thanks for this comment. We will consider this and discuss this accordingly.

Figure 2:

Check TC date formatting standards - I initially read this as MM.DD If you’re going to remake this figure, it might be better to alter the aspect ratio to reduce the width of the x axis, so we can better see the magnitude of the change over the study period (right now all lines look really flat). Either that or add thin horizontal gridlines and a complementary right axis label.

We will change to the TC formatting standards and try to improve the readability of the figure.

Figure 4:

I would move this to supplemental figure - it is awfully large for the information you're trying to convey, or could be presented as a table Need to define HS in caption

I'm still confused by comparison 3. Why is comparison 3 HS_platform_ALS?

We created this flowchart to give an overview over the different comparison strategies. We find this figure necessary given how many data products are discussed and presented in the manuscript. We will define HS in the caption.

We find comparison 3 important because otherwise we won't have a comparison or an evaluation of the snow depth maps on larger area. Certainly, a snow depth map for the whole recorded area would be interesting as well as a winter ALS scan over the whole area. However, these data were not captured as part of this study, but we believe we have nonetheless sufficiently imaged an area large enough for a valuable comparison of snow depth distribution.

Figure 5:

d) I don't see the violet stars? If they are present, recommend making larger and using a color that won't blend in with the orthoimage

We will add the purple stars, they disappeared in the cycles of redesigning the figure.

Figure 6:

The color ramp used here makes it very difficult to distinguish snow depth values between 0-1 m. It would be better to use a perceptually uniform, linear color ramp, ideally with labels for increments of 1.0 or 0.5 m intervals. I realize this may not be straightforward in ArcGIS.

We have used our organization's standard color ramp for snow depth maps, which we feel is sufficient for depicting the overall snow depth distribution across the study site. This color ramp also highlights well the features of the snow depth maps. But we will add the figure shown below to the supplement where we masked all values smaller 0 and greater than 1. Also we changed the color ramp of figure 7 (see figure 7 in the general comments).

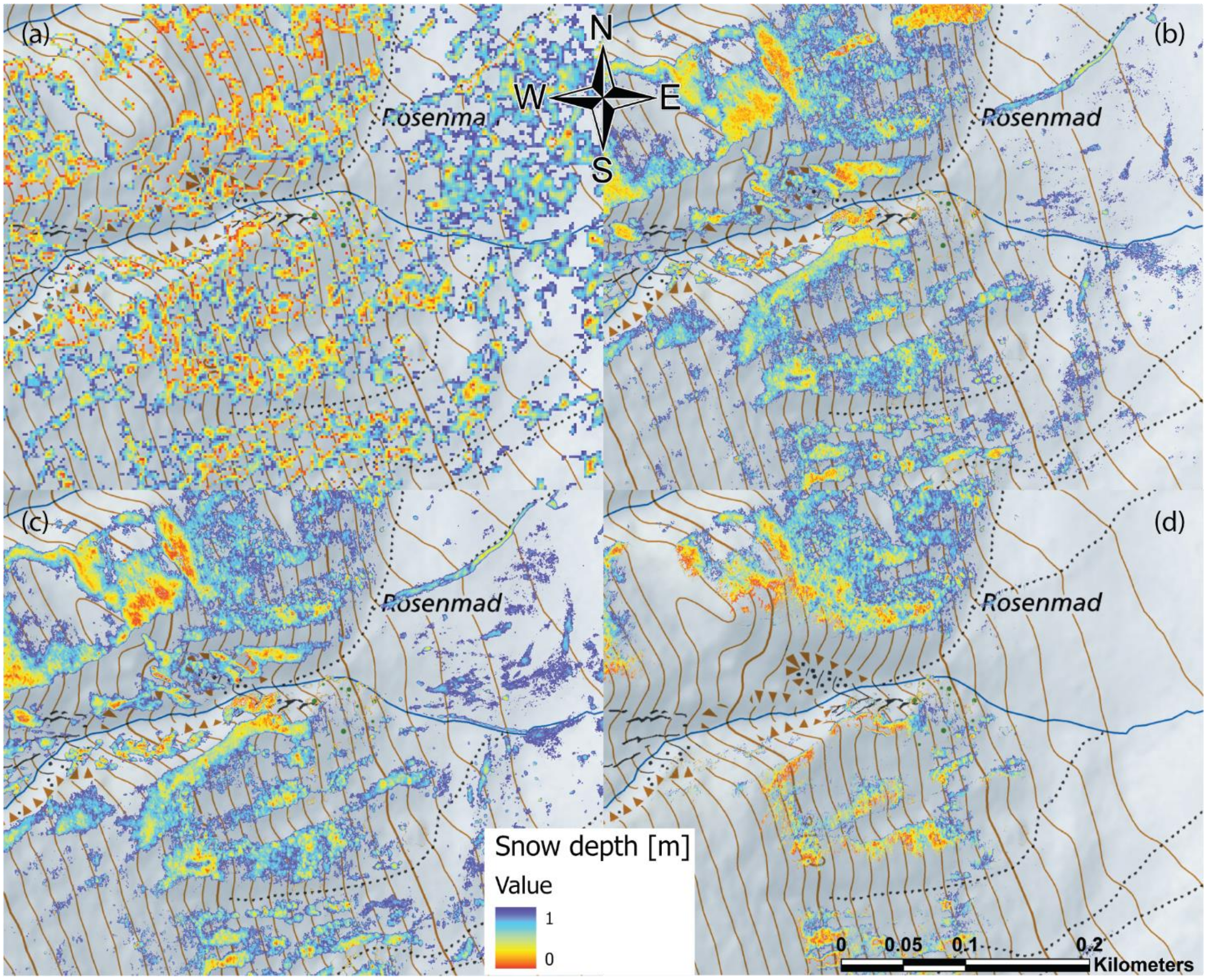

Figure 7:

Maybe use “apparent snow depth” or “snow depth estimate” here and elsewhere in the paper, as it’s not physically possible to have a negative snow depth

Why did color ramp change here to what looks like matplotlib plasma? Also, since you are showing values from -3 to 3 m, could be better to use a diverging color ramp. Lots of good resources on the theory behind these visualization approaches: https://matplotlib.org/3.1.1/tutorials/colors/colormaps.html

Yes, it’s not possible to have a negative snow depth but we think is all right to use only “snow depth” because we do not start from the absolute truth.

We thank you a lot for the input with the color ramp. We adapted Figure 7 with a diverging color ramp (see general comments above.)

Figure 8:

This is a nice figure, but why such a large bin size??? The quantization here makes comparison between different sources really challenging. I would recommend bin size of <5-10 cm, so we can properly assess each distribution. Also, it would be valuable to create a mask for the common intersection of valid HS pixels (ie pixels where all 4 DSMs have a valid elevation), clip each input HS to the same mask, then produce a similar histogram, maybe as a second panel in this figure. This provides an "apples to apples" comparison, as your current histograms are sampling different portions of the domain, and there is no reason to expect your reported mean and std statistics to be the same.

We will change the bin size of the histogram to 0.1 m. Below you find the new graph with the bin size of 0.1 m. We agree with you but the nice thing to see in this graph, is that also for different sizes of snow depth maps the relative distribution of the snow depth is similar. Therefore, we will keep this graph the way it is.

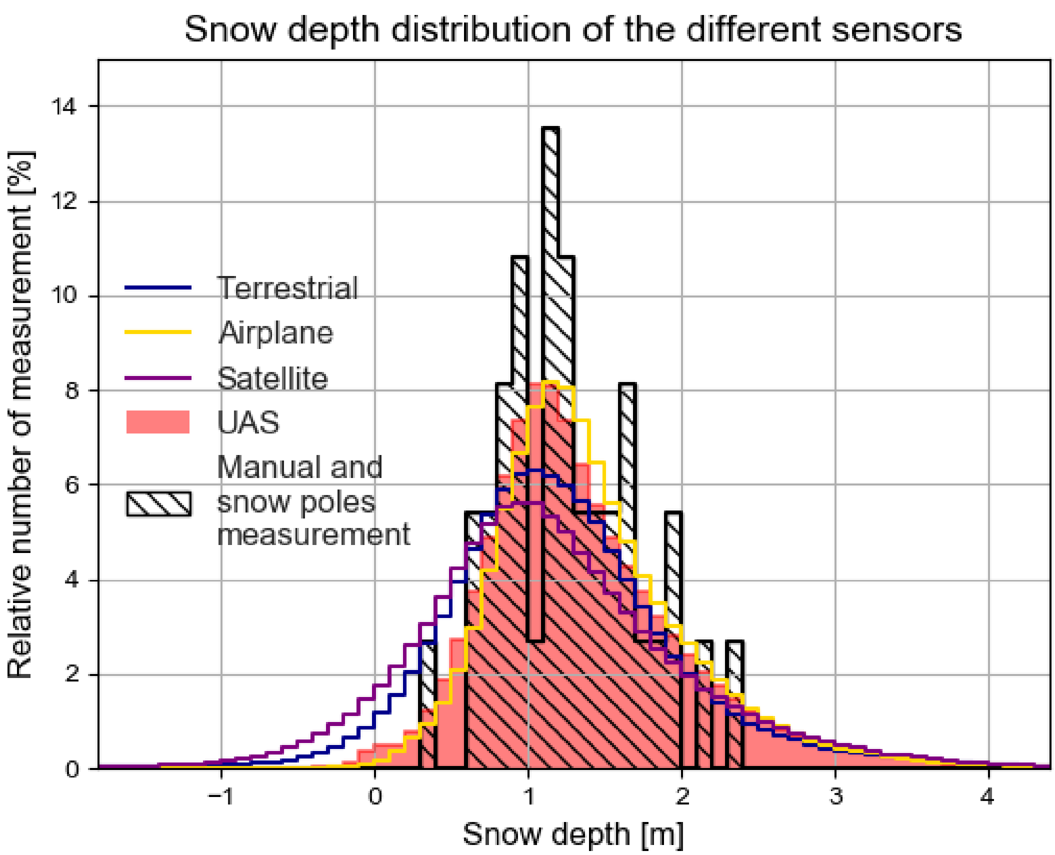

In the caption, you can just say "normalized histogram" without details about dividing by total number and multiplying by 100.

We will make the caption more precise.

What does "all not shown" mean? You have the Manual and snow poles measurement on histogram on the plot.

The “all not shown” means that the mean and STD are not shown but this is misleading formulation. We will change this formulation.

Figure 9:

Is “the median” the same as your MABE metric? I think MBE is just the mean error, right? 5th and 95th are not quartiles, they are percentiles. Fix in all other captions for box plots.

Yes, the median is the same as the MABE. We will change this in the caption of all boxplot. MBE is just the mean bias error as defined in the section 4.6.4. We will clarify this point. We update the captions for the figures using the 5th and 95thpercentiles.

Figure 11:

I think this is a 2-D histogram showing density? So, not a scatterplot. I don’t think your current caption says what color represents.

It’s a scatterplot showing the density. We will rework the caption and state what the color represents.

Probably want to say “y = x”

Yes, we will change this.

Should mention in caption why the bottom row is limited to range of 0-5 m on y axis. I think this is labeled “cleaned” but you’re adding another filter here.

We will mention that in the caption and change the name “cleaned” to “filtered”. We also will clarify this filtering in the method section for consistency.

Table 1:

Time is local or UTC?

It’s local time, which we will state with LT.

Add a row for sensor dimensions in pixels and/or mm. 450 MP is not really a “resolution” and we don’t know dimensions.

See comment above. We will add a row.

What do you mean by Pleaides mean GSD of 0.7 (resampled to 0.5). Did you intentionally oversample, or are the L1B products delivered at higher res after some super-resolution processing beyond normal TDI?

Pleiades native Ground Sampling Distance (nadir) are Panchromatic: 0.7m; Multispectral: 2.8m. the shipped products are resampled by ground segment to 0.5 and 2m, see section “B.2.2 Why 50 cm?” in Pleiades User Manual (https://www.cscrs.itu.edu.tr/assets/downloads/PleiadesUserGuide.pdf).

Table 3:

Threshold for classifying outliers

We will change “detecting” to “classifying”.

References:

Several of these are “gray literature” and some contain errors (e.g., Deems and Painter, 2006 has no journal information, year listed twice)

Authors should review all references carefully, update according to TC policy, remove gray literature, and update lingering errors from citation manager software

We will carefully check the references. Thank you for identifying the mistake with the Deems and Painter, 2006 citation.

Responses to the review of Mr. Deschamps-Berger

Eberhard et al. present an inter-comparison of methods to measure distributed snow depth maps in alpine terrain. They combined snow-on and snow-off digital terrain models (DTM) calculated with various methods to produce snow depth maps. In particular, they evaluated the accuracy of a snow depth map derived from spaceborne photogrammetry (satellite Pléiades) using snow depth maps measured with ground based photogrammetry (1.12 km2), UAS photogrammetry (3.59 km2) and airplane photogrammetry (75.7 km2). They found that the accuracy of the Pléiades snow depth map depends on the reference snow depth map and on the use of a 2 x STD filter of the snow depth residuals (STD: Standard Deviation).

In section 6.1, the authors compared the accuracy of a Pléiades snow depth map with previous studies of Marti et al. (2016), Deschamps-Berger et al. (2020). Using the accuracy of their Pléiades maps and the one obtained from an Unmanned Aircraft System (UAS) survey over 3.59 km2 (RMSE*=0.44 m, NMAD**=0.38 m), they concluded that they achieved higher accuracies than above cited works. We think that this comparison should be discussed in the light of two important methodological differences.

First, the reference snow depth map was calculated with different methods. This impacts the accuracy calculation as each method has its own uncertainty and are not available on the same areas. Deschamps-Berger et al. (2020) evaluated their snow depth maps against a reference snow depth derived from airplane laser scanning over 138 km2 (RMSE=0.80, NMAD=0.69). In Eberhard et al. (2020), the reference dataset was obtained using UAS photogrammetry over 3.59 km2 (RMSE*=0.44 m, NMAD**=0.38 m). At this spatial scale, UAS photogrammetry is expected to have a higher accuracy than airplane laser scanning. The accuracy assessment in Deschamps-Berger et al. (2020) actually compares well to the one calculated by Eberhard et al. (2020) with the reference snow depth map measured by airplane photogrammetry over 75.7 km2 (RMSE = 0.92, NMAD = 0.65 m). Eberhard et al. (2020) puts more weight on the validation using UAS photogrammetry because of the lack of validation for the airplane survey for the whole study site. However this airborne method was well evaluated in previous studies (Nolan et al., 2015, Bühler et al., 2015).

Second, in Eberhard et al. (2020), only the snow-on DTM was calculated with Pléiades images. The snow-off DTM is always common to the evaluated and the reference snow depth map. It is calculated with the same method as the reference snow-on DTM (ground-based, UAS, airplane photogrammetry) which are expected to have higher accuracy than Pleiades-derived DTM. In Marti et al. (2016) and Deschamps-Berger et al. (2020), both the snow-on and snow-off DTM were calculated with Pléiades images. This is a major difference as the accuracy of a snow depth map results from the combination of the accuracy of the snow-on and the snow-off DTM.

Dear Mr. Deschamps-Berger

Thank you very much for the comments. The point you make about the methodological differences that led to the reported values in each paper is very important and should have been clarified and discussed in Section 6.1, so that the relative performance across the three studies can be better interpreted.

We agree with your first point that we should discuss our results in relation to the size of the test area, which at 3.59 km^2 is very small. But we put a lot of emphasis on the validation with the eBee+, because the ultracam has never been tested on snow. Bühler et al, 2015 used an ADS80-SH52 sensor

which is an optoelectronic line scanner and not an aerial camera. Furthermore, the imagery was processed with ATE SOCET SET. Also, the imagery had an average GSD of 0.25 m and not 0.06 m as we had. Nolan et al, 2015 used an aerial camera system but nothing similar to Ultracam.

To your second point we would like to say that we do calculate snow depth maps but we only compare the snow-on DSMs. Whenever we compare two snow depth maps, the snow-off reference is the same. Therefore, the error from the snow-off DSM is the same for both subsequent comparison DSMs and will not influence the results.

We will therefore refine our discussion, especially section 6.1 to clarify and expand the methodological differences you pointed out.

References:

Bühler, Y., Marty, M., Egli, L., Veitinger, J., Jonas, T., Thee, P. and Ginzler, C.: Snow depth mapping in high-alpine catchments using digital photogrammetry, The Cryosphere 9(1), 229–243, doi:10.5194/tc-9-229-2015, 2015.

Deschamps-Berger, C., Gascoin, S., Berthier, E., Deems, J., Gutmann, E., Dehecq, A., Shean, D., and Dumont, M.: Snow depth mapping from stereo satellite imagery in mountainous terrain: evaluation using airborne lidar data, The Cryosphere Discuss., https://doi.org/10.5194/tc-2020-15, in review, 2020.

Marti, R., Gascoin, S., Berthier, E., De Pinel, M., Houet, T. and Laffly, D.: Mapping snow depth in open alpine terrain from stereo satellite imagery, The Cryosphere 10(4), 1361–1380, doi:10.5194/tc-10-1361-2016, 2016.

Nolan, M., Larsen, C. and Sturm, M.:Mapping snow depth from manned aircraft on landscape scales at centimeter resolution using structure-from-motion photogrammetry, The Cryosphere, 1445–1463, doi:10.5194/tc-9-1445-2015, 2015.

Relevant changes

We have implemented everything we answered to the reviewers. The most important points are summarized below:

- Proof reading and overall improvement of writing
- Improvement of the result and conclusion section
- Improvement of the Figures, 2 figures moved to the supplements
- Check of the references

Intercomparison of photogrammetric platforms for spatially continuous snow depth mapping

Lucie A. Eberhard[1, 2], Pascal Sirguey[3], Aubrey Miller[3], Mauro Marty[4], Konrad Schindler[2~~5~~], Andreas Stoffel[1], Yves Bühler[1]

[1]WSL Institute for Snow and Avalanche Research SLF, Davos Dorf, 7260, Switzerland
[2]Institute of Geodesy and Photogrammetry~~D-Baug~~, ETH Zu~~ü~~rich, Zu~~ü~~rich, 809~~2~~3, Switzerland
[3]National School of Surveying, University of Otago, PO Box 56, Dunedin, New Zealand
[4]Swiss Federal Institute for Forest, Snow and Landscape Research WSL, Birmensdorf, 8903, Switzerland
~~[5]Photogrammetry and Remote Sensing Group, ETH Zurich, Switzerland~~

Correspondence to: Lucie A. Eberhard (lucie.eberhard@slf.ch)

Abstract. Snow depth has traditionally been estimated based on point measurements collected either manually or at automated weather stations. Point measurements, though, do not represent the high spatial variability of snow depths present in alpine terrain. Photogrammetric mapping techniques have ~~made significant~~ progressed in recent years and are ~~suitable to~~capable of accurately maping snow depth in a spatially continuous manner, over larger areas, and at various spatial resolutions. However, the strengths and weaknesses associated with specific platforms and photogrammetric techniques, as well as the accuracy of the photogrammetric performance on snow surfaces have not yet been sufficiently investigated. Therefore, industry-standard photogrammetric platforms, including high-resolution satellites (Pléiades), airplane~~s~~ (Ultracam Eagle M3), Unmanned Aerial System~~s UAS~~ (eBee+ with S.O.D.A. camera) and ~~ground-based~~terrestrial (single lens reflex camera, Canon EOS 750D), were tested ~~in a timely manner~~ for snow depth mapping in the alpine Dischma valley (Switzerland) in spring 2018. Imagery was acquired with airborne and space-borne platforms over the entire valley, while Unmanned Aerial Systems (UAS) and ~~ground-based~~terrestrial photogrammetric imagery ~~were~~was acquired over a subset of the valley. For independent validation of the photogrammetric products, snow depth was measured by probing, as well as using remote observations of fixed snow poles.

When comparing snow depth maps with manual and snow pole measurements the root mean square error~~s~~ (RMSE~~s~~) values and the normalized median deviation~~s~~ (NMAD~~s~~) values ~~are~~ were 0.52 m and 0.47 m respectively for the ~~Pléiades~~ satellite snow depth map, 0.17 m and 0.17 m for the ~~Ultracam~~ airplane snow depth map, 0.16 m and 0.11 m for the UAS snow depth map. ~~Ground-based~~The area covered by the terrestrial snow depth map only intersected with 4 manual measurements and did not generate ~~-~~ statistically relevant measurements.~~had to few measurements to be statistically relevant.~~ When using the UAS~~eBee+~~ snow depth map as ~~ground truth~~a reference surface, the RMSE~~s~~ and NMAD~~s~~ values ~~are~~were 0.44 m and 0.38 m for the satellite~~Pléiades~~ snow depth map, 0.12 m and 0.11 m for the ~~Ultracam~~ airplane snow depth map, 0.21 and 0.19 m for the ~~ground-based~~terrestrial snow depth map. When compared to the ~~Because of the accuracy and precision of the Ultracam~~ airplane dataset over a large part of the Dischma valley (40 km^2), the ~~we finally compared the Ultracam~~ snow depth map from

Formatiert: Englisch (Vereinigtes Königreich)

Formatiert: Hochgestellt

the ~~to the Pléiades~~ satellite~~snow depth map over a large part of the Dischma valley and calculated~~ yielded a RMSE value of 0.92 m and a NMAD value of 0.65 m. ~~By comparing for the first time more than two platforms, t~~This study provides comparative measurements between photogrammetric platforms to evaluate th~~e~~ire~~e~~ specific advantages and disadvantages ~~of them~~ for operational, spatially continuous snow depth mapping in alpine terrain over both small and large geographic areas.

Keywords: Snow depth, Snow Water Equivalent, Photogrammetry, Satellite, Airplane, UAS, ~~Ground-based~~Terrestrial

1 Introduction

The range of applications for accurate high-resolution snow depth mapping is diverse. Snow depth or height of snowpack (HS) is defined as the vertical distance from the base to the surface of the snowpack (Fierz et al., 2009) and can vary significantly over short horizontal distances ~~horizontally within a meter-scale~~ (Lundberg et al., 2010; Griessinger et al., 2018; Dong, 2018). Several fields rely on accurate information about how snow depth changes across a landscape. First, accurate snow depth distribution estimates are necessary for snow water equivalent (SWE) modelling in snow hydrology (Steiner et al., 2018). SWE and snow depth are also important to estimate and model glacier mass balance (Gascoin et al., 2011; McGrath et al., 2015). Moreover~~Second~~, modelling snow drift accumulations and detecting avalanche release zones to estimate avalanche hazard requires ~~reliable~~precise information on snow depth (Schön et al., 2015). Furthermore, mapping the mass balance of avalanches is important for numerical avalanche dynamic simulation tools such as Rapid Mass Movement Simulation (RAMMS) (Christen et al., 2010; Bartelt et al., 2016). ~~In addition, snow~~Snow depth mapping also enables rapid documentation of avalanche accidents, which is required immediately after the event due to rapidly changing weather and snow conditions (Bühler et al., 2009; Lato et al., 2012; Korzeniowska et al., 2017). The tourism industry would also benefit from high-resolution snow depth maps in ski resorts to assist in snow redistribution ~~better redistribute snow~~ on slopes throughout the season (Spandre et al., 2017). ~~Furthermore~~Finally, mapping snow depth at high spatial resolution is desirable to support the monitoring of sensitive alpine ecosystems in a changing climate (Wipf et al., 2009; Bilodeau et al., 2013) because the seasonal snow cover is a rapidly changing climate characteristics ~~(IPCC 2007)~~.

Traditionally, snow depth measurements have been obtained as point measurements manually or at automated weather stations. Manual snow depth can be done by manual probing, with ground penetrating radar (GPR, e.g. McGrath et al., 2019) or other more automated field measurement techniques such as the magnaprobe (Sturm and Holmgren, 2018). Manual snow depth measurement techniques require access to challenging terrain, which is in alpine regions often prone to avalanche hazards, and may leave significant areas unsampled. Automated weather stations include a range of snow depth measurement techniques, such as snow pillows or sonic rangers (Nolan et al., 2015). Still, ~~T~~these measurement methods have ~~obvious~~ limitations because point measurements are sparse and give little indication about the spatial distribution of snow depth. This is particularly challenging when estimating snow depth over larger geographic areas (Nolan et al., 2015). Snow depth distribution can

~~eventually~~ be approached by interpolating sparse values (Cullen et al., 2016) ~~.~~ though the point measurement distribution may lead to biases and fail to fully capture the high variability of the snow depth. ~~Furthermore, manual snow depth probing disturbs the snow surface and may leave significant areas of terrain unsampled because of avalanche danger or challenging topography.~~

Emerging technologies such as laser scanning (LiDAR) have ~~already~~ produced continuous snow depth maps with high accuracy (e.g., Hopkinson et al., 2001; Hopkinson et al., 2004; Deems et al., 2013; Telling et al., 2017). Airborne laser scanning (ALS) typically covers ~~typically~~ large areas with ~~an average spatial resolution of 1 m~~a sampling density of ca. 1 pt/m^2 and can achieve a vertical accuracy of 0.1 m (Deems and Painter; Deems et al., 2013; Painter et al., 2016). ~~However, ALS remains expensive and requires an available aircraft (_ENREF_38). Also, not every laser scanner is suitable for snow depth mapping.~~ A laser (airborne or terrestrial) with a wavelength of 1064 µm ~~is the best choice~~ offers good compromise ~~for obtaining~~ to measure snow depth~~acceptable results on snow~~ due to the physical properties of the snowpack, i.e. dry or wet snowpack (Deems et al., 2013). Furthermore, a small laser beam footprint is desirable and can be achieved by ensuring that the laser beam remains perpendicular to the snow surface. Terrestrial laser scanning (TLS) can ~~achieve~~ measure the distance between scanner position and snow surface with accuracies below 0.10 m beyond 1000 m (Prokop, 2008). Recently, very long-range TLS have been used ~~for analysis~~ to map~~of~~ the spatial distribution of a snowpack up to 3000 m with absolute errors ranging from 0.2 to 0.6 m (Lopez-Moreno et al., 2017).

~~Laser scanning techniques remain relatively expensive compared with photogrammetry.~~ Satellite-based, airplane-based, Unmanned Aerial Systems (UAS)-based and ~~ground-based~~terrestrial data have been used for photogrammetric snow depth mapping, although rarely compared in a single study. A first study using imagery from the Pléiades satellites constellations mapped snow depth at 2 m spatial resolution with a standard deviation of 0.58 m compared to manual measurements and 1.47 m compared to UAS measurements (Marti et al., 2016). Recently, _ENREF_22 Deschamps-Berger et al. (2020) found a RMSE value of 0.8 m for Pléiades snow depth maps (resolution 3m) in comparison to ALS. ~~-~~ WorldView-3 satellite-derived snow depths were calculated by McGrath et al. (2019) who found a RMSE value of 0.24 m compared to GPR measurements. Aerial images acquired with a Leica ADS80/100 optical scanner have allowed snow depth to be produced with a RMSE value of 0.3 m (Bühler et al., 2015; Boesch et al., 2016). Using a consumer camera on a manned aircraft, a standard deviation of 0.1 m was determined for the snow depth compared to manual measurements (Nolan et al., 2015). Meyer and Skiles, 2019 produced digital surface models (DSMs) from snow covered surfaces with the RGB camera installed on the LiDAR-based Airborne Snow Observatory and compared them to simultaneously collected LiDAR data. At a spatial resolution of 1 m, the DSMs achieved a NMAD of 0.17 m and a mean relative elevation difference of 0.014 m. Photogrammetric UAS surveys are a promising method used and characteri~~s~~zed by several studies to map snow depth due to its high spatial resolution. With UAS data, vertical snow depth accuracies of 0.1 to -0.15 m have been achieved by several ~~researchers~~ studies (Vander Jagt et al., 2015; Bühler et al., 2016; De Michele et al., 2016; Harder et al., 2016; Cimoli et al., 2017; Redpath et al., 2018; Avanzi et al., 2018; Eker et al., 2019). Finally, ~~ground-based~~terrestrial photogrammetry has been used for snow observation, snow drift

Feldfunktion geändert
Feldfunktion geändert
Feldfunktion geändert
Feldfunktion geändert
Feldfunktion geändert
Formatiert: Hochgestellt
Feldfunktion geändert
Feldfunktion geändert
Feldfunktion geändert
Feldfunktion geändert
Feldfunktion geändert
Feldfunktion geändert
Feldfunktion geändert
Feldfunktion geändert
Feldfunktion geändert
Feldfunktion geändert
Feldfunktion geändert
Feldfunktion geändert
Feldfunktion geändert
Feldfunktion geändert
Feldfunktion geändert
Feldfunktion geändert
Feldfunktion geändert
Feldfunktion geändert
Feldfunktion geändert
Feldfunktion geändert
Feldfunktion geändert
Feldfunktion geändert
Feldfunktion geändert

tracking and avalanche detection with accuracies of 0.1 to -0.3 m (Prokop et al., 2015; Basnet et al., 2016). ~~Ground-based~~Terrestrial photogrammetry is currently the only method which can produce ~~digital surface models (~~DSMs~~)~~ of an avalanche flowing downwards during ~~an avalanche~~a release experiment (Vallet et al., 2001; Vallet et al., 2004; Dreier et al., 2016). Other techniques such as laser scanning have acquisition times that only allow the ~~acquisition~~ collection of DSMs before and after the avalanche release (Prokop et al., 2015). This makes ~~ground-based~~terrestrial photogrammetry a valuable monitoring solution, benefitting also from a relatively lower cost compared with other monitoring solutions such as TLS (Toth and Jozkow, 2016; Basnet et al., 2016).

Feldfunktion geändert
Feldfunktion geändert
Feldfunktion geändert
Feldfunktion geändert
Feldfunktion geändert
Feldfunktion geändert
Feldfunktion geändert
Feldfunktion geändert

Promising results from a range of photogrammetric~~y~~ techniques and platforms demonstrate the potential to operationalise photogrammetric snow depth mapping. Many studies have investigated the performance of photogrammetry for different surface types and mapping ~~To~~applications. However, only few studies have examined the available photogrammetric platforms for their performance on snow ~~date, the available photogrammetric platforms have only been partially investigated w.r.t. their performance on snow~~ (e.g., Bühler et al., 2017; Deschamps-Berger et al., 2020). Therefore, a comprehensive assessment is necessary to compare the snow depth products from terrestrial, UAS, aircraft and satellite platforms. ~~A comprehensive assessment is needed to compare snow depth products from ground-based, UAS, airplane and satellites platforms against each other.~~ Each platform has its advantages and disadvantages, but each must be able to cope with the challenges of imaging alpine environments, including steep terrain (high-parallax) ~~and rapidly changing weather conditions~~, high-albedo surfaces (sensor saturation) and limited surface texture for fresh snow (poor stereo-correlation). ~~A key advantage of photogrammetric satellite and airplane data is the large area that can be mapped promptly and the mapping of completely inaccessible terrain. Also, UASs allow decimetre-scale snow depth maps even when the accessibility of terrain is restricted i.e. because of avalanche danger and perform well in a winter alpine environment. UAS with photogrammetric platforms are fast, easy to handle and have a high recording availability, i.e. if the operator owns a UAS, they can fly whenever required. Ground-based photogrammetry achieves reasonable results for small areas of interest such as avalanche release zones if the areas are nearly perpendicular to the camera locations. Therefore, the different platforms available today for photogrammetric snow depth mapping can improve the research in alpine environments and fulfil the needs of spatially continuous snow depth mapping on different scale.~~

Feldfunktion geändert
Feldfunktion geändert

This study ~~documents~~ presents a photogrammetric intercomparison campaign ~~on 6 April, 7 April, and 11~~performed in April 2018 close to Davos, Switzerland. For the first time, optical data from a high-resolution satellite, an airplane, an UAS and ~~ground-based~~terrestrial platform were collected over the same area ~~and~~ within a short time frame. ~~(6 days). To validate the photogrammetric results with independent snow depth values, manual snow depth measurements were collected and fixed snow poles were used.~~

2 Test site Dischma valley and Schürlialp

The Dischma valley is an alpine valley in the region of Davos, Switzerland, which has been the focus of a range of snow-related studies (Baggi and Schweizer, 2008; Bühler et al., 2015). For a representative photogrammetric study, a test site with a diversity of terrain types was selectedneeded, including both artificially disturbed and undisturbed terrain. The Dischma valley covers altitudes from 1550 m a.s.l. to 3150 m a.s.l. with prevailing northeast and southwest aspects. In the south part of the Dischma valley, the vegetation changes between flat alpine meadows on the bottom to bushes and alpine roses on the slopes and hilly alpine terrain on the upper slopes. The northern and lower elevation region of the Dischma is dominated by alpine forests. The year-round inhabited areas are located in the northern region of the Dischma, the alpine pasture areas in the southern part are only inhabited in summer.

Satellite and aerial data were captured over an area that included the Dischma and surrounding ridges covering an extent of approximately 140 km^2. For the UAS and the ground-basedterrestrial platformss, a smaller test site was selected around Schürlialp, covering ca. 4 km^2 and reaching up to ca. 2350 m a.s.l. on each side of the valley (Figure 1). In winter the Schürlialp test site is only accessible by ski and In the Schürlialp test site the predominantmain aspects are northeast and southwest. The slope anglesurface slope ranges from 0° to 45°, with a typical slope anglesurface slope between 30° to 35°. Interesting features of the Schürlialp area are gullies channeling downslope winds and producing contrasted snow depth distributionwhich produces snow deposits on the bottom of the gullies. Manual snow depth measurements as well as 15 fixed snow poles observable from a distance with binoculars provided reference measurements in inaccessible terrain in the Schürlialp test site, including steep and inaccessible terrain.

Data from snow measurement stations distributed sparsely around our study site provides context for general snowfall patternssnow depth evolution in the Dischma valley during our study period. In particular, it the snow measurement stations documented that less than 10 cm of snow melted between 6 and 11 April (Figure 2see Figure S1). Only the low elevation stations Davos Flüelastrasse (5DF, 1560 m a.s.l) and Matta Frauenkirch (5MA, 1655 m a.s.l) lost more than 20 cm of snow. At higher altitudes, a small amount of new snow was measured (2 cm above an altitude of 2400 m. a.s.l.). These measured values support our assumption that the change in snow depth was minimal despite the time difference between data acquisition and a comparison of datasets could be made.

Feldfunktion geändert

Feldfunktion geändert

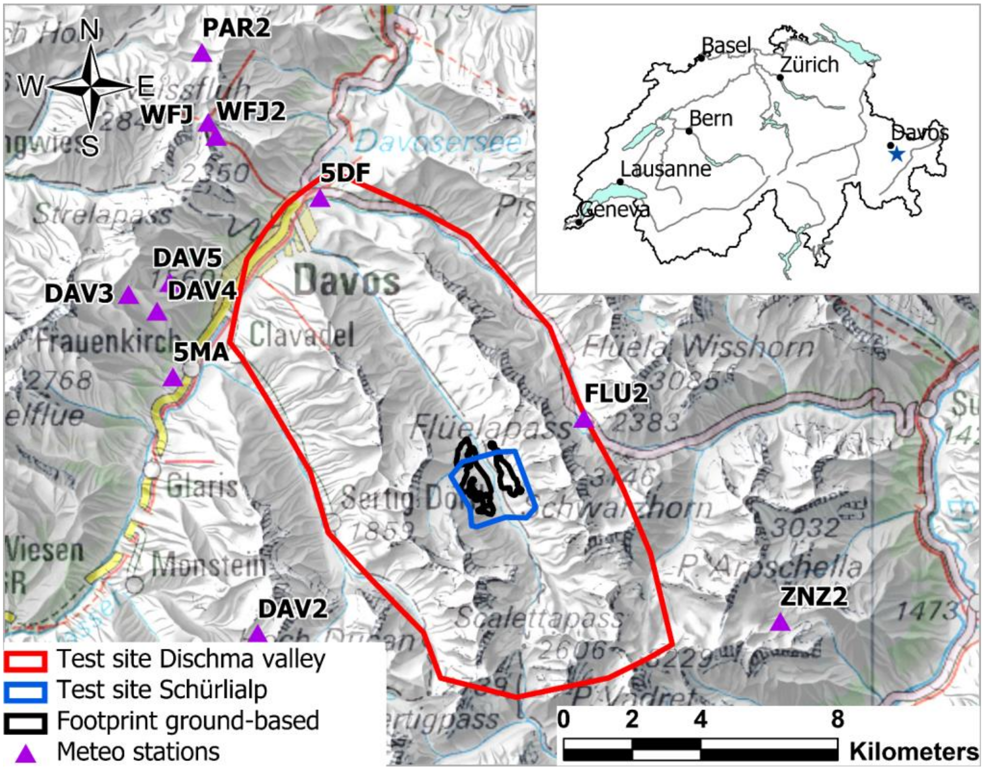
N
W
E
S
PAR2
WFJ
WFJ2
5DF
Davos
Davosersee
Strelapass
DAV5
DAV3
DAV4
Frauenkirch
Clavadel
5MA
Flüela Wisshorn
FLU2
Flüelapass
Glaris
Monstein
DAV2
Scalettapass
P. Arpschella
ZNZ2
Basel
Zürich
Bern
Davos
Lausanne
Geneva
Test site Dischma valley
Test site Schürlialp
Footprint ground-based
Meteo stations
0 2 4 8
Kilometers

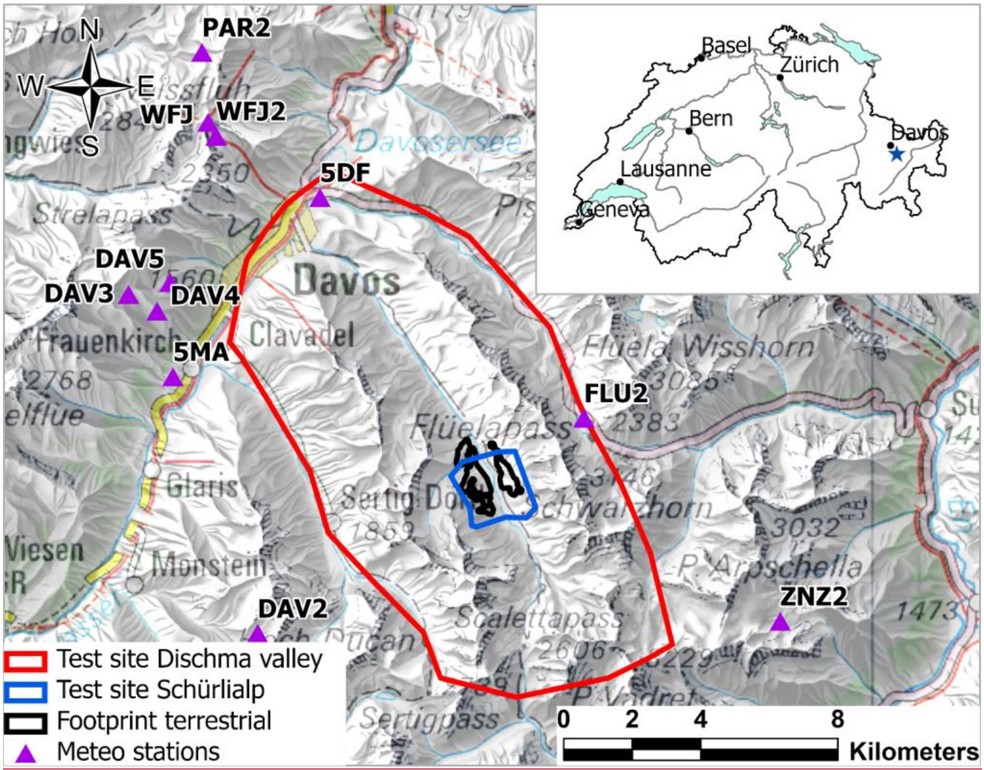

Figure 1: Overview of the test sites: ~~the red polygon is the~~ area ~~which was~~ recorded by the ~~Pléiades~~ satellite and ~~the Ultracam~~airplane imagery (red)~~,~~. ~~The blue polygon is the~~ area covered by the ~~eBee+~~UAS imagery (blue) and ~~the black polygons represent the~~ area covered by the ~~ground-based~~terrestrial images (black). The purple triangles represent the location of automatic and manual snow measuring stations around Davos. The abbreviations correspond to the snow measuring stations shown in Figure S1. The blue star in the inset map shows the location of the Schürlialp test site. (Swiss Map Raster© 2019 swisstopo (5 704 000 000), reproduced by permission of swisstopo (JA100118).)

Feldfunktion geändert

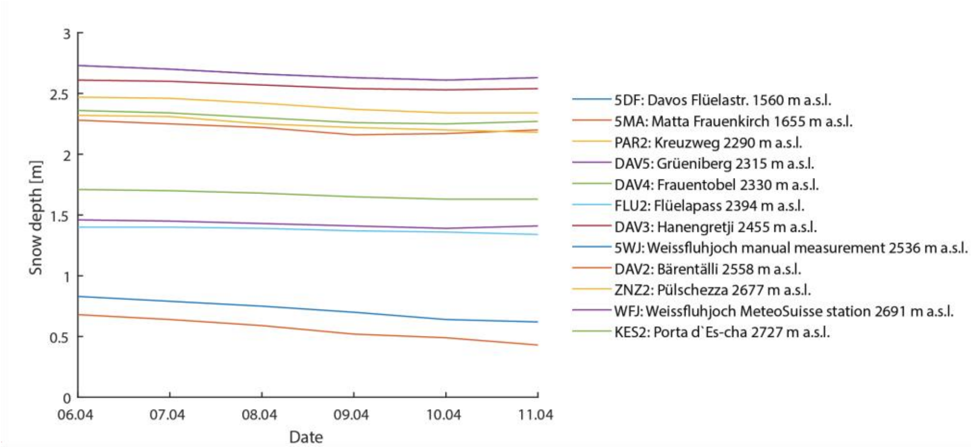

~~**Figure 2: Overview of the measured snow depth of the automatic and manual snow measuring stations around Davos for the period of photogrammetric data acquisition (see Figure1 for locations). (Data © SLF and MeteoSchweiz)**~~

3 Platforms and data

By acquiring satellite, airplane, UAS and ~~ground-based~~terrestrial data over a short timeframe (6 days), a comprehensive dataset bringing together small- and large-scale photogrammetric platforms is available for intercomparison. The ~~Pléiades~~ satellite constellation (Pléiades) ~~involves~~ consists of two very high-resolution optical satellites with proven performance to derive ~~digital surface model~~DSMs (Stumpf et al., 2014). The airplane platform (Ultracam Eagle M3) is a digital aerial ~~high-resolution~~ large format camera ~~from the Ultracam series~~ for state-of-the-art high-resolution aerial photogrammetry ~~()~~. The UAS (eBee+ RTK) is a fixed-wing survey drone ~~(UAS)~~ equipped with high-resolution camera and a dual-frequency differential ~~GNSS~~ Global Navigation Satellite System (DGNSS) sensor capable of Real Time Kinematic (RTK) positioning, all contributing to deliver very accurate digital surface models (Benassi et al., 2017). The camera used to capture ~~ground-based~~terrestrial data is a digital single reflex (SLR) Canon 750D. With this set of photogrammetric platforms, the Ground Sampling Distance (GSD) range from 0.04 m/pixel (UAS) to 0.5 m/pixel (satellites). To achieve the ~~triangulation~~ consistent geolocation of satellite data and ~~the~~ airplane data, independent ground control points (GCPs) and check points (CPs) were collected around Davos during summer. They consisted of features such as roof corners, bridges and other clearly distinguishable man-made features. However, many of these points are not visible in ~~the~~all imagery, either as they are covered by snow in winter or because of ~~the low~~ challenging interpretation due to the spatial resolution (Pléiades). Therefore 10 additional control points were distributed throughout Dischma, six of them on the test site Schürlialp. Seven of the GCPs were laid out on 6 April and 3 more on 7 April. They consisted of 0.8 x 0.8 m white tarps with a black cross and a white square in the middle. The positions of all GCPs were

Formatiert: Englisch (Neuseeland)

Feldfunktion geändert

Feldfunktion geändert

determined using ~~All GCPs were positioned with~~ a ~~differential~~ DGNSS (Trimble Geo XH 6000) with a ~~position~~ horizonal and vertical accuracy of 0.1m. In the following subsections, we present each platform and the corresponding data.

3.1 Satellite: Pléiades

A cloud-free Pléiades-1B stereo image triplet was acquired on 7 April 2018 between 10:17 LT and 10:19 LT ~~am~~. The panchromatic and multispectral bands (red, green, blue, near-IR) of Pléiades very-high resolution sensor achieve a spatial resolution of 0.5 and 2 m, respectively. The 12-bit radiometric resolution of Pleiades imagery provides a dynamic range capable to resolve contrast in dark shaded areas, as well as across highly reflective snow surfaces. From 694 km above ground, the image triplet was acquired along a descending orbit tracking east of Switzerland (across-track incidence angles of 17.4°, 12.1° and 9.7°, respectively). Along-track incidence angles of -16.3°, 7.6° and 17.9° resulted in three stereo pairs with Base-over-Height ratio (B/H) of 0.42 (images 1 and 2: pair P12), 0.19 (images 2 and 3: pair P23) and 0.62 (image 1 and 3: pair P13). Although both P12 and P13 have B/H recommended for photogrammetric work (>0.25, Astrium, 2012), P23 is below the usual standard to process an accurate DSM due to acute parallax angles. Meanwhile, larger B/H ratio, such as stereo P12, can yield unresolved areas due to terrain obstruction in steep topography. In addition, complicated parallax can modify the appearance of ground features~~,~~ and in turn challenging stereo-matching. For this study, we processed the three stereo pairs and considered occlusion and accuracy of each DSM to create a single merged surface product, as explained in section 4.2.

Feldfunktion geändert

3.2 Airplane: Ultracam Eagle M3

Airborne imagery was acquired with an Ultracam Eagle M3 by the company Flotron on 11 April 2018 between 11:00 LT and 12:00 LT. Unfortunately, the data could not be acquired on the same day as the satellite triplet due to technical issues on the airplane. The meteorological conditions during the data acquisition were partly cloudy and only the northern part of the Dischma valley was cloud free. From 512 images, only 242 images could be used for photogrammetric processing. Fortunately, no noticeable snow~~-~~fall event occurred between 6 April and 11 April 2018, and the temperature was too low to allow for significant snow melt (maximum 10 cm between 6 and 11 April at the low elevation stations, see graph in Figure S1 ~~Figure 2~~). The Ultracam Eagle M3 features a large-format CCD image sensor with 450 megapixel (MP) and a pixel size of 4 µm ~~x~~× 4 µm (see Table 1 for more information). The Ultracam Eagle M3 was mounted with the 122.7~~0~~ mm focal length lens and flown at a mean altitude of 1780 m above ground level (a.g.l.), resulting in a GSD of ca. 6 cm/pixel. The Ultracam images were recorded with a radiometric resolution of 14 bit. The images delivered were 4 band~~s~~ (RGB and NIR~~I~~) geotagged images. Furthermore, the data were delivered with camera positions and orientations with a DGNSS accuracy of 0.2 m, an Inertial Measurement Unit (IMU) accuracy of 0.01° (omega, phi, kappa) and corrected for lever arm and boresight calibration.

Feldfunktion geändert

3.3 UAS: eBee+ with S.O.D.A. camera

UAS ~~data~~ imagery of the Schürlialp area was collected on 7 April 2018 at 9:27 ~~am~~ LT for 1.5 h (three flights) with an eBee+ RTK of SenseFly equipped with the S.O.D.A camera~~, changing the battery twice~~. This imaging payload features a 1-inch

CMOS sensor with 20 MP (see Table 1 for more information) built specifically for photogrammetric applications. The images were recorded in the JPEG format with a radiometric resolution of 8-bit for each channel. Flying at 182 m a.g.l. on average and with lateral and forward overlaps of 70% and 60%, respectively, the eBee+ survey capturedyielding 1550 images with an average GSD of 0.04 m. A characterizing feature of the eBee+ RTK is the onboard differential DGNSS which measured the camera positions with a mean horizontal accuracy of the camera positions around ca. 0.02 m and mean vertical accuracy aroundof ca. 0.03 m. For RTK operation, of the eBee+ was referenced directly in the Swiss coordinate system LV95LN02, relative to mount point VRS_GISGEOLV95LN02 of the national DGNSS network.

3.4 Ground-basedTerrestrial: Canon EOS 750D

The ground-basedterrestrial images were collected manually on a tripod with a SLR camera Canon EOS 750D on 7 April 2018 starting at 10.37 am LT for 1 hour. The Canon EOS 750D is a digital SLR camera featuring an APS-C CMOS sensor with 24,2 MP resolution. We used a zoom lens (18-55 mm) and set the focal length at 43 mm. We chose the focal length of 43 mm as a compromise to achieve a mean GSD in the range of the other platforms for the selected camera locations. To ensure stable recording conditions, a tripod was used to take pictures from 5 different vantage points. The tripod was placed at each location and the camera was rotated on the tripod head. The entire setup was moved in one piece so that the focal length stayed fixed. To document the camera location, the DGNSS (Trimble Geo XH 6000) was placed on the top of the camera and this position was measured with a horizontal and vertical accuracy of 0.1 m. The GSD of this ground-basedterrestrial recording changes strongly across the slope, which affects the photogrammetric results. Also, for a stable and accurate photogrammetric model In order to achieve accurate measurement in all directions, the ray intersection angle is optimal around 90° to-100° and which requires a defined by a sufficient B/H ratio (Luhmann et al., 2014, p. 547), while also promoting terrain occlusions. When taking photos from the ground, there are many occlusions. This are all configuration elements that make ground-based making terrestrial recording challenging. With the camera positioned at the bottomSince we took the pictures from the bottom of of the Dischma valley, some slopes to the southwest and to the northeast are more than one kilometer away. Thus, the GSD varies between 0.01 m/pixel and 0.1 m/pixel with a mean GSD of 0.05 m/pixel. Towards the north and south sides, we havethe a flat valley floor for which our ground-based setup is not suitable for snow depth mapping. Therefore, we use the focal length of 43 mm as a compromise to achieve a mean GSD in the range of the other platforms for the selected camera locations. To ensure stable recording conditions, a tripod was used to take pictures from 5 different vantage points. The tripod was placed at each location and then the camera was rotated on the tripod head. The entire setup was moved in one piece so that the focal length stayed fixed. To have information about the camera location, the differential GNSS (Trimble Geo XH 6000) was placed on the top of the camera and this position was measured with an accuracy of 0.1 m. Finally, a A total of 268 images were recorded on the 7 April 2018 with a radiometric resolution 8-bit in JPEG format . With this ground-based setup we covered the covering the slopes of the northern part of the Schürlialp test site (see Figure 1).

Feldfunktion geändert

Table 1: Summary of the photographic data collection with the satellite, airplane, UAS and ~~ground-based~~terrestrial platforms.

		Satellite: Pléiades	**Airplane: Ultracam Eagle M3**	**UAS: eBee+ with SODA camera**	**~~Ground-based~~Terrestrial: Canon EOS 750D**
Platform information	**Sensor type**	Pushbroom scanner TMA optics	CCD image sensor	1-inch CMOS-sensor	APS-C CMOS-s~~S~~ensor
	Sensor resolution	Panchomatic array assembly: 5 ~~x~~× 6000 (30,000 cross-track) pixels Multispectral array assembly: 5 ~~x~~× 1500 (7500 in cross-track) pixels	450 MP	20 MP	24.2 MP
	Focal length	12.905 m	122.7 mm	10.6 mm	43 mm
	Pixel size	13 µm ×~~x~~ 13 µm in panchromatic band	4 ×~~x~~ 4 µm	2.4 ×~~x~~ 2.4 µm	3.7 ~~x~~× 3.7 µm
	Sensor Dimensions	-390 mm × 3 mm	105.85 × 68.03 mm	13.2 × 8.8 mm	22.3 × 14.9 mm
	Radiometric resolution	12-bit	14-bit	8-bit	8-bit
	Image type	Multispectral TIFF and panchromatic TIFF	High resolution multi-channel RGBI TIFF	sRGB JPEG	sRGB JPEG
Acqu...	**Acquisition date**	07~~.04.~~ April 2018	11~~.04.~~ April 2018	07 April ~~.04.~~2018	07~~.04.~~ April 2018

	Start of Acquisition	10:~~.~~17 ~~am~~LT	11:05 LT~~am~~	9:27 ~~am~~LT	10.37 ~~am~~LT
	Number of pictures	3	521 (242 cloud free)	1550	268
	Area covered	140 km^2	75.7 km^2	3.59 km^2	1.12km^2
	Mean flight height	694 km a.g.l.	1780 m a.g.l.	181 m a.g.l.	Mean distance from the Target: 1 km
	Mean GSD	0.7 (resampled to 0.5) m/pixel for the panchromatic band (nadir) 2.8 (resampled to 2) m/pixel for the multispectral bands (nadir)	0.06 m/pixel	0.04 m/pixel	0.05 m/pixel

3.5 Reference datasets

3.5.1 Manual snow depth measurements and fixed snow depth poles

Manual snow probing measurements at 27 locations in the Schürlialp test site were performed on 6 April (17 measurements) and 7 April 2018 (10 measurements). ~~Between 6 April and 7 April 2018, the weather was sunny, not too warm and without precipitation making the manual measurements comparable.~~ The automatic stations around Davos (Figure 1~~, Figure 2~~) ~~had lost a maximum~~ measured a decrease in snow depth of 0.04m between these two days at the lowest elevation station Davos Flüelastrasse (5DF~~) at an altitude of~~, 1560 m a.s.l.). For each snow probing location, the snow depth was measured plumb ~~vertical~~ with an avalanche probe at each corner and in the middle of a 1 ~~x~~× 1 m square. The position of the square center was recorded with a ~~differential~~ DGNSS (Trimble Geo XH 6000). As manual snow probe measurements are only possible in terrain safe from avalanches, 15 fixed snow poles were installed throughout the Schürlialp area in summer (see Figure 2~~Figure 3~~). The snow depths values were read off the poles with ~~the help of~~ binoculars or zoomed photos. The snow poles ~~had~~ were marked every half meter ~~marked~~ by pointer and red tape at every 0.1~~10c~~ m ~~red tape subdivided the pole further leading to~~allowing a measuring accuracy of ~~around~~ ca. 0.05 ~~c~~m (see Figure 2~~Figure 3~~). We estimate this uncertainty because a small depression often exists around the pole and it is possible that the snow pole is slightly tilted by the snow load. At the time of the campaign, the snow depth could be read from 10 snow poles. The other five poles were not visible due to a lack of contrast against the snow, or ~~previous~~ avalanches that ~~had~~ bent them previously.

Feldfunktion geändert

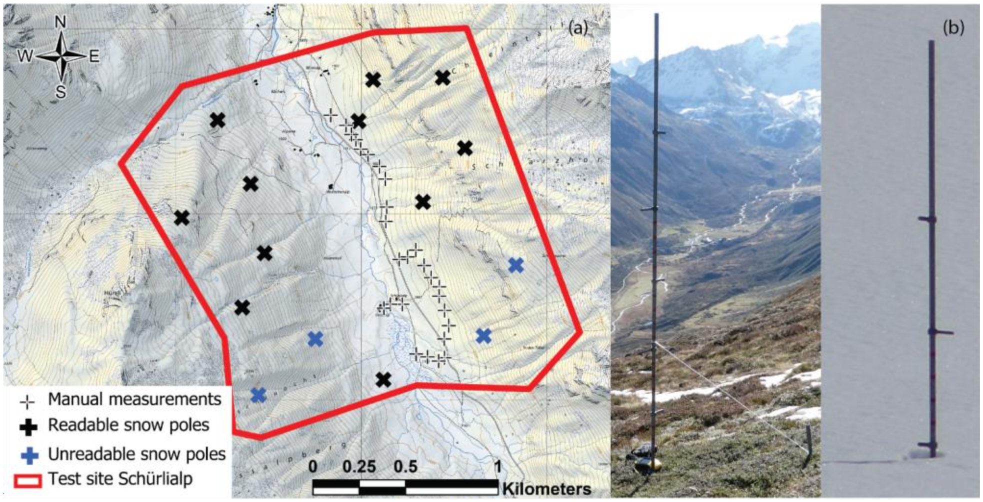

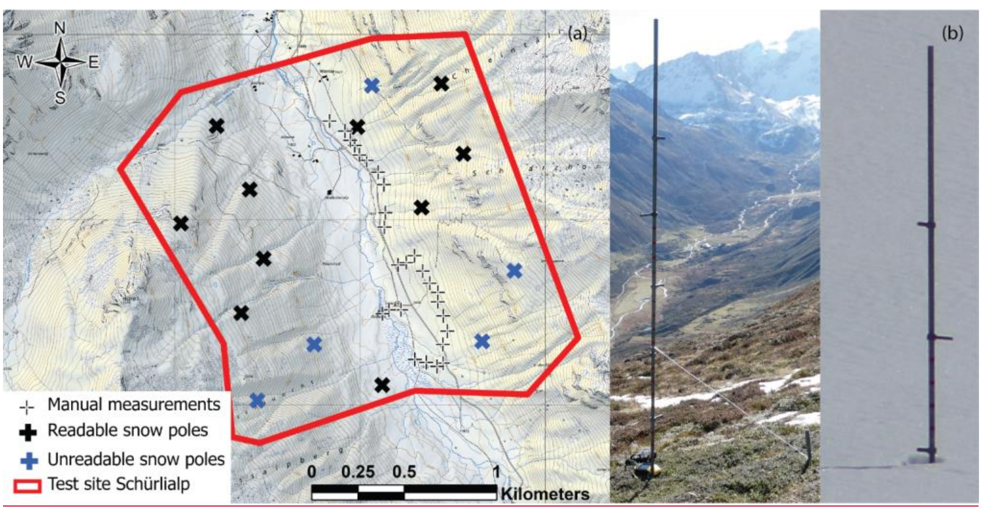

Figure 2~~3~~: ~~Panel~~ (a) shows the distribution of the snow poles and the manual snow measurements on the Schürlialp test site. The snow poles are separated into the readable (black crosses) and unreadable ones (blue crosses). The thin black crosses show the locations of the manual measurements. The two images ~~on panel~~in (b) show a snow pole in summer and winter. The snow poles have a hinge at the foot and are tensioned back with a nylon cord. This way they simply fold down in the event of an avalanche and are not dragged along. (Swiss Map Raster© 2019 swisstopo (5 704 000 000), reproduced by permission of swisstopo (JA100118)).

3.6 Summer reference data sets

Mapping snow depth map requires an accurate snow-free reference surface. For this study two completely snow-free summer DSMs were considered. For the snow depth maps on the Schürlialp test site, an UAS (eBee+ RTK) flight was performed on 27 June 2018 yielding a final DSM with spatial resolution of 0.09 m. For further information about the processing workflow see section 4.4. For producing snow depth maps extending beyond the Schürlialp test site, a DSM with a spatial resolution of 0.5m derived from an airborne laser scan (ALS) of the Dischma valley was used. The flight covered the Dischma valley but not the entire area captured by the satellite and airplane imagery. The ALS flightIt was carried conducted out on 5 and 6 August 2015 by Milan geoservice GmbH with a n ALS of type Riegl LMS-Q 780 scanner. Milan geoservice GmbH delivered an oriented, unclassified point cloud in the reference system LV03 LN02. Ground points classification and DSM generationderivation was done using the software LASlastools (Isenburg, 2014) (ground classification: lasground_new with flags wilderness and ultra_fine).

Feldfunktion geändert

Table 2: Description of the summer data sets used for the calculation of the snow depth maps.

		UAS: eBee+	ALS: LMS-Q 780
Acquisition details	**Acquisition date**	27 June .06.2018	05 August .08.2015 – 06 August .08.2015
	Number of pictures	1449	-
	Covered area	3.66 km^2	100 km^2
	Mean flight height	184 m a.g.l.	2330 m a.g.l.
	Point density	155 points/m^2	11.8 points/m^2 (after postprocessing)
	GSD	0.04 m/pixel	-
	Resolution DSM	0.09 m/pixel	0.5 m/pixel

4 Data processing

Before a photogrammetric snow depth map or an orthoimage can be generated, a DSM must first be produced from the images of each platform. We used the software packages Agisoft Metashape version 1.5.3/1.5.5 (for aAirplane, UAS, ground-basedterrestrial data) and a combination of ERDAS Imagine 2018, Ames Stereo Pipeline (ASP 2.6.2) and GDAL (for satellite data) for photogrammetric triangulation, restitution of DSM, and production of orthoimages from the different platforms. Once DSMs and orthoimages were created as raster datasets, snow depth maps were calculated using ArcGIS Pro version 2.4.2 by subtracting the summer DSM from the winter DSM. The resulting snow depth maps were validated and compared using 2 two different ~~comparison~~ strategies in order to evaluate the performance of the individual platforms and workflows. More specific aspects of data processing and performance evaluation are provided in the following sections.

4.1 Coordinate systems

~~Using~~ Analysing data in the same horizontal coordinate system with the same vertical datum is fundamental for the calculation of snow depth maps. This requires documentation and verification of the coordinate systems and vertical datums used across the processing workflow for each dataset. For example, the geometry of ~~Pléiades~~ the satellite ~~data~~imagery is defined in terms of WGS84 ellipsoid, both for planimetry and elevation (height above ellipsoid, HAE). Other data such as the summer ALS DSM were delivered in the Swiss coordinate system LV03/LN02. All DGNSS data (GCP, ~~eBee+~~UAS) was recorded in RTK mode based on a swipos-GIS/GEO correction stream using the LN02 height system.

Because the conversion from ellipsoidal heights (WGS84) to LN02 is only achieved by means of interpolation, we defined the new swiss height system LHN95 and the local reference system LV95 as the main reference frame for this study. The height system LHN95 (Landeshöhennetz 1995) is derived from geopotential number and provides rigorous orthometric heights with consideration of the Alpine uplift (Schlatter and Marti, 2005). However, because of its official and legal status, most of the data in Switzerland is measured in the LN02 height system. Therefore,~~Since~~ the datasets were provided either on LN02 or on WGS84 and~~,~~ all conversions from LN02 to LHN95 and WGS84 to LHN95 were handled using the REFRAME library provided by swisstopo. REFRAME was used to create conversion grids to accommodate: (i) WGS84 to Bessel ellipsoidal height separation (deterministic calculation); (ii) Bessel to LHN95 separation (CHGEO2004 geoid model), and (iii) LHN95 to LN02 separation (HTRANS).

Feldfunktion geändert

4.2 Satellite data processing workflow

Processing of Pléiades satellite images involved triangulation in ERDAS Imagine 2018, surface restitution in NASA Ames Stereo Pipeline ~~(ASP 2.6.2,)~~ (ASP, Shean et al., 2016; Beyer et al., 2018) version 2.6.2 (https://doi.org/10.5281/zenodo.3247734), and DSM post-processing and production of orthoimage with custom scripts in GDAL 2.4.1. Satellite image triplet bundle block triangulation (BBA) is best performed on WGS84 to ensure unambiguous Rational Polynomial Coefficient (RPC) modelling. The 14 GCPs from the field survey (see section 3) with decimeter accurate coordinates on LV95 and Bessel HAE were converted with REFRAME to UTM32N (ETRS89) and WGS84 HAE. BBA ~~T~~triangulation was completed on the 50-cm resolution panchromatic images with manual input and manual refinements of the 14 GCPs and 32 Tie Points to achieve robust BBA solution. Final quality assessment of the triangulation was derived from Leave-One-Out Cross-Validation (LOOCV) (Sirguey and Cullen, 2014) whereby each GCP is set as a check point in turn~~s~~ to generate an independent residual, yielding 0.43 m CE90 (Circular Error of 90%) and 0.43 m LE90 (Linear Error of 90%).

Feldfunktion geändert

Feldfunktion geändert

Feldfunktion geändert

Dense stereo-matching at full resolution (50 cm) was completed with ASP using a hybrid global-matching approach (Hirschmuller, 2008; d'Angelo, 2016; Beyer et al., 2018). DSMs were produced from a point cloud at 2 m resolution on UTM32N/WGS84, reprojected to LV95 with GDAL (cubic convolution) and height adjusted to LHN95 using conversion grids mentioned in section 4.1. Maps of ray-intersection errors from stereo-matching with ASP measure the minimal distance between rays for pairwise stereo, and are indicative of the quality of the match. ~~In tri-stereo configuration, maps of intersection errors are used to weight the contribution of pairwise DSMs into a blended DSM with GDAL~~ In tri-stereo configuration, we generated a DSM and map of ray intersection error for each stereo-pair. We blended DSMs with GDAL using a weighted arithmetic mean, whereby the elevation from each constituent DSM was weighted by its corresponding ray intersection error (Sirguey and Lewis, 2019). A map of standard error of the weighted mean was generated by uncertainty propagation. The relatively small B/H ratio of the pair P23 resulted in significantly higher noise that compromised the tri-stereo blending. Alternatively, blending only ~~both~~ DSM members P12 and P13 provided a better surface, with noise comparable or better than the bi-stereo with the largest B/H ratio (P13). P23 was only used to fill gaps remaining from the two-members blending. The final DSM was used to orthorectify each of the three images, and the three pan-sharpened orthoimages were then blended together to create a single final orthoimage. ~~Finally~~Finally, the ~~ray-intersection error~~ map of standard error for the blended DSM was used to set all cells of the DSM to no data where the ray intersection error was~~is~~ greater than one panchromatic pixel ~~or~~ (0.5 m) as larger errors were found to ~~be~~ often be indicative of erroneous stereo-matching

Despite the robust survey quality indicated by LOOCV, a remaining 27.5 arcsec tilt (66.7 ppm, or ±1m over 15km) along the northwest-southeast axis of the imagery was detected in the blended DSM after differencing with the summer ALS DSM. To correct the tilt, points were manually placed along snow-free roads in the imagery, and spot elevations were extracted from the blended DSM and ALS surfaces. The distribution of offsets along roads in the city and inside the valley revealed enough linearity to justify the fitting of a plane in 3D space. This hyperplane was fit via least-squares through the residuals ~~A hyperplane was fit through the residuals~~ to create a corrective grid covering the imagery footprint which was used to adjust the blended DSM. ~~Finally, the ray-intersection error map for the blended DSM was used to set all cells of the DSM to no data where the ray intersection error is greater than one panchromatic pixel or 0.5 m as larger errors were found to be often indicative of erroneous stereo-matching~~

4.3 Airplane data processing workflow

The Ultracam images are distinguished by a ~~their~~ high dynamic range ~~of a~~ (14-bit radiometric resolution). ~~There are different software solutions provided to process such images but we decided to use~~ We used Agisoft Metashape for image processing. ~~Agisoft Metashape is used for~~which can be applied for images acquired with frame sensors of RGB or multispectral type (Westoby et al., 2012)~~.~~ ~~Agisoft Metashape supports also the high dynamic range associated with the~~ and supports up to 1~~4~~6 bits radiometric ~~resolution of the Ultracam images~~. Since the southern part of the Dischma valley was cloud-covered, the ~~Ultracam~~ images were manually sorted into cloud-free and cloud-covered images. ~~As t~~The ~~Ultracam~~ camera positions ~~were~~

Feldfunktion geändert
Feldfunktion geändert
Feldfunktion geändert
Feldfunktion geändert
Feldfunktion geändert

delivered in the height system LN02~~, the coordinates of the positions had to be~~ were converted into LHN95 with REFRAME for input into Agisoft Metashape. The use of the CHGeo2004 geoid model in Agisoft Metashape then allows for consistent processing in the vertical height system LHN95.

~~After sorting, t~~The images were imported into Agisoft Metashape and aligned. The Ultracam is a professional photogrammetric camera that has been accurately calibrated by the vendor so that a refinement of the internal camera parameters by Agisoft are not desirable. Therefore ~~B~~before alignment, the camera parameters were fixed in Agisoft Metashape to a focal length of 122.7 mm and 0.004 mm ~~x~~× 0.004 mm pixel sizes (see Table 1). All the other camera model parameters (cx, cy, b1, b2, k1, k2, k3, k4, p1, p2, see Agisoft LLC, 2019 for more information about the frame camera model) were fixed to 0 according the calibration report of the camera. ~~The Ultracam is a professional photogrammetric camera that has been accurately calibrated by the vendor so that a refinement of the internal camera parameters by Agisoft are not desirable.~~ To improve the geolocation accuracy after alignment, 29 GCPs distributed over the Dischma valley were imported into Agisoft. Fifteen CPs were used to control the geolocation accuracy (see section 3 for more information about GCP and CP). The CPs resulted in a RMSE value of 0.14 m for the XY coordinates and a RMSE value of 0.19 m for the Z~~ coordinates (see for exact definition of the RMSE)~~. After alignment and refinement of the geolocation accuracy, the dense point cloud was~~ built~~ produced with the depth filtering method “aggressive”. The filtering method “aggressive” gives, in our experience, the best results for snow-covered surfaces and filters out most outliers, leading to cleaner surface models. The DSM was~~ made~~ generated from the dense point cloud at a 0.11 m/pixel resolution without interpolating voids. Finally, an orthoimage at a resolution of 0.5 m/pixel was created based on the DSM.

Feldfunktion geändert

4.4 UAS processing workflow

~~We processed the eBee+ data using integrated sensor orientation (ISO) without GCPs and using only CPs to assess the accuracy of the DSM. SenseFly, the manufacturer of the eBee+, claims that the eBee+ can achieve accuracies in order 0.03 m horizontal and 0.05 m vertical (level of accuracy of 1-3 x GSD) using this method (). proved a RMSE of 0.02 - 0.03 m for the horizontal coordinates of checkpoints and a RMSE of 0.02 – 0.1 m for the vertical coordinates of CPs for a flight with RTK solution but without GCPs.~~

The eBee+ RTK has an IMU on board for flight control for which the accuracy and calibration are not given by the manufacturer. Therefore, we have processed the imagery in Agisoft Metashape without IMU but with the DGNSS data only. Since the mount point applied the corrections for the Swiss coordinate system LV95 LN02 during the flight, the camera positions of the eBee+ had to be transformed into the vertical coordinate system LHN95 before processing could take place. This was done by first exporting the camera position of the eBee+ images stored in EXIF metadata~~ Exif~~ to a text file~~. This text file served~~ used as input for REFRAME to convert the positions into ~~the correct vertical coordinate system~~ LHN95~~. The transformed positions were then imported back into~~ for use in Agisoft Metashape~~ to overwrite the old camera positions~~. Again, the use of the CHGeo2004 geoid model in Agisoft Metashape allowed for consistent processing in the vertical height system LHN95. The images were then aligned. and georeferenced without GCPs and using only CPs to assess the accuracy of the triangulation. SenseFly, the manufacturer of the eBee+, claims that this approach of integrated sensor orientation (ISO) can achieve accuracies in order 0.03 m horizontal and 0.05 m vertical (level of accuracy of 1 to 3 × GSD) (Benassi et al., 2017; Roze et al., 2017). Benassi et al. (2017) showed a RMSE value of 0.02 to 0.03 m for the horizonal coordinates of checkpoints and a RMSE value of 0.02 to 0.1 m for the vertical coordinates of CPs for a flight with RTK solution but without GCPs. We assessed the model accuracy using six of the signaled CPs on the Schürlialp test site, resulting in total RMSE values for XY and Z coordinates of 0.05 m and 0.1 m respectively. A dense point cloud was produced with the filtering mode “aggressive”. Finally, the DSM was created with a resolution of 0.09 m/pixel withoutwith no interpolation which was used to produce an. An orthoimage was produced with a resolution ofat 0.04 m/pixel using the DSM.. We checked accuracy using six of the signaled CPs on the Schürlialp test site. They resulted in a total RMSE for the XY coordinates of 0.05 m and a total RMSE for the Z coordinates of 0.1 m.

Feldfunktion geändert

Feldfunktion geändert

Feldfunktion geändert

Formatiert: Englisch (Vereinigtes Königreich)

The summer eBee+ flight was processed with the same workflow as the winter eBee+ flight. This resulted in a DSM with a resolution of 0.09 m/pixel and an orthoimage of 0.04 m/pixel. For the summer eBee+ flight sSix CPs markers were signaled on the ground for the summer eBee+ survey and measured with a Stonex S800 receiver and S4II Win Mobile 6.5 controller providing accuracy for the horizontal position between 0.014 m to 0.022 m and a vertical position accuracy of 0.02 m. The RMSE of the CPsPhotogrammetric modeling in Agisoft resulted in a RMSE values for the XY position and Z of 0.02 m and a RMSE of and 0.05 m, respectively. for the Z coordinate.

Formatiert: Englisch (Vereinigtes Königreich)

4.5 Ground-basedTerrestrial processing workflow

Ground-basedTerrestrial snow depth mapping is a compromise between measurement requirements and time. Therefore, due to the avalanche situation and the logistical effort that would have been necessary, no control points could be distributed over the area during the recordingdata capture. Furthermore, tThe GCPs/CPs used for the Pléiadessatellite, Ultracam airplane and eBee+UAS are not visible on the ground-basedterrestrial images. Only the camera positions were measured with a DdGNSS (see section 3.4) during recording. However, with this method it was not possible this did not allow to determine the precise offset between the DGNSS antenna phase and the principal point ofexact center of the camera. For this reason, the measurement accuracy of the camera position when input into used in Agisoft Metashape was set to 0.2 m.

To refine the georeferencing of the ground-basedterrestrial images, features such as stones, bushes and house corners emerging from the snow were detected manually on the ground-basedterrestrial images to serve as GCP. The features of nine GCPs were then identified on the eBee+orthoimage and DSM products from the UAS summer surveyflight and from which their coordinates were extracted. Nine GCPs were identified with this approach. For this comparison we did not use CPs, because

~~the model was aligned to the eBee+ summer DSM. To process ground-based images with our acquisition setting, it was necessary to define camera stations for each acquisition location in Agisoft Metashape.~~ The images were therefore sorted into the five camera stations in Agisoft Metashape, aligned and georeferenced with GCPs.~~. Using the previously defined GCPs, the images were aligned and the geolocation accuracy was refined.~~ Again, the dense point cloud was created with the “aggressive” filter~~ mode "aggressive"~~ and a~~. Finally, a~~ DSM and ortho image produced at ~~with a resolution of~~ 0.11 m/pixel ~~was calculated~~ and ~~an ortho image with a resolution of~~ 0.06 m/pixel, respectively ~~was created~~.

4.6 Snow depth map validation and comparison strategies

Three comparison strategies were developed to compare the photogrammetric data and investigate the performance of the different platforms (see Figure 3~~Figure 4~~). Comparison 1 aims to validate the snow depth maps for the Schürlialp test site using the manual and snow pole measurements (described in detail in section 4.6.1). Comparison 2 compares the different snow depth maps with the spatially dense ~~eBee+~~UAS snow depth map used as ~~ground truth~~spatial reference (described in detail in section 4.6.2). The ~~eBee+~~UAS summer reference is used for calculating the snow depth maps of comparison 1 and comparison 2. Finally, in comparison 3,~~ to show the potential of measuring snow depth distribution over larger areas,~~ snow depth maps of ~~the Pléiades~~ satellite and ~~the Ultracam~~airplane imagery are calculated and compared with the ALS summer scan (described in section 4.6.3) to show the potential of measuring snow depth distribution over larger areas. Section 4.6.4 describes the accuracy measures used within this paper.

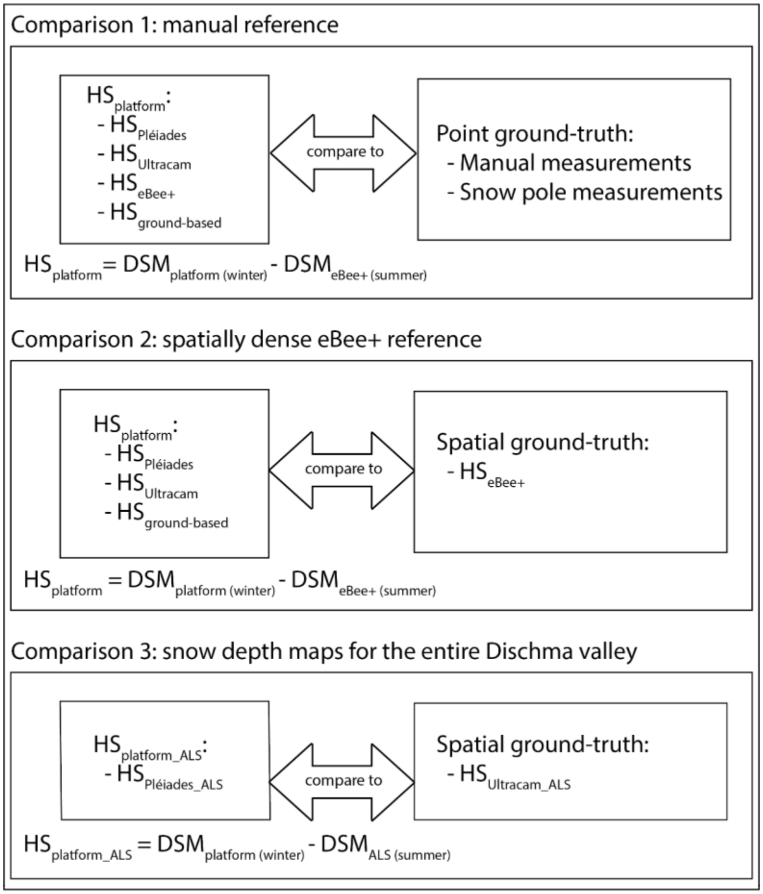
Comparison 1: manual reference
HSplatform:
- HSPléiades
- HSUltracam
- HSeBee+
- HSground-based
compare to
Point ground-truth:
- Manual measurements
- Snow pole measurements
HSplatform = DSMplatform (winter) - DSMeBee+ (summer)
Comparison 2: spatially dense eBee+ reference
HSplatform:
- HSPléiades
- HSUltracam
- HSground-based
compare to
Spatial ground-truth:
- HSeBee+
HSplatform = DSMplatform (winter) - DSMeBee+ (summer)
Comparison 3: snow depth maps for the entire Dischma valley
HSplatform_ALS:
- HSPléiades_ALS
compare to
Spatial ground-truth:
- HSUltracam_ALS
HSplatform_ALS = DSMplatform (winter) - DSMALS (summer)

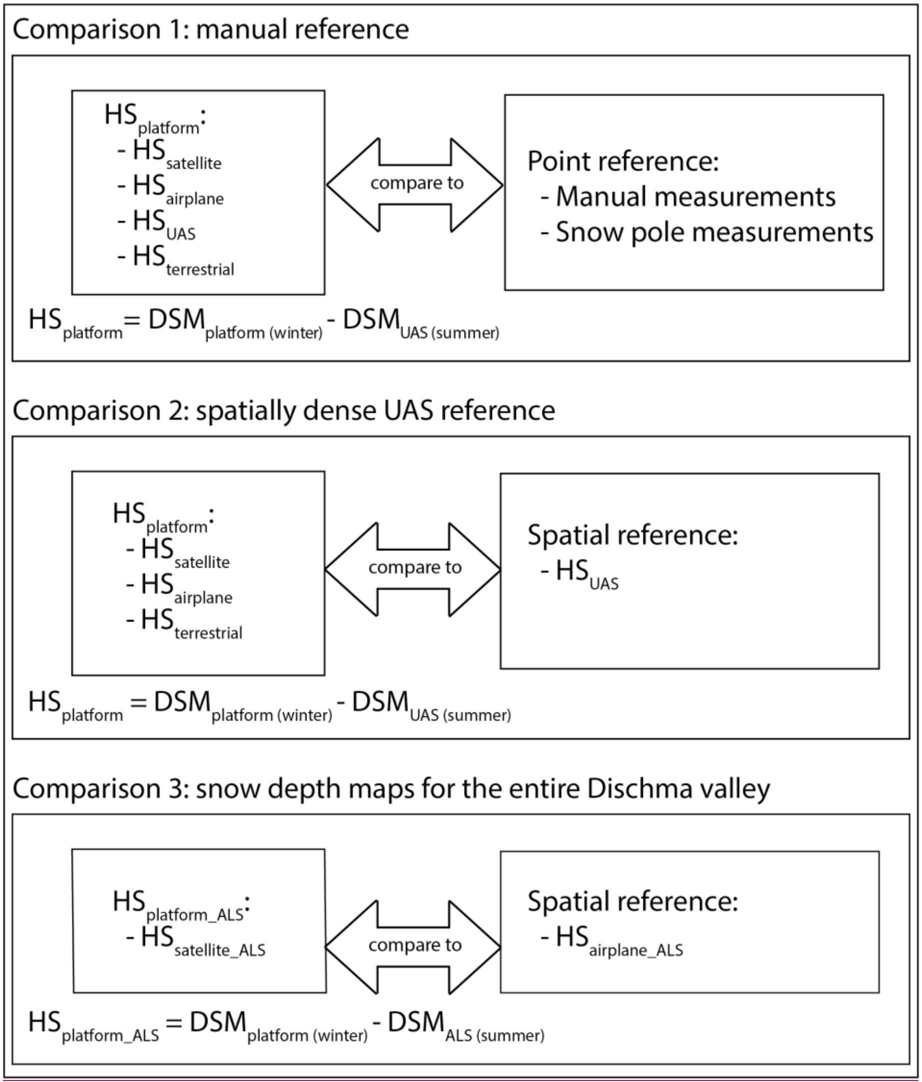

Figure 34: Flowchart illustrating the three comparisons strategies. With $HS_{platform}$ we refer to the snow depth map of the respective platform. $HS_{platform\_ALS}$ is the snow depth map of the respective platform calculated with the ALS summer DSM.

Formatiert: Tiefgestellt

Formatiert: Tiefgestellt

4.6.1 Comparison 1: manual reference

For comparison 1 only the Schürlialp (3.59 km^2) test site was considered. This ~~allowed us~~provided a detailed comparison of each platform's accuracy against ~~to investigate accurately the performance of the individual platforms by comparing them with~~ the manual measurements and the snow poles measurements ~~(manual ground truth)~~. The snow depth maps are calculated with the ~~eBee+~~UAS summer DSM of 27 June 2018. To keep interpolation errors as low as possible, the Winter DSMs were exported at their highest ~~resulting~~native spatial resolution: ~~Pléiades~~ Satellite DSM 2 m~~/pixel~~, ~~Ultracam~~ airplane DSM 0.11 m~~/pixel~~, ~~eBee+~~UAS DSM 0.09 m~~/pixel~~ and ~~ground-based~~terrestrial DSM 0.11 m~~/pixel~~. ~~For the calculation of~~Prior to generating the snow depth maps ~~by subtracting grids~~, ~~it is important that~~ the summer and winter DSMs ~~have not only the same cell size, but also identically aligned grid cells~~ were made coincident (equal size and winter DSM snapped to summer DSM). ~~Therefore, to ensure that the cells were completely congruent, the eBee+ summer DSM was exported in Agisoft Metashape with the same cell size as the winter DSM of each platform, and each winter DSM was then aligned to the later via resampling with cubic convolution in Arcgis Pro.~~ The summer DSM was then subtracted from the winter DSM resulting in the corresponding platform snow depth map. Finally, to compare the snow depth maps ~~of the~~ from each ~~different~~ platform~~s~~ with the manual reference measurements~~ground truth~~, a buffer with a radius of 0.7 m (i.e. the half-diagonal of the 1 m ~~x~~× 1 m sample square) was created from the center position of the manual ~~ground truth~~measurement. For each snow depth map, the mean value and the standard deviation were calculated within this buffer area. Because the selected buffer has a smaller area than the resolution of the satellite~~Pléiades~~ data, the cell value was extracted at the position of the snow depth measurements and the snow poles for this data. In section 4.6.4 further details of the accuracy and precision measures calculated are defined.

4.6.2 Comparison 2: spatially dense ~~eBee+~~UAS reference

The high accuracy of UAS data for snow depth mapping has been successfully tested in various studies (Vander Jagt et al., 2015; Bühler et al., 2016; De Michele et al., 2016; Harder et al., 2016; Cimoli et al., 2017; Redpath et al., 2018; Avanzi et al., 2018; Eker et al., 2019). With comparison 2, we compare the spatially continuous snow depth map of the UAS~~eBee+~~ with the snow depth maps of the other three platforms. Therefore, the winter and summer DSM of the ~~eBee+~~UAS were exported from Agisoft Metashape at a spatial resolution of 0.11m~~/pixel~~ (for ~~ground-based~~terrestrial and ~~Ultracam~~ airplane comparison) and 2 m~~/pixel~~ (for ~~Pléiades~~ satellite comparison). These DSMs ~~are~~ were then aligned to the snow depth maps ~~to be~~ used in the comparison ~~compared~~ via cubic convolution resampling. Finally, the winter DSMs ~~are~~were ~~again~~ subtracted from the summer DSMs resulting in three snow depth maps with that from~~of~~ the ~~eBee+~~UAS used as ~~ground truth~~reference for comparison 2. With these snow depth maps the metrics and plots described in section 4.6.4 were~~are~~ calculated.

Feldfunktion geändert
Feldfunktion geändert
Feldfunktion geändert
Feldfunktion geändert
Feldfunktion geändert
Feldfunktion geändert
Feldfunktion geändert
Feldfunktion geändert

4.6.3 Comparison 3: Snow depth maps of the entire Dischma valley

The summer ALS scan covers ~~the entire Dischma valley,~~ a much larger area (100 km^2) compared with~~than~~ the ~~eBee+~~UAS summer flight. ~~Therefore, w~~We calculated the snow depth maps from ~~of~~ the ~~Pléiades~~ satellite and the ~~Ultracam~~ airplane ~~data~~

Formatiert: Hochgestellt

imagery using the summer ALS scan. We re-exported the Ultracam airplane DSM at in a 2 m resolution withfrom Agisoft Metashape. With the cubic convolution resampling function, wWe aligned the Pléiades satellite and the Ultracam airplane DSM to the ALS DSM and subtracted the summer ALS DSM from each Winter DSM with cubic convolution resampling. To compare at a larger scale snow depth measurements over a much larger area, we usednow use the Ultracam airplane snow depth map as ground trutha reference to calculate the accuracy and precision of the satellite mapmeasures described in section 4.6.4..

4.6.4 Accuracy and precision measures

For the evaluationWe evaluated of the snow depth maps according in to the different comparisons using, a selection of accuracy and precision measures is calculated (see Table 3). Accuracy defines how close an estimated value is to a standard or accepted value of a given quantity (). Precision (dispersion) on the other handside is a measure describes for how close measurements agree with each other despite a possible systematic bias (). The root mean square error (RMSE) is a common measure of accuracy. and tThe standard deviation (STD) is a common measure of precision and measures the dispersion of the data in relation to the mean (Maune and Naygandhi, 2018). To detect systematic vertical offsets of the snow depth maps, the mean bias error (MBE) and the Median of the bias errors (MABEMdBE) were calculated. The MABEMdBE is less sensitive to outliers than the MBE and the difference between the two measures gives an indication of the role of outliers in the metrics. whether large outliers are present. Similarly, the normalized median absolute deviation (NMAD) is a measure of precision that A more robust measure to outliers than the STD is the normalized median absolute deviation (NMAD) (Höhle and Höhle, 2009).

Boxplots and normalized histograms were calculated for the first two comparison strategies Tto illustrate the accuracy measuresassessment by graphical means. boxplots were calculated for the first two comparison strategies. The boxplot summarizes the statistical measures of the median, quartilesquantile, span and interquartilentile distance in one graph and allowsthat supports a graphical interpretation of the dataresults. For the histogram the values were normalized and the y-axes shows the relative frequency of the values. We decided to also considered a cleaned filtered version of the errors of each platform comparison whereby errors greater than 2*STD were classified as outliers and removed. There are different methods described in literature to remove outliers, one is to remove data in excess of 3*STD (Höhle and Höhle, 2009; Novac, 2018). We prefer to be more rigorous more liberal and exclude (almost) all outliers, so wefiltered the data only with a threshold of used 2*STD where, for normal distribution. In case of a normal distribution 95.45% of all measured the values can be would be found in the interval of plus-minus 2*STD. With the cleaned data. We also filter out only the largest outliers and are close to the original product. Tthe accuracy and precision measures as well as the boxplot and histogram were calculated again with the filtered data. The boxplot of the cleaned data should serve mainly as control and should have smaller whiskers and boxes than the boxplot of the raw data. Additionally, we calculated generated scatterplots for comparison 2 and comparison 3 to illustrate the dispersion between the in snow depth from satellite, airplane and terrestrial, maps compared to the reference from

Feldfunktion geändert

Feldfunktion geändert

Feldfunktion geändert

Feldfunktion geändert

UAS, as well as~~ snow depth map (eBee+ snow depth map for comparison 2 and Ultracam snow depth map for comparison 3). We~~ calculated the Pearson correlation coefficient (R^2)~~ to evaluate the relationship between the reference snow depth and the model snow depth~~. To analyze only the per-pixel value correlation of the snow depth maps in the positive realistic range we calculate a second scatterplot where all negative values and values higher than a maximum snow depth (5 m defined by expert opinion and based on the snow depth distribution) of the reference snow depth map are deleted and the Pearson correlation coefficient (R^2) is calculated again. This gives us an indication of how the snow depth maps correlate in the positive and most relevant range for most modelling purposes.

Table 3: Accuracy and precision measures adapted from Höhle and Höhle, 2009.

ΔHS_j: error of the snow depth at location *j* HS_j^{ref}: reference snow depth at location *j* HS_j^{model}: model snow depth at location *j*	$\Delta HS_j = HS_j^{\text{model}} - HS_j^{\text{ref}}$
Root mean square error (RMSE)	$RMSE^{\text{model}} = \sqrt{\frac{1}{n}\sum_{j=1}^{n}\Delta HS_j^{\,2}}$
Mean bias error (MBE)	$\hat{\mu}^{\text{model}} = \frac{1}{n}\sum_{j=1}^{n}\Delta HS_j$
Standard deviation (STD)	$\hat{\sigma}^{\text{model}} = \sqrt{\frac{1}{(n-1)}\sum_{j=1}^{n}(\Delta HS_j - \hat{\mu})^2}$
Median of the bias errors (~~MABE~~MdBE, 50% quantile)	$m_{BE}^{\text{model}} = median(\Delta HS)$
Normalized Median Absolute Deviation (NMAD)	$NMAD^{\text{model}} = 1.4826 * median(\lvert \Delta HS_j - m_{BE} \rvert)$
Threshold for ~~detecting outliers~~classifying outliers	$\lvert \Delta HS_j \rvert > 2 * \hat{\sigma}^{\text{model}}$

5 Results

The~~ largest area of~~ satellite imagery covered 140 km^2~~ was covered by the Pléiades satellite~~, the ~~Ultracam flight~~airplane imagery ~~covered a surface of~~ 75.7 km^2 in the northern part of the Dischma valley, the ~~eBee+~~UAS imagery ~~a surface of~~ 3.59 km^2 around Schürlialp and finally the ~~ground-based~~terrestrial ~~data~~ images covered the smallest ~~surface~~area of 1.12 km^2.The orthoimages in Figure 4~~Figure 5~~ show~~s the orthoimages and thus the extent of the area~~ the footprint covered by each platform. ~~The red polygon indicates the extent of the Schürlialp test site on each orthoimage.~~ The orthoimages of both~~the~~ ~~Pleiades~~ satellite and UAS ~~is~~are cloud-free, while ~~completely cloudless in contrast to~~ the orthoimage of the ~~Ultracam~~airplane~~ which~~ only covers the

Formatiert: Hochgestellt

Feldfunktion geändert

northern part of the Dischma~~tal~~ valley because of clouds. ~~The orthoimage of the eBee+ illustrates the good quality of the eBee+ flight. Finally, t~~The orthoimage of the ~~ground-based~~terrestrial imagery reveals ~~the problem of~~ the suboptimal recording geometry and large terrain occlusions.

The following subsections will present the results in detail according to the comparison strategies described in section 4.6. Section 5.1 shows the results of the comparison 1. Section 5.2 continues with the results of comparison 2. Finally, in section 5.3 the snow depth maps of the entire Dischma valley are illustrated.

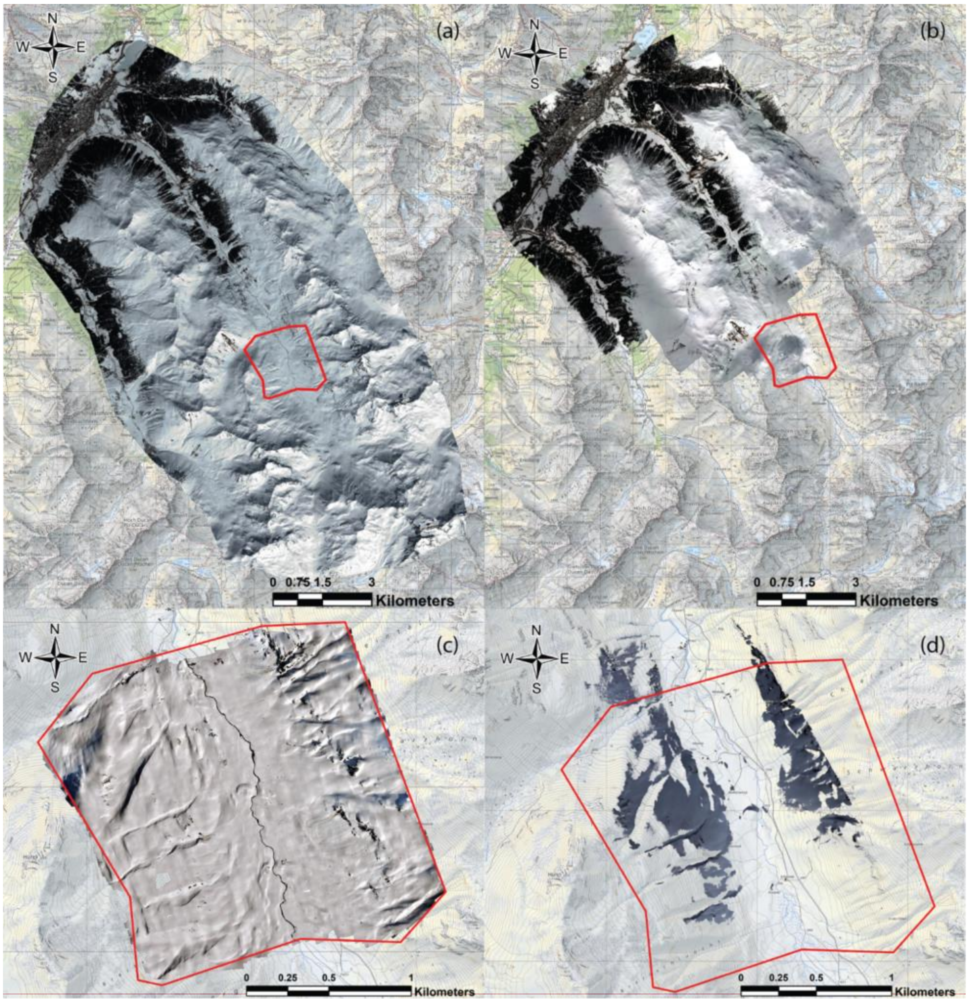
(a)
(b)
(c)
(d)
N
W
E
S
0 0.75 1.5 3
Kilometers
0 0.25 0.5 1
Kilometers

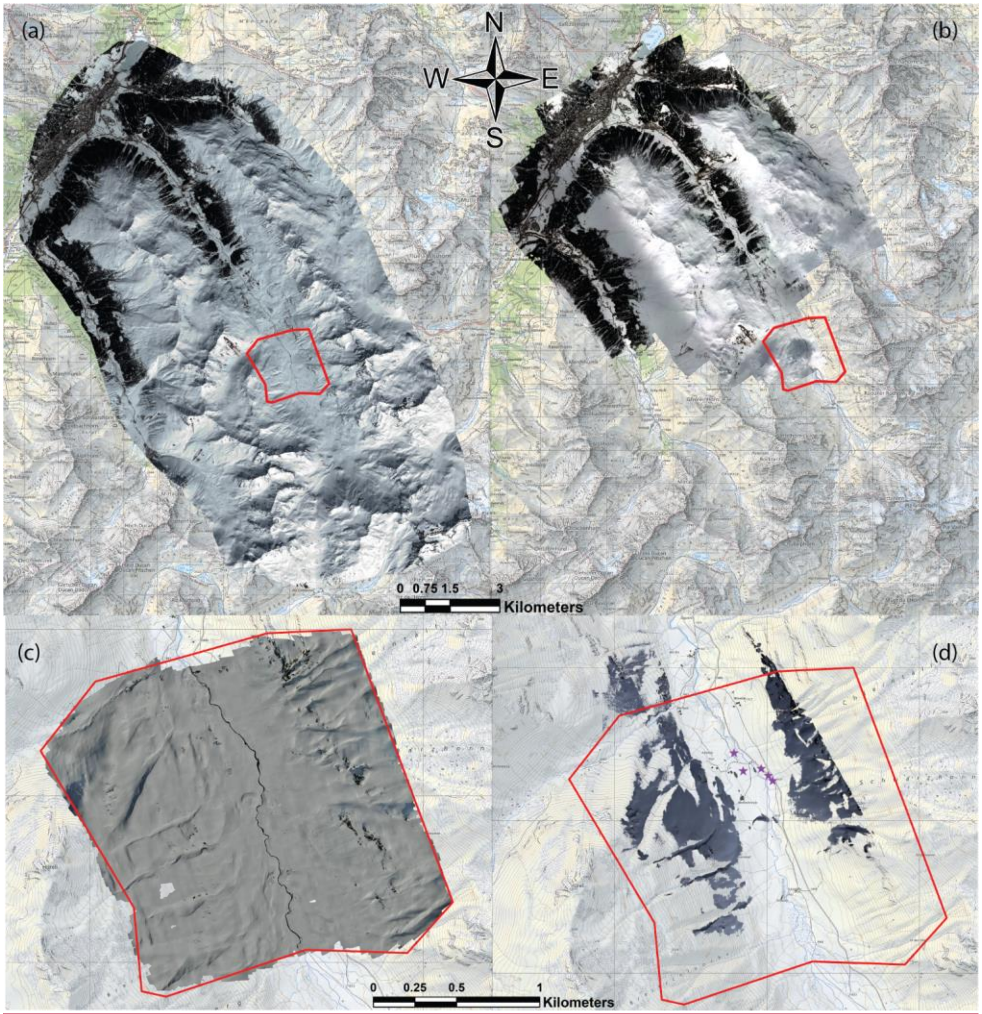

Figure ~~4~~5: ~~Panel~~ (a) orthoimage of the satellite~~Pléiades~~ data, ~~panel~~ (b) orthoimage of the ~~Ultracam~~ airplane data. The area recorded by the ~~Ultracam~~ airplane is theoretically larger than the area recorded by the satellites, but due to the clouds only part of the images could be used for producing DSM and orthoimage. ~~Panel~~ (c) the orthoimage of the ~~eBee+~~UAS data and ~~panel~~ (d) orthoimage of the ~~ground-based~~terrestrial data. The red polygon in ~~panel~~ (a), (b), (c) and (d) indicates the Schürlialp site test. The violet stars in ~~panel~~

(d) indicate the five camera positions of the ground-basedterrestrial recordings. (Swiss Map Raster© 2019 swisstopo (5 704 000 000), reproduced by permission of swisstopo (JA100118), Pléiades data© CNES 2018, Distribution Airbus DS).

5.1 Results of comparison 1: manual reference

Using the workflows described in the section 4.6.1, a snow depth map was calculated for each platform. The snow depth maps are shown in Figure 5Figure 6 and an extract of them a zoomed inset in Figure 6Figure 7. When comparing the maps graphically, aAll four maps show similar snow depth distribution patterns, including characteristic snow features such as wind deposits.. Figure 6 illustrates how vegetation (here the bush species *alnus alnobetula)* can influence the snow depth when using a DSM as summer reference. Also, the histogram in Figure 8 illustrates the similar snow depth distribution between the different platforms. The fact that the manual and snow pole measurements do not show negative values in the histogram is due to the measurement method. Negative values for manual and snow pole measurements are gross human errors and can be excluded. However, negative values exist on photogrammetric snow depth maps due to vegetation (Figure 7) but also photogrammetric processing. The negative values due to vegetation result from the fact that our summer reference for the calculation of snow depth maps is a DSM. Since some vegetation is pressed down by the snow load in winter, lower or even negative snow depths result. have also identified this effect. investigated in field studies on how much vegetation can be pushed down by the snow load. Depending on the vegetation type the difference between the summer height and the height below snow was between 10 and 20cm. They examined only certain vegetation types, namely long grass, short grass and dwarf shrubs. So other alpine vegetation types as green alder (*alnus alnobetula*) are missing. *Alnus alnobetula* is a vegetation type present at different places on the Schürlialp test site. It is pressed down by the snow and negative snow depth spots are visible on the snow depth maps (Figure 7, violet negative patterns visible on every snow depth map).

The Pleiades satellite data snow depths have the largest dispersion (STD = 0.77 m and NMAD = 0.43 m) in comparison to the manual and snow pole measurements. The boxplots and the histograms (Figure 7Figure 9) illustratesillustrate the dispersion as well. The negative MBE (-0.46 m) and negative MABEMdBE (-0.40 m) suggest that the Pléiades satellite snow depth map is systematically lower compared to the manual and fixed snow pole measurements. This is again depicted by the boxplot where almost 75% the error values are below zero. The difference between the STD and NMAD indicates a large outlier and justifies the removal of all values greater than 2*STD to further characterize errors. Subsequently,After filtering the raw data, the satellite RMSE value is (0.52 m) and the STD is (0.39 m) of the Pleiades data improve significantly. The NMAD has deteriorated by 0.04 m. This improvement can be partially explained by acomes from the fact, that the Pléiades data had one single large outlier (ΔH = -4.47 m) which influenced the NMAD the other way around. Removed with the filter. The Pleiades satellite snow depth map however remains negatively biased at the location of manual and snow pole measurements. It is important to note here the limitation of the triangulation of the Pléiades imagery. Most of the GCPs were collected in summer and only a few could be identified and placed in the images of the Pleiades. Also remains the placement uncertainty of the GCPs due to the resolution of the imagery. The remaining shift was corrected on the basis of points along the roads in three

~~valleys (Sertig valley, Dischma valley, Flüela valley), but without specifically targeting the Schürlialp test site. Thus, the shift does not characterize the technology, but shows the limitation due to triangulation and absolute orientation approach. Also, it should be kept in mind that the Pléiades images are obtained from space and the resolution of the DSM is 2m.~~

The ~~Ultracam~~ airplane returns a RMSE value of 0.20 m and~~,~~ the ~~eBee+~~UAS a RMSE value of 0.21 m.~~. The difference is negligible, i.e., the accuracies can be considered equal (note, for the Ultracam~~ ~~o~~ Only 27 out of 37 measurements could be considered for the airplane~~)~~. ~~Also, t~~The STD of the airplane~~Ultracam~~ and the ~~eBee+~~UAS are the same (STD = 0.20 m). The NMAD (0.17 m) of the ~~Ultracam~~airplane is 0.03 m higher than the one of the ~~eBee+~~UAS (0.14 m) but again the difference is small. The boxplot and the histogram illustrate~~s~~ ~~finally a higher~~greater dispersion of the errors of the ~~Ultracam~~airplane despite the small differences in the accuracy and precision measures compared to the ~~eBee+~~UAS. The MBE (0.03 m) of the ~~Ultracam~~ airplane is slightly positive but ~~MABE~~MdBE (-0.03 m) is negative by the same value. Therefore, we consider this difference of 0.06 m negligible and assume that the ~~Ultracam~~ airplane snow depth map is not biased. This result is also supported by the boxplot for both ~~not cleaned~~raw and ~~cleaned~~ filtered data. By applying the threshold for outliers RMSE, STD and NMAD are found to be equal at 0.17 m for ~~Ultracam~~airplane, and slightly better (0.11 to 0.16 m) for ~~eBee+~~UAS. The MBE (-0.07 m) and ~~MABE~~MdBE (-0.07 m) indicate that the ~~eBee+~~UAS snow depth map has a slight negative bias. ~~The boxplot supports this finding.~~ This is again consistent with Bühler et al., 2016 who found a slight underestimation of snow depth for UAS. Normally it should be the same for the ~~Ultracam~~ airplane but this can be due to the difference in processing ~~workflow~~ as the airplane~~Ultracam~~ was processed with GCPs and the ~~eBee+~~UAS without. However, boxplots, histograms and accuracy measures of ~~cleaned~~filtered versions of the snow depth maps, show that the UAS~~eBee+~~ has the best accuracy compared to manual ~~ground truth~~reference measurement. For the ~~ground-based~~terrestrial snow depth map, only four snow pole measurements could be considered and therefore the statistical statements are not meaningful. For completeness they are nevertheless listed in Table 4.

Feldfunktion geändert

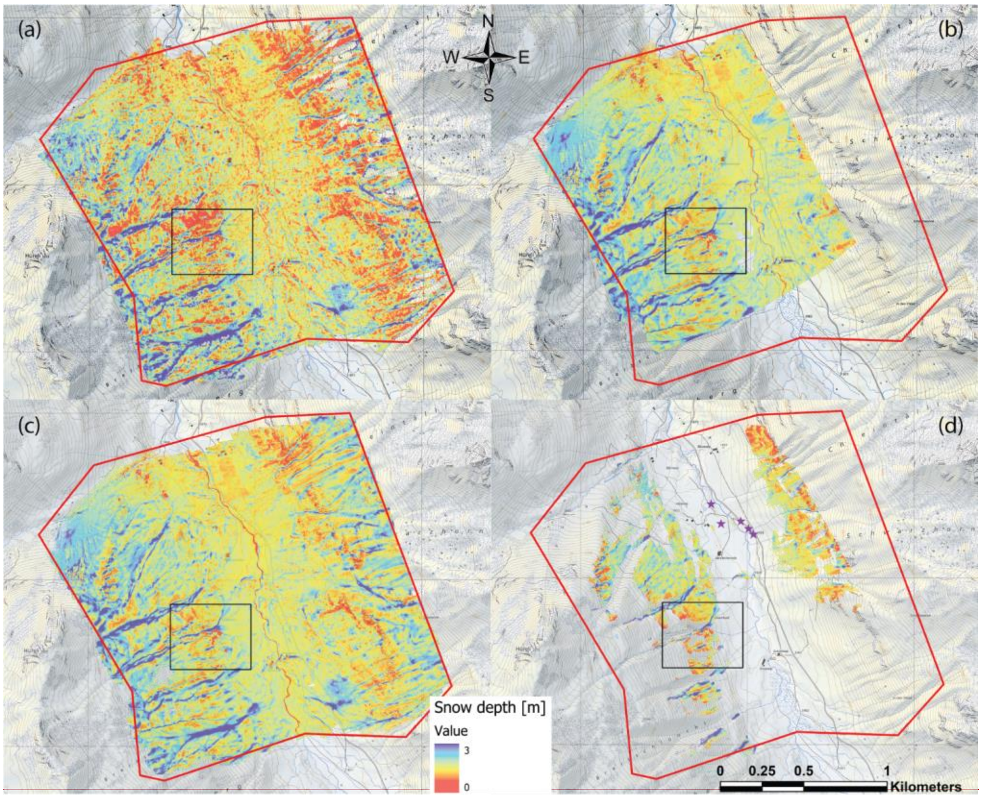

(a)
(b)
(c)
(d)
N
W
E
S
Snow depth [m]
Value
3
0
0
0.25
0.5
1
Kilometers

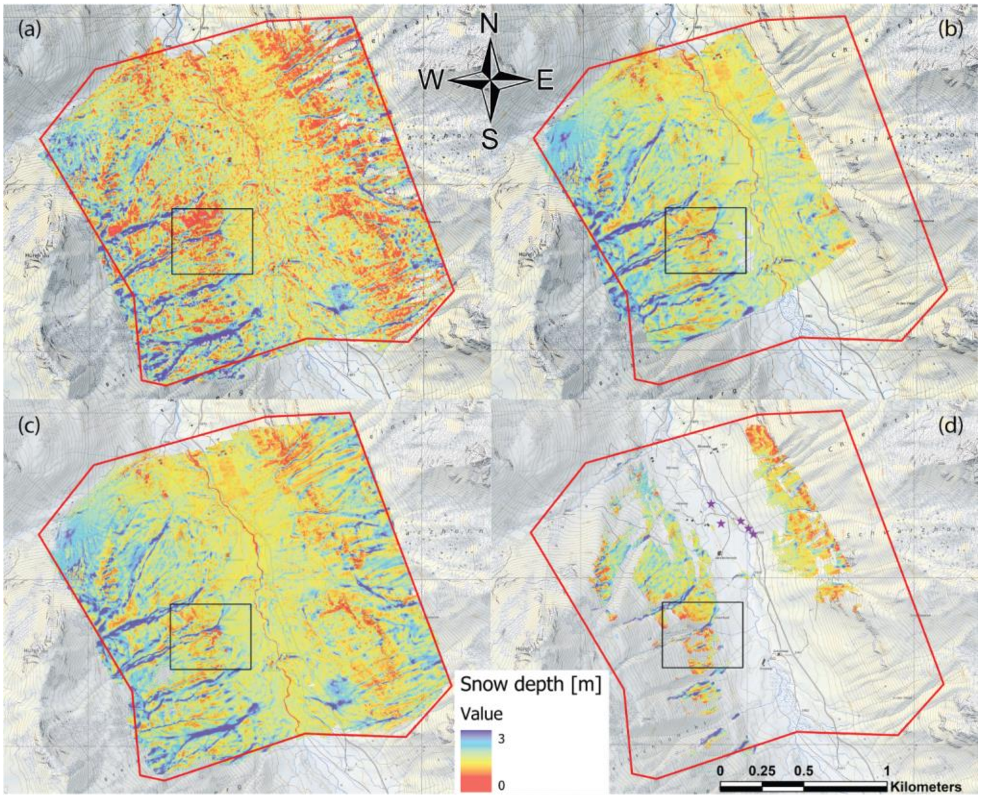

Figure 56: Snow depth maps of the Schürlialp test site from the Pléiades satellite(panel (a)), the Ultracam airplane(panel (b)), the eBee+UAS (panel (c)) and the ground-basedterrestrial data (panel (d)). On the ground-basedterrestrial snow depth map the camera positions are indicated with violet stars. The scale on the snow depth maps ranges from 0 m (red) to 3 m (blue). The red polygon delimitspicts the extent of the Schürlialp test site. The black box polygon indicates the zoomed insetextract shown in Figure 6Figure 7. (Swiss Map Raster© 2019 swisstopo (5 704 000 000), reproduced by permission of swisstopo (JA100118))

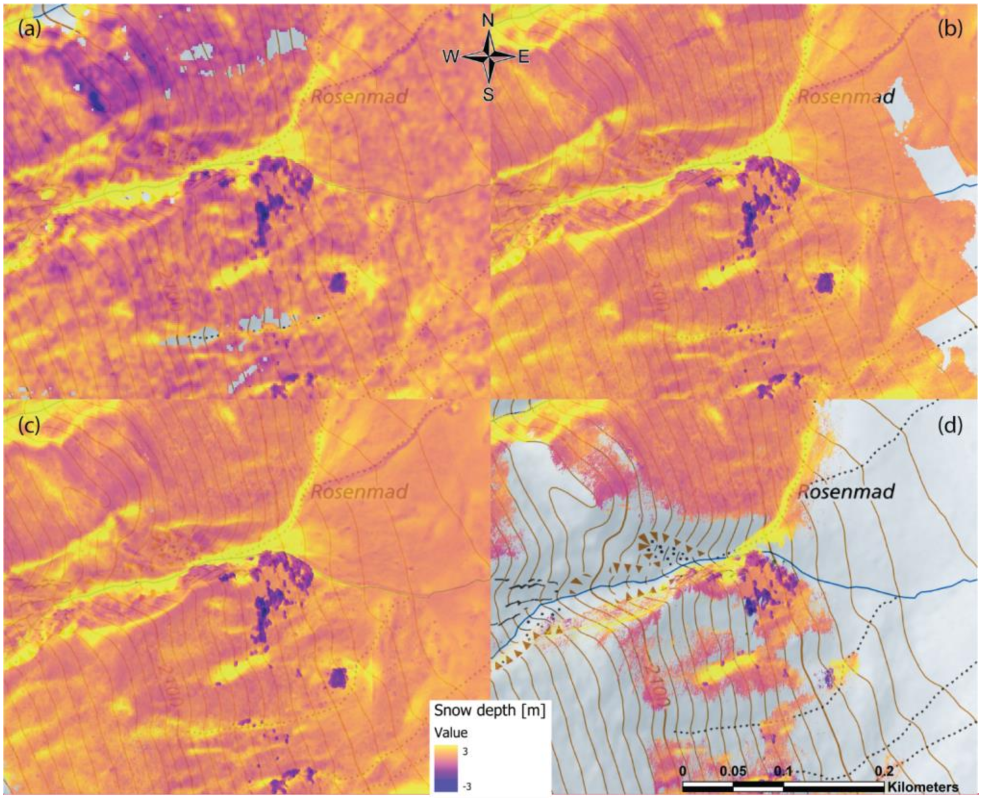

(a)
(b)
(c)
(d)
N
W
E
S
Rosenmad
2100
Snow depth [m]
Value
3
-3
0
0.05
0.1
0.2
Kilometers

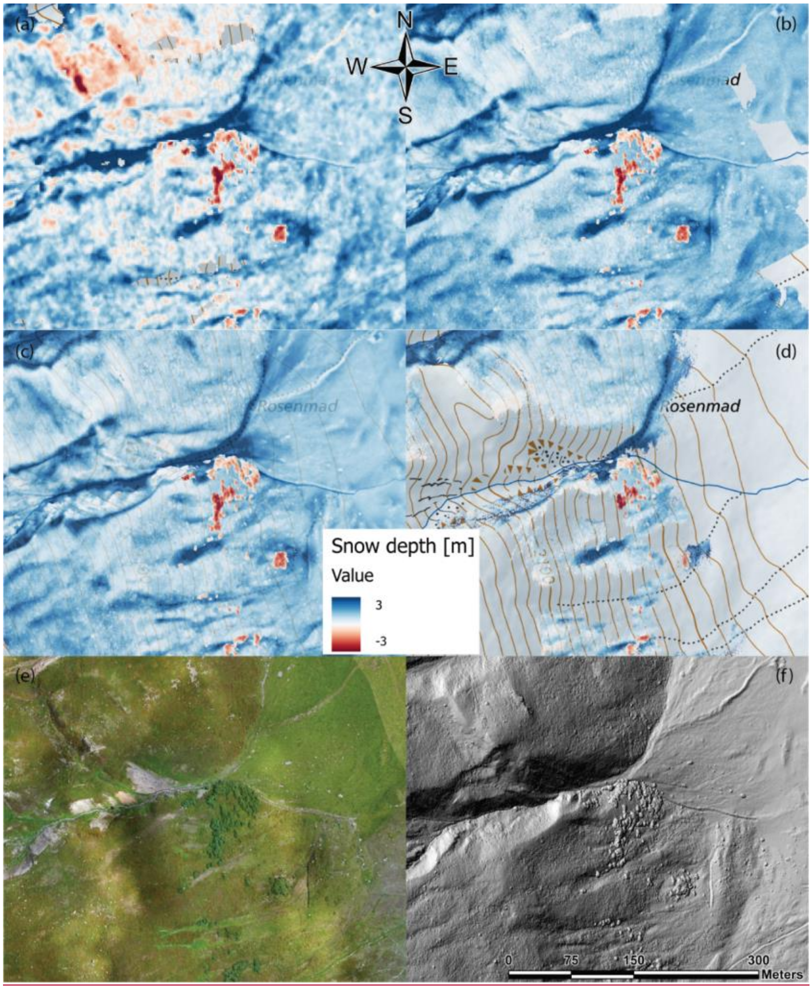

Figure 6~~7~~: Inset ~~Extract~~ of the Schürlialp snow depth maps shown in Figure 5~~Figure 6~~ with the scale ranging from -3 m to 3 m to illustrate the negative snow depths caused by the vegetation. ~~In this extract the dark violet spots are mainly~~The effect of bushes ~~of the (~~species *alnus alnobetula*) under ~~pressed down~~compression by the snow is visible as the greatest negative snow depth values (dark red) in ~~.~~ (a) satellite, (b) airplane, (c) UAS and (d) terrestrial draped over the swisstopo basemap. An orthoimage for the same extent is shown in (e) from the UAS summer flight and, shows a hillshade of the summer ALS scan. Positive snow depth values reach up to 5m in the gulley features in the study site. (Swiss Map Raster© 2019 swisstopo (5 704 000 000), reproduced by permission of swisstopo (JA100118))

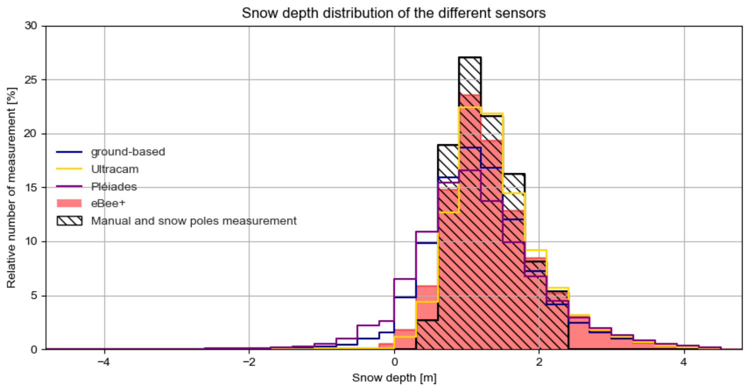

~~**Figure 8: Histogram of the snow depth distribution of the different platforms over their entire processed extent (Figure 6). The snow depth is shown on the x-axis with a bin size of 0.3 m. The y-axis shows the relative number of measurements. This is the total number of counts per bin divided by the total number of measurements and multiplied by 100. The average snow depth calculated with the Pléiades snow depth map is 1.15 m with a STD of 0.96 m. The average snow depth derived from the Ultracam snow depth map is 1.41 m with a STD of 0.67 m. The eBee+ data shows an average snow depth of 1.35 m measured with a STD of 0.68 m. The average snow depth of the ground-based data is 1.22 m with a STD of 0.80 m. The manual and snow pole measurements resulted in an average snow depth of 1.27 m and a STD of 0.44 m (all not shown).**~~

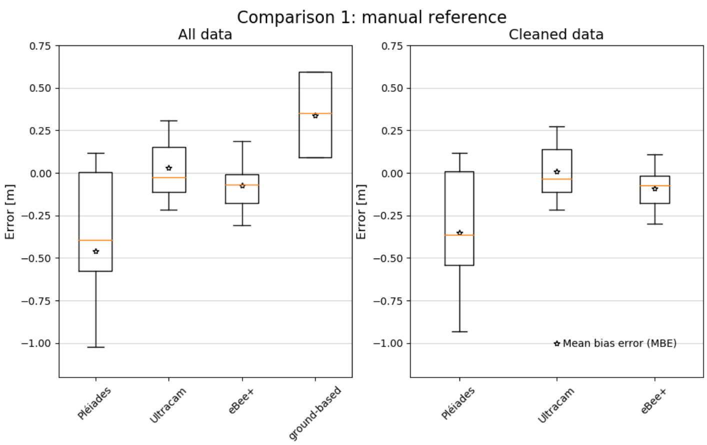

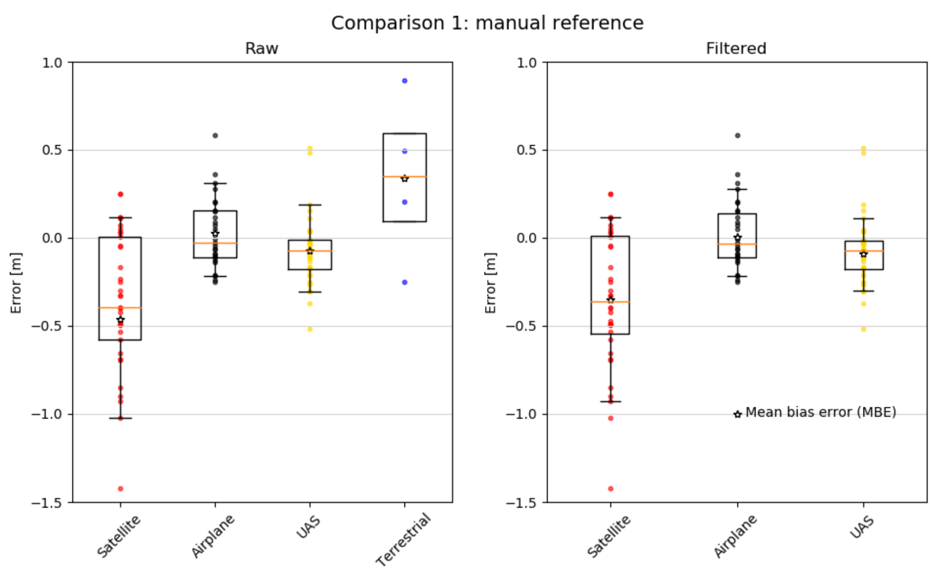

Figure 79: Boxplots with single value plots for of Comparison 1. The orange line depicts the median, the star the mean bias error (MBE). The 25th and 75th quartile are represented by the boxes and the 5th and 95th quartilepercentile by the whiskers. The left boxplot shows the raw data and the right boxplot the data where plus or minus 2*STD is removed. Because of the small low sample size of the ground-basedterrestrial data applying such a threshold doesn't have a statistical relevance and therefore the ground-

basedterrestrial data is not shown in the- right boxplot anymore. To better illustrate the distribution of the error we calculated single value plots and included them into the boxplots. Note the single large outlier (- 4.47 m) from the satellite data is not shown in the raw data to improve interpretation.

Table 4: A summary of the accuracy measures assessment of snow depths maps compared to the manual and snow pole measurements for the Pléiadessatellite, Ultracamairplane, eBee+UAS and ground-basedterrestrial imagery. For the Pléiadesatellite, Ultracamairplane and the eBee+UAS the threshold of plus or -minus 2*STD was applied and the newly calculated accuracy measures updated values are depicted in the column clean"Filtered".

	PléiadesSatellite		AirplaneUltracam		eBee+UAS		ground-basedTerrestrial
	Raw	Filtered Clean	Raw	Filtered Clean	Raw	CleanFiltered	Raw
RMSE [m]	0.90	0.52	0.20	0.17	0.21	0.16	0.54
MBE [m]	-0.46	-0.35	0.03	0.01	-0.07	-0.09	0.34
STD [m]	0.77	0.39	0.20	0.17	0.20	0.13	0.42
MABEMdBE [m]	-0.40	-0.36	-0.03	-0.04	-0.07	-0.07	0.35
NMAD [m]	0.44	0.47	0.17	0.17	0.14	0.12	0.51
Number of measurements	37	36	27	26	37	34	4

Formatierte Tabelle

5.2 Results of comparison 2: spatially dense eBee+UAS reference

The fact that UAS imagery allows for an aAccurate and spatially distributed calculation of the snow depth even in alpine terrain from UAS imagery has been well-documenteddemonstrated in recent publications by (e.g., Vander Jagt et al., 2015; Bühler et al., 2016; De Michele et al., 2016; Harder et al., 2016; Cimoli et al., 2017; Redpath et al., 2018; Avanzi et al., 2018; Eker et al., 2019) and supported by our results. Comparison 1 has also confirmed that the with an RMSE value of 0.16 m and a NMAD value of 0.11m for the filtered data, the eBee+UAS snow depth map with an RMSE of 0.16 m and a NMAD of 0.11 m for the cleaned data is within the expected accuracy for processing with ISO and without GCP. However, Ddue to the rather low number of manual and snow pole measurements, which are also mainly located at the valley floor, the accuracy analysis of comparison 1 may not fully capture the true accuracy of the snow depth productsdata analysis of comparison 1 is limited. Therefore, comparison 2 allow us to more comprehensively analyse the performance of Pléiadessatellite, Ultracamairplane and ground-basedterrestrial snow depth maps against the entire surface of mapped by the UAS winter flight in the Schürlialp study site. The boxplot (Figure 8Figure 10) shows that all three platforms estimates snow depth withmaps are in a similar range also after filteringcleaning the data by the threshold of 2*STD. Furthermore, the normalized histograms of the raw and the filtered data show that the errors are normally distributed.

Feldfunktion geändert
Feldfunktion geändert
Feldfunktion geändert
Feldfunktion geändert
Feldfunktion geändert
Feldfunktion geändert
Feldfunktion geändert
Feldfunktion geändert

Again, the Pléiades satellite data show the largest highest error dispersion compared to the Ultracam airplane and ground-basedterrestrial data. The boxplot and histogram of the cleaned satellite data confirmillustrates that the Pléiades satellite snow depth map isare slightly negatively biased over the Schürlialp test site (MBE = -0.21 m, MABEMdBE = -0.19 m.). Even aAfter cleaningfiltering, MBE and MABEMdBE remain negative with -0.18 m (Table 5). The scatter plot of the Pléiades satellite data in Figure 9Figure 11 also illustrates the lower snow depths offrom the HS map Pléiades satellite snow depth map compared to the HS map eBee+UAS snow depth map which explains also the lowest (correlation of R^2 = 0.62).

According to Comparison 1, we assume that the HS map Ultracam airplane snow depth map must correlate strongly with the HS map eBee+UAS snow depth map. The MBE and the MABEMdBE as well as the scatterplot confirm this assumption (with a R^2 =of 0.94). The RMSE of the filteredcleaned Ultracam snow depth map from airplane improved by 0.04 m, from 0.17 m to 0.12 m. All other values did notshowed minimal or no improvement at all or by 0.02 m at most when applying the thresholdfilter. The right boxplot in Figure 8Figure 10 also displays the low dispersion of the Ultracam airplane data compared to the eBee+UAS data, which is exemplified further underlined by the lower value of around 0.12 m of RMSE, STD and NMAD value of 0.12 m for the (cleaned filtered data).

For the ground-basedterrestrial data, the snow depth map correlates also strongly well with the the eBee+UAS snow depth map with a (R^2 = 0.81). (Figure 11). The MBE of 0.0 m and the MABEMdBE of -0.02 m show that the ground-basedterrestrial HS snow depth map has no overall shift. This was to beis expected since the ground-basedterrestrial snow depth map was georeferenced with the summer eBee+UAS DSM. The Boxplot (Figure 8Figure 10) shows a larger dispersion of the measurements than for the airplane Ultracam. The threshold filter has removed the major outliers and RMSE (0.21 m), STD (0.21 m), and NMAD (0.19 m) are now very similar.

Finally, to limit the effects of any outliers we assess the correlation between the satellite, airplane and terrestrial snow depth maps against the UAS snow depth map for values the lower scatter plots in Figure 11 assess the correlation of the eBee+ snow depth map with only the snow depths in the range from 0 m to 5 m (Figure 9)to the corresponding snow depth of the different platforms. This gives us an indication of how the snow depth maps correlate in the positive and most relevant range for most modelling purposes. The interval from 0 m to 5 m was selected based on the snow depth distribution shown in the histogram of Figure S2 Figure 8. The histogram shows the main snow depth distribution in this range. The R^2s of the lower scatterplots show that even in only positive range of eBee+ snow depth map the snow depth maps of the different platforms correlate still strongly and the R^2s show hardly any difference. The results show minimal difference in the correlation for each platform when focusing only on the positive 0 to 5 m snow depth values.

Feldfunktion geändert

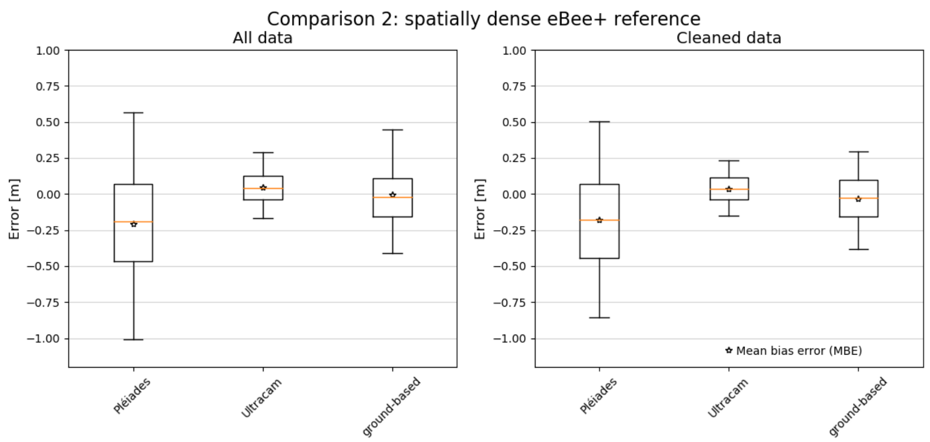
Comparison 2: spatially dense eBee+ reference
All data
Cleaned data
Error [m]
1.00
0.75
0.50
0.25
0.00
−0.25
−0.50
−0.75
−1.00
Pléiades
Ultracam
ground-based
Mean bias error (MBE)

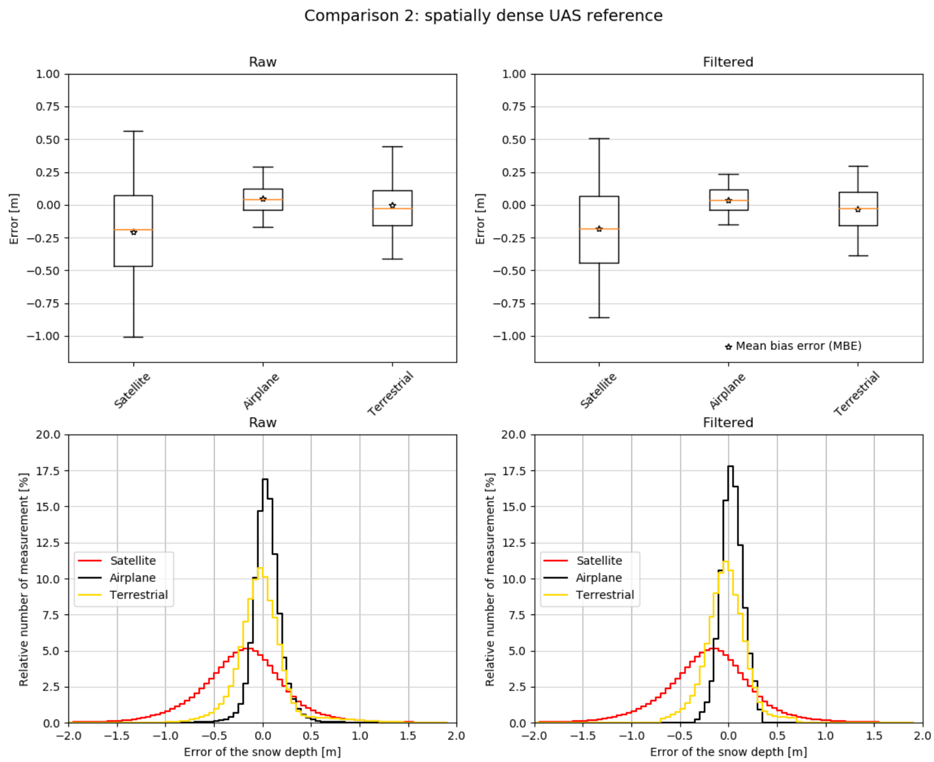

Figure 810: Boxplot of Comparison 2. The orange line depicts the median, the star the mean bias error (MBE). The 25th and 75th quartile are represented by the boxes and the 5th and 95th quartile percentile by the whiskers. The upper left boxplot shows the raw data and the upper right boxplot the data where plus- or minus 2*STD is removed from the raw data. To better illustrate the distribution of the error we calculated normalized histograms for the raw and filtered data. The bottom left plot shows the raw data and the bottom right plot the filtered data.

Table 5: Accuracy and precision measures assessment calculated for comparison 2: The column "rRaw" contains the values for the accuracy measures for all the values and the column "Filtered"cleaned shows the results of the accuracy measures where any values

exceeding the threshold of plus or -minus 2*STD are removed. For the ~~Pléiades~~ satellite data 4.2 % of the data ~~is~~were removed with the filter, while~~. For the Ultracam~~ 4.9% of the airplane data~~ is removed.~~ and~~ Overall,~~ 4 % of the ~~ground-based~~terrestrial data were ~~not considered when thresholded at plus-minus 2*STD.~~removed.

	~~Pléiades~~Satellite		**~~Ultracam~~Airplane**		**~~Ground-based~~Terrestrial**	
	Raw	**~~Cleaned~~Filtered**	**Raw**	**~~Cleaned~~Filtered**	**Raw**	**~~Cleaned~~Filtered**
RMSE [m]	0.63	0.44	0.17	0.12	0.35	0.21
MBE [m]	-0.21	-0.18	0.05	0.04	0.0	-0.03
STD [m]	0.59	0.4	0.16	0.12	0.35	0.21
~~MABE~~MdBE [m]	-0.19	-0.18	0.04	0.04	-0.02	-0.03
NMAD [m]	0.4	0.38	0.12	0.11	0.19	0.19
Number of measurements	854,519	818,834	174,072,072	165,622,459	43,554,271	41,797,672

Formatierte Tabelle

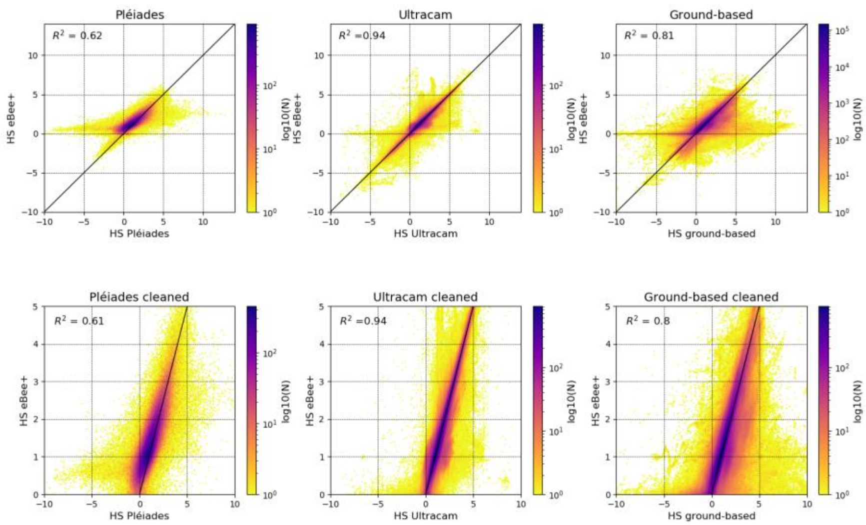
Pléiades
R^2 = 0.62
HS eBee+
HS Pléiades
log10(N)
Ultracam
R^2 =0.94
HS eBee+
HS Ultracam
log10(N)
Ground-based
R^2 = 0.81
HS eBee+
HS ground-based
log10(N)
Pléiades cleaned
R^2 = 0.61
HS eBee+
HS Pléiades
log10(N)
Ultracam cleaned
R^2 =0.94
HS eBee+
HS Ultracam
log10(N)
Ground-based cleaned
R^2 = 0.8
HS eBee+
HS ground-based
log10(N)

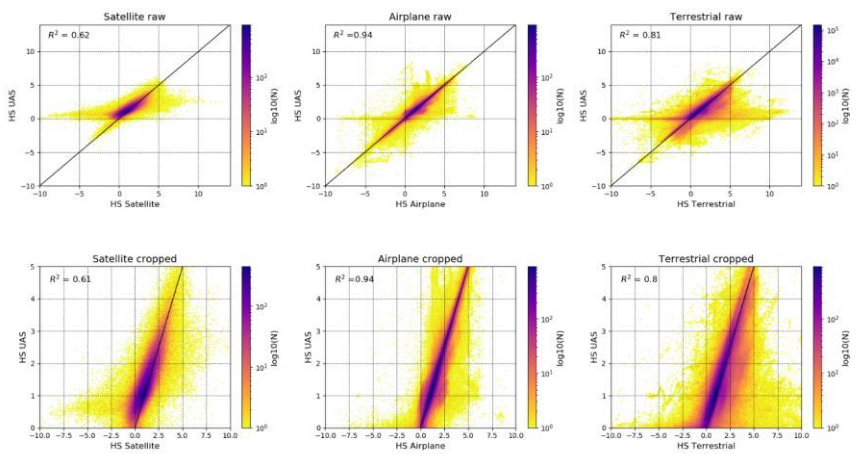

Figure 911: Scatterplot of Comparison 2: The three upper scatterplots show the platform snow depth on the x-axis and the corresponding eBee+UAS snow depth on the y-axis. For the lower scatterplots only the snow depths of the eBee+UAS snow depth map in the range of 0 m to 5 m were considered and compared to the corresponding values from each of the platform to bewere compared. For the satellite, 0.8 %, airplane 0.8 %, and 1.9% of the terrestrial data were removed. The black line is the regression line x = y. The scatterplots have a logarithmic scale, which is shown on the right side with a plasma colour bar. R^2 is calculated given for each scatterplot.

5.3 Result of comparison 3: Snow depth maps of the entire Dischma valley

A large-area, high-resolution snow depth map opens up benefitswould be of great value for many different applications. Therefore, thewe produced a snow depth map of the entire Dischma valley is calculated with the summer ALS scansurface as a reference for the winter Pléieades satellite and Ultracam airplane imagery DSMsand is shown in (Figure 10Figure 12. BecauseBased on the performance of the results of in comparison 1 and comparison 2 we use the airplane datanow the Ultracam snow depth map as a ground truth to assess the accuracy of the satellite snow depth map. What can be seen well on both snow depth maps in Figure 11 are the photogrammetric problems of the forest. For forested areas ALS or TLS provide better results as they can penetrate the vegetation layers and record signals from the ground. We have not performed a segmentation into snow and forest for these snow depth maps, so wWe have a high RMSE (2.2 m) and STD (2.2 m) (summarized indepicted in Table 6) as well as a large difference between MBE (-0.02 m) and MABEMdBE (-0.18 m) when using all data. . Again, this underlines the benefit of the strict threshold of 2*STD. After thresholdingfiltering, the RMSE (0.92 m) and STD (0.9 m) reduce considerablydiminished by half and indicate an accuracy and precision in the same order.

When looking at the correlation We found between Pléiades the satellite and Ultracam airplane data were well correlated (in Figure 14, an R^2 of= 0.74, see Figure 12) indicates a strong correlation. The correlation was weaker (R^2 = 0.21) when only focusing on the snow depth estimates betweenAs we are also interested in the correlation in the range 0 m to 5 m. m of the reference data set, we calculate the scatterplot and the correlation for this range as well. There the correlation is clearly weaker with R^2 = 0.21. This again comes on one hand from can be partially explained by the slight negative bias of the Pléiades satellite snow depth maps which is also shown by the MBE (raw: -0.02 m, cleaned: -0.17) and the MABEMdBE (raw: -0.18 m, filteredcleaned: -0.19 m). This bias is also visible graphically in the boxplot (Figure 11Figure 13) as well as in the scatterplot (Figure 12Figure 14). On the other hand, we do not know how the Ultracam snow depth map is biased over this entire area. The normalized histograms (Figure 11) show that the errors are normally distributed.

Formatiert: Hochgestellt

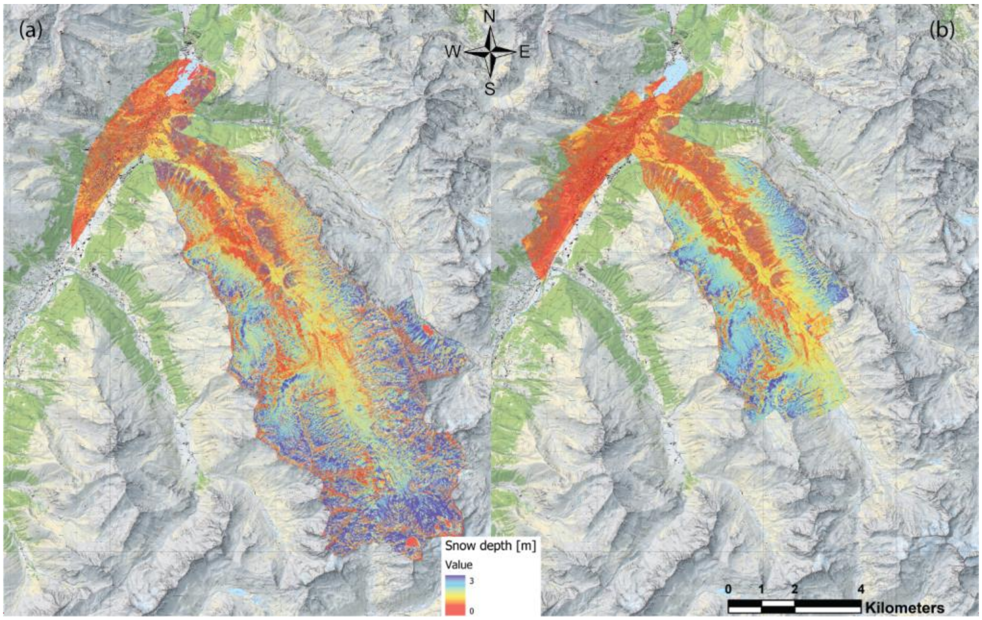
(a)
(b)
N
W
E
S
Snow depth [m]
Value
3
0
0
1
2
4
Kilometers

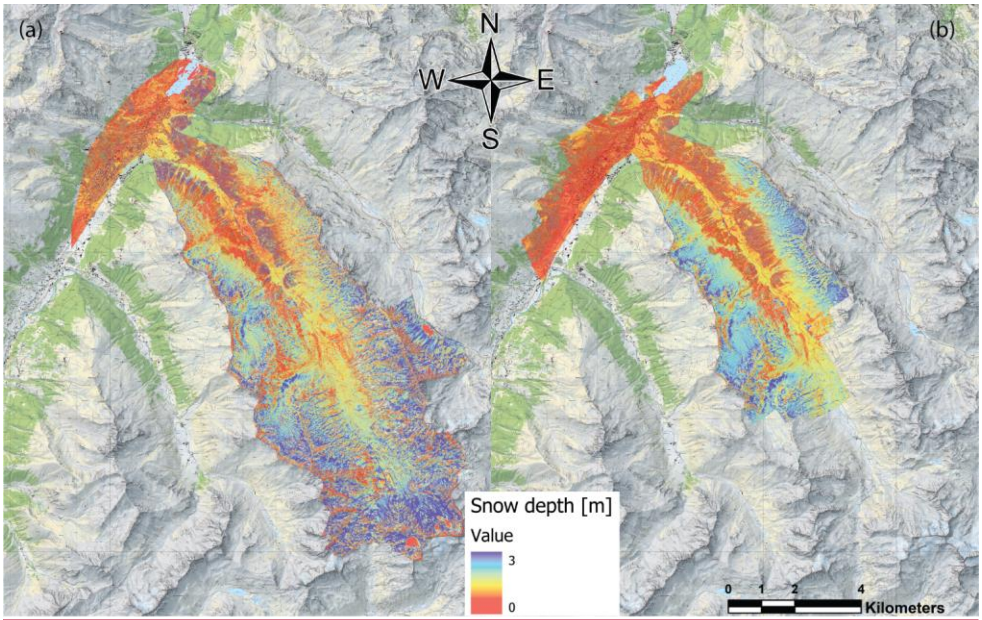

Figure 10~~12~~: Snow depth maps of the ~~Pléiades~~ satellite (a) and the ~~Ultracam~~ airplane (b) platforms for the whole Dischma valley. The snow depth is ranging from 0 m (red) to 3 m (blue) based on the summer ALS reference surface (Swiss Map Raster© 2019 swisstopo (5 704 000 000), reproduced by permission of swisstopo (JA100118)).

Table 6: Accuracy and precision ~~measures~~ assessment~~calculated~~ for comparison 3 where the satellite data are assessed against the airplane data: The column "R~~r~~aw" contains the results for all the values and the column "Filtered~~cleaned~~" the results where plus or minus 2*STD are removed. The filter removed 3.5 % of the data ~~is removed by applying the threshold of 2*STD.~~.

	Raw	**~~Cleaned~~Filtered**
RMSE [m]	2.2	0.92
MBE [m]	-0.02	-0.17
STD [m]	2.2	0.9
~~MABE~~MdBE [m]	-0.18	-0.19
NMAD [m]	0.95	0.65
Number of measurements	8,637,387	8,333,955

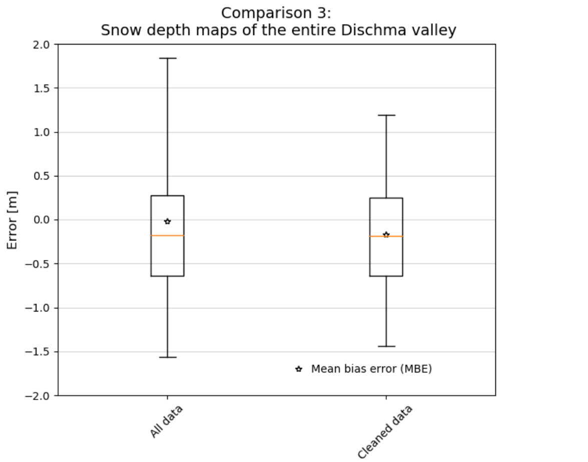

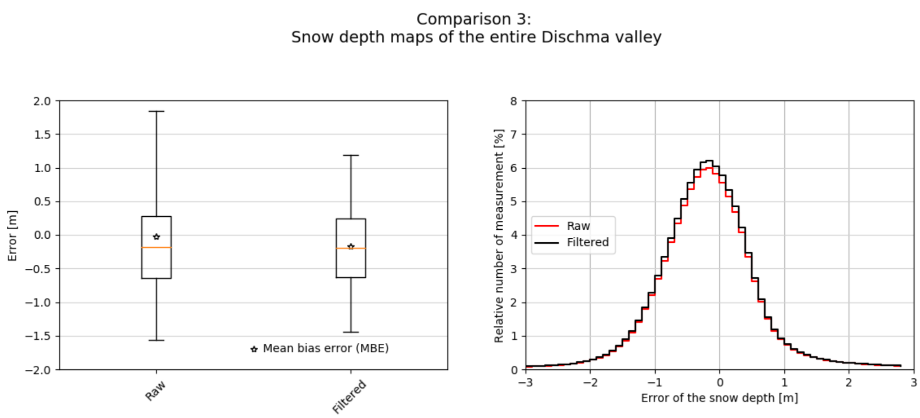

Figure 1113: Boxplot of Comparison 3, the satellite data assessed against the airplane data. The orange line depicts the median, the star the mean bias error (MBE). The 25th and 75th quartile are represented by the boxes and the 5th and 95th quartile percentile by the whiskers. The left boxplot of the boxplot graph contains all dataillustrates the raw data and the right boxplot the filtered data where plus or -minus 2*STD is removed. To better illustrate the distribution the right plot shows a normalized histogram of the raw and the filtered data.

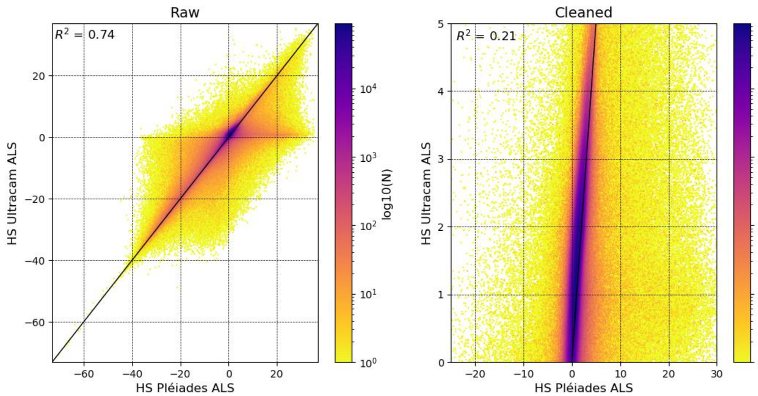

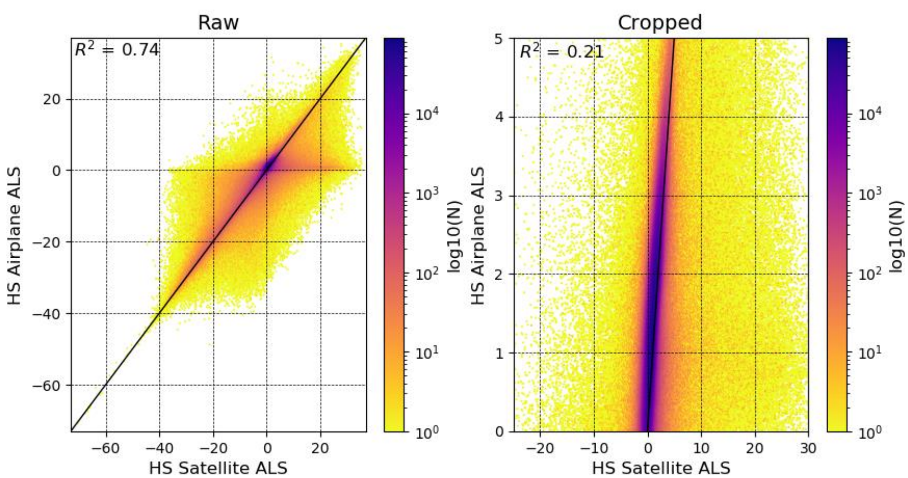

Figure 1214: Scatterplot for comparison 3 where of Pléiadessatellite snow depth ismap compared to the Ultracamairplane snow depth map. The left scatterplot shows all the data plotted. The right scatterplot shows only the snow depth estimatespoints where the airplane Ultracam snow depth is between 0 and 5 m. This cropping removed and the corresponding Pléiades snow depths. 21.27% of the data. The black line is the regression line x = y. The scatterplots have a logarithmic scale, which is shown on the right side with a plasma colour bar. R^2 is given for each scatterplot.The square of the correlation coefficient is calculated for each scatterplot.

Formatiert: Hochgestellt

6 Discussion

In this study we compare four different photogrammetric platforms focusing on their performance for spatially continuous snow depth mapping in high alpine terrain. EachEvery platform has its distinctunique advantages and disadvantages, which we (summarized in Table 7 at the end of the discussion). In this section we discuss the results presented in section 5 from the three comparisons and describe our experiences using these platforms. Furthermore, wWe conclude by providinggive recommendations on potential applications of the platforms.

6.1 Satellite photogrammetry: Pléiades

Very high-resolution optical satellites (GSDs of 0.3 to 0.7 m) have the main advantage that they can cover image several hundreds of square kilometers from space in a few secondsa single acquisition under cloud-free conditions if there are no clouds present. Today only two Few studies have are published investigatinged the performance of satellites Pléiades DSMs for snow depth mapping: in alpine terrain. Marti et al., 2016, with a Pléiades snow depth map at a resolution of 2 m, achieved achieve a STD of 0.581.47 m and a NMAD value of 0.78 45m in comparison to an UAS datasetmanual snow probing. By comparing the same snow depth map to a UAS snow depth map they calculated a STD of 1.47 m and a NMAD value of 0.78 m.; Shaw et al., 2020 found an NMAD value of 0.36 m and a RMSE value of 0.52 m for a snow depth map of 4 m resolution compared to terrestrial LiDAR. Finally, Deschamps-Berger et al., 2020 ENREF_22 achieve a RMSE value of 0.8 m and a NMAD value of 0.69 m in comparison to airborne LiDAR snow depth maps covering an area over 137 km^2 at a resolution of 4 m ENREF_44. Also, they performed filtering operations and in their Pléiades snow depth maps they set snow heights lower than -1 m and higher than 30 m to no data. In this investigation we achieve a RMSE value of 0.6344 m (0.630.44 m uncleanedfiltered) and a NMAD value of 0.4 38 m (0.38 m filtered0.4 m uncleaned) in comparison to a UAS snow depth map. This is higher than the previously reported accuracies, but oOur multi-platform ur validation wasis limited to an area of 3.6 km^2 at the Schürlialp test site and the comparison methods used in these studies are not all the same. Our snow depth maps are always calculated with the identical summer reference, so we only compare and validate winter DSMs.

Our nested validation method (with probe measurements in comparison 1 to UAS surface in comparison 2 to airplane surface in comparison 3) provides a multi-scale approach to assess accuracy and precision of photogrammetrically-derived snow depth mapsOur RMSE is in the range of the GSD of the input satellite imagery (0.5 m) and we therefore assume that we are very close to the maximum achievable accuracy. Even though we have compared the satellite snow depth maps with the snow depth maps of the Ultracam, we cannot accept this as a complete validation. Although we know that the airplane product appears highly accurate and preciseUltracam has a high accuracy and precision atover the Schürlialp test site, we could not validate it over the entirelack validation for the whole valley. and therefore the RMSE (0.92 m) and NMAD (0.65 m) of this comparison are of limited value. Nevertheless, they show that the Pléiades snow depth map is similarly accurate over the whole area as on the Schürlialp test site. It is also important to note some limitation associated with the triangulation of the satellite imagery.

Feldfunktion geändert

Feldfunktion geändert

Feldfunktion geändert

Feldfunktion geändert

Feldfunktion geändert

Most of the GCPs were collected in summer and only a few could be identified and placed when the images of the satellites were acquired. This compounds with uncertainty in the placement of the GCPs due to the resolution of the imagery. The remaining tilt was assessed and corrected on the basis of points along the roads in three valleys (Sertig, Dischma, Flüela), but without regards for the Schürlialp test site in particular. Thus, the shift does not characterize the technology, but shows a limitation of absolute orientation approach for snow-covered images.

A photogrammetric challenge also arises from stereo-matching in low contrast snow-covered surfaces which combines with imaging geometry and the relatively coarser spatial resolution of satellite imagery, decreasing signal-to-noise ratio in the DSM. This is exacerbated by lower B/H ratio (P23 in particular) which led to substantially greater noise on smooth, undisturbed areas of the snowpack. Lower contrast appeared to promote variability in stereo-matching which compounds with lower parallactic angles when B/H decreases, thus increasing the dispersion in the triangulated heights on poorly textured areas. With some contrast or texture in the snow (e.g., avalanches deposits), then stereo-matching performed similarly across every stereo-pairs with no substantial differences in surface height dispersion. This indicates that image contrast and B/H ratio combine to govern the dispersion of the restitution. An in-depth study may be desirable to characterize this effect further, including testing more stereo-matching options and satellite geometry in such environments.

~~Our findings limit the range of applications for satellite-based snow depth maps.~~ Our testing shows that given the resolution of the Pleiades imagery, the uncertainty in snow depth retrieval challenges the mapping of ~~S~~shallow snow packs~~, present over large parts of the tundra regions of the northern hemisphere, have~~ with mean snow depth values in the range of 0.5 m (Sturm et al., 2008)~~ and can therefore not be captured with sufficient reliability by the Pléiades platform~~. In mountain regions on the other hand, where larger mean snow depth values are present and the amplitude of the values is generally larger, satellite-based snow depth maps will ~~could~~ provide important estimates of snow distribution~~information~~. Typical applications that could benefit~~profit~~ are the mapping of snow avalanches (Bühler et al. 2019) and the estimation of water resources stored in snow (Jonas et al. 2009) for drinking water supply or hydropower (Farinotti et al. 2012). In many remote regions of the world, where access is difficult and dangerous, satellite photogrammetry proves to be a competitive~~is the only feasible~~ method to gather spatial continuous snow depth information even though the achievable accuracy is limited.~~. However, to orientate the imagery and to accurately align the snow-free and the snow-covered DSMs, ground control points GCPs, well distributed over the entire area, are necessary. If this is not possible, the DSMs could be aligned based on a master scene but this is often very difficult in alpine, snow covered terrain because not enough points can be identified in both scenes accurately.~~

Formatiert: Schriftart:

Feldfunktion geändert

6.2 Airplane photogrammetry: Ultracam

~~Airborne~~ Airplane photogrammetry campaigns depend on the availability of suitable airplanes and camera systems as well as ~~on~~ flight permissions. E~~If this is given, e~~ntire catchments of several hundred~~s of km^2~~ square kilometers can be covered within 1 – 2 hours of flying with ground sampling distances of 0.05 to 0.25 m. Despite today's availability of high-end camera systems only few studies have used airplane photogrammetry for snow depth measurements. The investigations of Bühler et al., 2015 and Boesch et al., 2016 with an ADS80/100 optical scanner and Nolan et al., 2015 with a Nikon D800E frame camera reported accuracies of 0.10 m to 0.3 m. In our study we use an Ultracam Eagle M3 frame camera and achieve a RMSE value of 0.12 m (0.17 m ~~uncleaned~~raw) compared to the UAS snow depth values.

Feldfunktion geändert

Feldfunktion geändert

Feldfunktion geändert

~~Due to the higher GSD airborne~~Aerial photogrammetry allows for snow depth map~~s~~ping at~~ in~~ a higher spatial resolution than ~~the~~ satellite~~-based~~ photogrammetry ~~and~~ with~~reaches~~ accuracies close to UAS photogrammetry. This is particularly the case if low flying~~ flight~~ heights above ground are planned resulting in higher GSDs of 0.05 to 0.1 m. However, ~~I~~in alpine terrain the GSD varies a lot due to topography~~. Therefore,~~ as the airplane flight lines are usually at fixed elevations~~, highly elevated areas are closer to the sensor than regions in the valleys~~, resulting in varying GSDs within the investigation area. Airplanes can also fly below high clouds; however as for all photogrammetric sensors, diffuse illuminations corrupt the contrast of the snow-covered surfaces and may result in insufficient DSM qualities ~~with~~ resulting in holes and outliers. ~~Due to~~With~~ the medium to~~ high accuracy and precision and the large possible coverage, airplane photogrammetry is a~~ very~~ ~~valuable~~ promising tool for all applications where the investigation area is reachable with an airplane and an accuracy in the range of 0.1 to 0.3 m is acceptable. Also, airborne photogrammetry is costly depends on GCPs or the alignment to a master scene for orientation. Because of the smaller GSD ~~is higher t~~of the airplane data compared with ~~han in~~ the satellite data, the accurate photo-identification of points ~~might~~may be easier.

6.3 UAS photogrammetry: eBee+

UAS photogrammetry has proved to be an accurate, flexible and reliable tool for snow depth mapping achieving accuracies in the range of 0.05 to 0.2 m (Bühler et al., 2016; Harder et al., 2016; De Michele et al., 2016; Redpath et al., 2018). In this study we applied ISO based on onboard RTK without applying ground control points. Our experience with more than 150 flight missions shows, that the snow depth values generated under favorable illumination conditions are of very high quality. ~~and are often even more trustworthy than the manual probe measurements.~~ Comparison 1 supports this conclusion, which allows us to~~Therefore, we can~~ apply the ~~eBee+~~UAS snow depth map as ~~ground truth~~a reference for the validation of satellite and airplane platforms~~ photogrammetry~~.

Feldfunktion geändert

Feldfunktion geändert

Feldfunktion geändert

Feldfunktion geändert

The main limitation of UAS photogrammetry is that current systems ~~can~~cover only ~~cover limited areas in the range of~~ a limited area (on order of a few square kilometers)~~km^2~~ due to technical limitations~~ and legal regulations~~. ~~The p~~Pilots have to be ~~very~~

close to the study~~investigation~~ site to fly the ~~drone~~ UAS with~~in~~ line-of-sight. Furthermore, takeoff~~starting~~ and ~~in particular~~ landing the ~~drones~~UAS in high-alpine terrain is challenging, especially in particular if wind gusts of more than 15 m/s are present. ~~At present higher wind speeds make it impossible to operate any known mapping drone.~~ On the other hand, UAS enable the flexible generation of accurate and precise DSMs. Therefore, they can be applied for all applications requiring spatial continuous snow depth information as long as a limited area is acceptable. An example for such an application is the measurement of snow redistribution by wind at a specific mountain ridge (Walter et al., 2020_ENREF_71).

Feldfunktion geändert

Feldfunktion geändert

6.4 ~~Ground-based~~Terrestrial photogrammetry: Canon EOS 750D

~~Ground-based~~Terrestrial photogrammetry needs no high-end photogrammetric equipment and only a ~~powerful~~ consumer camera can be enough to fulfill the task. ~~Ground-based photogrammetry~~Therefore, it is a suitable tool if only smaller areas mainly in steep terrain facing towards the cameras should be covered. If fixed installation~~ed~~ cameras are used, a ~~very~~ high temporal resolution of several measurements per day is possible. The spatial resolution declines with the distance to the camera position and the inclination away from the sensor. Our results demonstrate that flat regions are often not visible unless you would map from above,~~.~~ ~~so~~ A~~a~~ spatial continuous coverage can only be achieved in ~~steep~~ terrain facing ~~to~~ towards the camera. The ~~achieved precision and~~ accuracy and precision achieved in this study ~~was~~ rang~~inged~~ from 0.2 ~~m~~ to 0.5 m. Terrestrial photogrammetry also encounters limitations such as georeferencing problems, logistic problems or access problems. We performed for example the georeferencing using a UAS flight. This can certainly be avoided with a clear ISO approach and well distributed GCPs points. But terrestrial photogrammetry remains the most challenging technique, because for a working setup, access to difficult terrain is necessary (distribution of the GCPs, camera position). Potential applications for such platforms ~~are e.g.~~ include the mapping of snow avalanche mass balances (e.g. Thibert et al., 2015) or the mapping of snow depth variations at confined locations such as mitigation measures along roads (e.g. Basnet et al., 2016) where large snow depth values are expected.

Feldfunktion geändert

Feldfunktion geändert

6.5 Influence of vegetation

Our study confirms the previously noted effect of~~at~~ vegetation ~~plays a not neglectable role for~~on snow depth ~~mapping~~ (Bühler et al., 2016; Harder et al., 2016; Redpath et al., 2018). Photogrammetr~~icy~~-derived DSMs over forested areas ~~are~~have limitations compared with ALS where above-ground returns can be removed from the surface ~~limited~~. ~~However, bushes~~ Dense vegetation can also produce holes and negative snow depth values in a snow depth map when using photogrammetry. For example, all four snow depth maps showed the same negative snow depth patterns due to the species *alnus alnobetula* (Figure 6~~Figure 7~~). These bushes stand tall (up to ~~2 –~~ 3 m) during summer and are pressed to the ground by the snow cover in winter resulting in negative snow depth values ~~of~~ up to 3 m (Figure 6~~Figure 7~~). Bühler et al., 2016 have also identified this effect. Feistl et al., 2014 investigated vegetation compression snow and found that depending on the vegetation type (long grass, short grass and dwarf shrub) the difference between the summer height and the height below snow was between 0.1 and 0.2 m. ~~Therefore, we suggest~~Our work affirms the utility of ALS ~~airborne laser scanning techniques~~ for investigating snow depth ~~near~~in densely

Feldfunktion geändert

Feldfunktion geändert

Feldfunktion geändert

Feldfunktion geändert

Feldfunktion geändert

vegetated or forested areas. forests. If bushes are present, fFiltering a summer laser scanALS for to producinge a digital terrain model (DTM) instead of a DSM can improve the snow depth measurements overin vegetated areas, however artefacts are likely to .-remain. Further investigations are needed to quantify the effects of vegetation in estimating snow depth with remote sensing techniques.

Table 7: Summary of the RMSEs and /NMADs values and main advantages/disadvantages of the investigated photogrammetric platforms. Except for the eBee+ the The reported RMSE s/and NMADs values for the satellite, airplane and terrestrial data are based on the cleaned filtered values from comparison 2. TheFor the eBee+ the RMSE and NMAD values shown for the UAS are the filtered values taken from the comparison 1, therefore they are higher than the once of the Ultracam.

Platform	RMSE [m] / NMAD [m]	Main advantages	Main disadvantages
Satellite (Pléiades)	0.44 / 0.38 (Comparison 2)	• Very large coverage possible • Fast acquisition times • Covering remote regions • High temporal resolution possible	• Limited Lower spatial resolution which results in limited reduced accuracy and precision • Data acquisition costly • GCPs / alignment necessary
Airplane (Ultracam)	0.12 / 0.11 (Comparison 2)	• Large coverage • High accuracy • Suitable for most applications	• Data acquisition costly • GCPs / alignment necessary • Dependent on external availability
UAS (eBee+)	0.16 / 0.112 (Comparison 1)	• Very high accuracy • Economic and flexible	• Limited coverage

		• No GCPs necessary	• Wind, especially gusts critical • Starting and landing demanding
~~Ground-based~~Terrestrial (Canon EOS 750D)	0.21 / 0.19 (Comparison 2)	• Minimal ~~material~~ equipment required • Economical and flexible • High temporal resolution possible	• Limited coverage with holes in flat/obstructed terrain • ~~Limited~~ Lower accuracy • GCPs / alignment necessary

7 Conclusions

In this study we tested and compared~~for the first time~~ a wide range of available photogrammetric platforms~~ in a timely manner covering the same area~~ for their performance in snow depth mapping. Satellite imagery (Pléiades)~~ imagery~~ demonstrated its capability to map large areas (> 100 km^2) in a single acquisition ~~with a high temporal resolution~~ but with a lower native spatial resolution (0.5 m) compared with the other platforms. We found a~~A~~ RMSE value of 0.44 m and a NMAD value of 0.38 m for the satellite-derived ~~at a~~ snow depth map at a spatial resolution of 2 m~~/pixel (cleaned data comparison 2) underline these statements~~. ~~For higher spatial resolution and large coverage but lower temporal resolution airplane (Ultracam) imagery is suitable.~~ The comparison to the UAS (eBee+) snow depth map demonstrated the high accuracy of the ~~Ultracam~~ airplane (Ultracam) snow depth map at a high spatial ~~(~~resolution of 0.11 m~~/pixel)~~ with a RMSE value of 0.12 m and a NMAD value of 0.11 m. UAS images are an economical and flexible method for mapping snow depth with high accuracy (RMSE value of 0.16 m and NMAD value of 0.11 m~~ in comparison 1~~) and high spatial resolution (0.09 m~~/pixel~~ snow depth map resolution)~~.~~, ~~B~~but coverage~~ and temporal resolution~~ of an UAS is limited. ~~Finally, one advantage of ground-based~~The terrestrial (Canon EOS 750D) ~~images~~platform ~~is that they~~ requires ~~minimal material~~less expensive equipment and ~~allow~~supports a high temporal resolution of data capture. However, coverage, accuracy and precision are limited and not possible for every application. ~~Nevertheless, t~~The snow depth map of ~~ground-based~~terrestrial images achieved a~~n~~ RMSE value of 0.21 m and a~~n~~ NMAD value of 0.19 m with a snow depth map resolution of 0.11 m~~/pixel (cleaned data in comparison 2)~~.

With these investigations we demonstrate that digital photogrammetry is a powerful tool to map spatially continuous~~ly map~~ snow depth distribution in alpine terrain.~~. As such information was mostly missing in the past, various i~~ Important applications such as avalanche warning, ecological investigations in alpine environments or hydropower generation can ~~profit~~ benefit from data acquired by this new technology~~ in the future~~. With further advancements in sensor technology for all tested platforms, we expect ~~even better~~improved accuracies and coverage~~s~~ in the future. ~~We assume that d~~Digital photogrammetry may be ~~could~~

~~become~~ the preferred method for snow depth mapping as it~~. It~~ is more flexible and less costly than laser scanning for most applications, as long as the vegetation cover is negligible and the snow is deep enough.

Data availability

The photogrammetric and reference data sets will be published on ENVIDAT (https://www.envidat.ch)~~ upon the final publication of this paper~~.

Author contribution

LE, YB and AS designed and performed the experiments. PS, AM and YB processed the satellite imagery. LE processed the ~~Ultracam~~airplane, UAS and ~~ground-based~~terrestrial imagery. LE and YB prepared the manuscript with contributions from all co-authors.

Competing interests

The authors declare that they have no conflict of interest.

Acknowledgements

We would like to thank the Swiss National Science Foundation (SNF) for funding this project under Grant N° 200021_172800 and Grant N° IZSEZ0_185651. P. Sirguey and A. Miller were funded by MBIE Endeavour Smart Idea research project "Quantifying environmental resources through high-resolution, automated, satellite mapping of landscape change" (UOOX1914). Methodological approaches for processing Pléiades data were developed in part with funding from University of Otago Research grant "Glaciers in the picture" (ORG-0118-0319) and GNS research grant "Topographic mapping of Franz Josef glacier "(GNS-DCF00043). We would also like to thank Elisabeth Hafner, Kevin Simmler, Konstantin Nebel, Daniel von Rickenbach, Julian Fisch, Michael Hohl and Christian Simeon for their help with the various fieldwork tasks.

References

Agisoft LLC: Agisoft Metashape User Manual Professional Edition, 1.5, https://www.agisoft.com/pdf/photoscan-pro_1_4_en.pdf, 2019.

Avanzi, F., Bianchi, A., Cina, A., De Michele, C., Maschio, P., Pagliari, D., Passoni, D., Pinto, L., Piras, M., and Rossi, L.: Centimetric Accuracy in Snow Depth Using Unmanned Aerial System Photogrammetry and a MultiStation, Remote Sens.-Basel, 10, https://doi.org/10.3390/rs10050765, 2018.

Baggi, S., and Schweizer, J.: Characteristics of wet-snow avalanche activity: 20 years of observations from a high alpine valley (Dischma, Switzerland), Nat. Hazards, 50, 97-108, https://doi.org/10.1007/s11069-008-9322-7, 2008.

Feldfunktion geändert
Feldfunktion geändert
Formatiert: Englisch (Vereinigtes Königreich)
Feldfunktion geändert
Formatiert: Englisch (Vereinigtes Königreich)
Formatiert: Englisch (Vereinigtes Königreich)
Formatiert: Italienisch (Italien)
Feldfunktion geändert
Formatiert: Italienisch (Italien)
Formatiert: Italienisch (Italien)
Formatiert: Englisch (Vereinigtes Königreich)
Feldfunktion geändert
Formatiert: Englisch (Vereinigtes Königreich)
Formatiert: Englisch (Vereinigtes Königreich)

Bartelt, P., Buser, O., Vera Valero, C., and Bühler, Y.: Configurational energy and the formation of mixed flowing/powder snow and ice avalanches, Ann. Glaciol., 57, 179-188, https://doi.org/10.3189/2016AoG71A464, 2016.

Basnet, K., Muste, M., Constantinescu, G., Ho, H., and Xu, H.: Close range photogrammetry for dynamically tracking drifted snow deposition, Cold Reg. Sci. Technol., 121, 141-153, https://doi.org/10.1016/j.coldregions.2015.08.013, 2016.

Benassi, F., Dall'Asta, E., Diotri, F., Forlani, G., di Cella, U. M., Roncella, R., and Santise, M.: Testing Accuracy and Repeatability of UAV Blocks Oriented with GNSS-Supported Aerial Triangulation, Remote Sens.-Basel, 9, 172, https://doi.org/10.3390/rs9020172, 2017.

Beyer, R. A., Alexandrov, O., and McMichael, S.: The Ames Stereo Pipeline: NASA's Open Source Software for Deriving and Processing Terrain Data, Earth and Space Science, 5, 537-548, https://doi.org/10.1029/2018EA000409, 2018.

Bilodeau, F., Gauthier, G., and Berteaux, D.: The effect of snow cover on lemming population cycles in the Canadian high Arctic, Oecologia, 172, 1007-1016, https://doi.org/10.1007/s00442-012-2549-8, 2013.

Boesch, R., Buhler, Y., Marty, M., and Ginzler, C.: Comparison of digital surface models for snow depth mapping with UAV and aerial cameras, Int Arch Photogramm, 41, 453-458, https://doi.org/10.5194/isprs-archives-XLI-B8-453-2016, 2016.

Bühler, Y., Hüni, A., Christen, M., Meister, R., and Kellenberger, T.: Automated detection and mapping of avalanche deposits using airborne optical remote sensing data, Cold Reg. Sci. Technol., 57, 99-106, https://doi.org/10.1016/j.coldregions.2009.02.007, 2009.

Bühler, Y., Marty, M., Egli, L., Veitinger, J., Jonas, T., Thee, P., and Ginzler, C.: Snow depth mapping in high-alpine catchments using digital photogrammetry, The Cryosphere, 9, 229-243, https://doi.org/10.5194/tc-9-229-2015, 2015.

Bühler, Y., Adams, M. S., Bosch, R., and Stoffel, A.: Mapping snow depth in alpine terrain with unmanned aerial systems (UASs): potential and limitations, The Cryosphere, 10, 1075-1088, https://doi.org/10.5194/tc-10-1075-2016, 2016.

Bühler, Y., Adams, M. S., Stoffel, A., and Boesch, R.: Photogrammetric reconstruction of homogenous snow surfaces in alpine terrain applying near- infrared UAS imagery, Int. J. Remote Sens., 38, 3135-3158, https://doi.org/10.1080/01431161.2016.1275060, 2017.

Christen, M., Kowalski, J., and Bartelt, P.: RAMMS: Numerical simulation of dense snow avalanches in three-dimensional terrain, Cold Reg. Sci. Technol., 63, 1-14, https://doi.org/10.1016/j.coldregions.2010.04.005, 2010.

Cimoli, E., Marcer, M., Vandecrux, B., Bøggild, C. E., Williams, G., and Simonsen, S. B.: Application of Low-Cost UASs and Digital Photogrammetry for High-Resolution Snow Depth Mapping in the Arctic, Remote Sens.-Basel, 9, https://doi.org/10.3390/rs9111144, 2017.

Cullen, N. J., Anderson, B., Sirguey, P., Stumm, D., Mackintosh, A., Conway, J. P., Horgan, H. J., Dadic, R., Fitzsimons, S. J., and Lorrey, A.: An 11-year record of mass balance of Brewster Glacier, New Zealand, determined using a geostatistical approach, J. Glaciol., 63, 199-217, https://doi.org/10.1017/jog.2016.128, 2016.

d'Angelo, P.: Improving Semi-Global Matching: Cost Aggregation and Confidence Measure, ISPRS - International Archives of the Photogrammetry, Remote Sensing and Spatial Information Sciences, XLI-B1, 299-304, https://doi.org/10.5194/isprs-archives-XLI-B1-299-2016, 2016.

De Michele, C., Avanzi, F., Passoni, D., Barzaghi, R., Pinto, L., Dosso, P., Ghezzi, A., Gianatti, R., and Della Vedova, G.: Using a fixed-wing UAS to map snow depth distribution: an evaluation at peak accumulation, The Cryosphere, 10, 511-522, https://doi.org/10.5194/tc-10-511-2016, 2016.

Deems, J. S., and Painter, T. H.: LiDAR measurement of snow depth: Accuracy and error sources, in: Proceedings of the 2006 International Snow Science Workshop, ISSW, Telluride, Colorado, 330–338, 2006.

Deems, J. S., Painter, T. H., and Finnegan, D. C.: Lidar measurement of snow depth: a review, J. Glaciol., 59, 467-479, https://doi.org/10.3189/2013JoG12J154, 2013.

Deschamps-Berger, C., Gascoin, S., Berthier, E., Deems, J., Gutmann, E., Dehecq, A., Shean, D., and Dumont, M.: Snow depth mapping from stereo satellite imagery in mountainous terrain: evaluation using airborne laser-scanning data, The Cryosphere, 14, 2925-2940, https://doi.org/10.5194/tc-14-2925-2020, 2020.

Dong, C.: Remote sensing, hydrological modeling and in situ observations in snow cover research: A review, J. Hydrol., 561, 573-583, https://doi.org/10.1016/j.jhydrol.2018.04.027, 2018.

Dreier, L., Bühler, Y., Ginzler, C., and Bartelt, P.: Comparison of simulated powder snow avalanches with photogrammetric measurements, Ann. Glaciol., 57, 371-381, https://doi.org/10.3189/2016AoG71A532, 2016.

Eker, R., Bühler, Y., Schlögl, S., Stoffel, A., and Aydın, A.: Monitoring of Snow Cover Ablation Using Very High Spatial Resolution Remote Sensing Datasets, Remote Sens.-Basel, 11, https://doi.org/10.3390/rs11060699, 2019.

Feistl, T., Bebi, P., Dreier, L., Hanewinkel, M., and Bartelt, P.: Quantification of basal friction for technical and silvicultural glide-snow avalanche mitigation measures, Nat. Hazard. Earth Sys., 14, 2921-2931, https://doi.org/10.5194/nhess-14-2921-2014, 2014.

Fierz, C., Armstrong, R. L., Durand, Y., Etchevers, P., Green, E., McClung, D. M., Nishimura, K., Satyawali, P. K., and Sokratov, S. A.: The international classification of seasonal snow on the ground, Paris, 80, 2009.

Gascoin, S., Kinnard, C., Ponce, R., Lhermitte, S., MacDonell, S., and Rabatel, A.: Glacier contribution to streamflow in two headwaters of the Huasco River, Dry Andes of Chile, The Cryosphere, 5, 1099-1113, https://doi.org/10.5194/tc-5-1099-2011, 2011.

Griessinger, N., Mohr, F., and Jonas, T.: Measuring snow ablation rates in alpine terrain with a mobile multioffset ground-penetrating radar system, Hydrol. Process., 32, 3272-3282, https://doi.org/10.1002/hyp.13259, 2018.

Harder, P., Schirmer, M., Pomeroy, J., and Helgason, W.: Accuracy of snow depth estimation in mountain and prairie environments by an unmanned aerial vehicle, The Cryosphere, 10, 2559-2571, https://doi.org/10.5194/tc-10-2559-2016, 2016.

Hirschmuller, H.: Stereo processing by semiglobal matching and mutual information, IEEE T. Pattern Anal., 30, 328-341, https://doi.org/10.1109/TPAMI.2007.1166, 2008.

Höhle, J., and Höhle, M.: Accuracy assessment of digital elevation models by means of robust statistical methods, ISPRS J. Photogramm., 64, 398-406, https://doi.org/10.1016/j.isprsjprs.2009.02.003, 2009.

Hopkinson, C., Demuth, M., Sitar, M., and Chasmer, L.: Applications of Airborne LiDAR Mapping in Glacierised Moountainous Terrain, 2, 949-951, 10.1109/IGARSS.2001.976690, 2001.

Hopkinson, C., Sitar, M., Chasmer, L., and Treitz, P.: Mapping snowpack depth beneath forest canopies using airborne lidar, Photogramm. Eng. Rem. S., 70, 323-330, https://doi.org/10.14358/PERS.70.3.323, 2004.

Isenburg, M.: LAStools - efficient LiDAR Processing Software, academic, http://rapidlasso.com/LAStools, 2014.

Korzeniowska, K., Bühler, Y., Marty, M., and Korup, O.: Regional snow-avalanche detection using object-based image analysis of near-infrared aerial imagery, Nat. Hazard. Earth Sys., 17, 1823-1836, https://doi.org/10.5194/nhess-17-1823-2017, 2017.

Lato, M. J., Frauenfelder, R., and Bühler, Y.: Automated detection of snow avalanche deposits: segmentation and classification of optical remote sensing imagery, Nat. Hazard. Earth Sys., 12, 2893-2906, https://doi.org/10.5194/nhess-12-2893-2012, 2012.

Lopez-Moreno, J. I., Revuelto, J., Alonso-Gonzalez, E., Sanmiguel-Vallelado, A., Fassnacht, S. R., Deems, J., and Moran-Tejeda, E.: Using very long-range terrestrial laser scanner to analyze the temporal consistency of the snowpack distribution in a high mountain environment, J. Mt. Sci.-Engl., 14, 823-842, https://doi.org/10.1007/s11629-016-4086-0, 2017.

Luhmann, T., Robson, S., Kyle, S., and Boehm, J.: Close-Range Photogrammetry and 3D Imaging, 2 ed., edited by: Thomas Luhmann, Stuart Robson, Kyle, S., and Boehm, J., De Gruyter, Berlin/Boston, 2014.

Lundberg, A., Granlund, N., and Gustafsson, D.: Towards automated 'Ground truth' snow measurements-a review of operational and new measurement methods for Sweden, Norway, and Finland, Hydrol. Process., 24, 1955-1970, https://doi.org/10.1002/hyp.7658, 2010.

Marti, R., Gascoin, S., Berthier, E., de Pinel, M., Houet, T., and Laffly, D.: Mapping snow depth in open alpine terrain from stereo satellite imagery, The Cryosphere, 10, 1361-1380, https://doi.org/10.5194/tc-10-1361-2016, 2016.

Maune, D. F., and Naygandhi, A.: Digital Elevation Model Technologies and Applications: The DEM Users Manual, 3 ed., edited by: Maune, D. F., and Naygandhi, A., 652 pp., 2018.

McGrath, D., Sass, L., O'Neel, S., Arendt, A., Wolken, G., Gusmeroli, A., Kienholz, C., and McNeil, C.: End-of-winter snow depth variability on glaciers in Alaska, J. Geophys. Res-Earth, 120, 1530-1550, https://doi.org/10.1002/2015JF003539, 2015.

McGrath, D., Webb, R., Shean, D., Bonnell, R., Marshall, H. P., Painter, T. H., Molotch, N. P., Elder, K., Hiemstra, C., and Brucker, L.: Spatially Extensive Ground-Penetrating Radar Snow Depth Observations During NASA's 2017 SnowEx Campaign: Comparison With In Situ, Airborne, and Satellite Observations, Water Resour. Res., 55, 10026-10036, https://doi.org/10.1029/2019WR024907, 2019.

Meyer, J., and Skiles, S. M.: Assessing the Ability of Structure From Motion to Map High-Resolution Snow Surface Elevations in Complex Terrain: A Case Study From Senator Beck Basin, CO, Water Resour. Res., 55, 6596-6605, https://doi.org/10.1029/2018WR024518, 2019.

Nolan, M., Larsen, C., and Sturm, M.: Mapping snow depth from manned aircraft on landscape scales at centimeter resolution using structure-from-motion photogrammetry, The Cryosphere, 9, 1445-1463, https://doi.org/10.5194/tc-9-1445-2015, 2015.

Novac, J.: Quality assessment of elevation data, in: Digital Elevation Model Technologies and Applications: The DEM Users Manual, 3rd Edition, 3 ed., edited by: Maune, D. F., and Nayegandhi, A., 455 - 544, 2018.

Painter, T. H., Berisford, D. F., Boardman, J. W., Bormann, K. J., Deems, J. S., Gehrke, F., Hedrick, A., Joyce, M., Laidlaw, R., Marks, D., Mattmann, C., McGurk, B., Ramirez, P., Richardson, M., Skiles, S. M., Seidel, F. C., and Winstral, A.: The Airborne Snow Observatory: Fusion of scanning lidar, imaging spectrometer, and physically-based modeling for mapping snow water equivalent and snow albedo, 184, 139-152, 10.1016/j.rse.2016.06.018, 2016.

Prokop, A.: Assessing the applicability of terrestrial laser scanning for spatial snow depth measurements, Cold Reg. Sci. Technol., 54, 155-163, https://doi.org/10.1016/j.coldregions.2008.07.002, 2008.

Prokop, A., Schon, P., Singer, F., Pulfer, G., Naaim, M., Thibert, E., and Soruco, A.: Merging terrestrial laser scanning technology with photogrammetric and total station data for the determination of avalanche modeling parameters, Cold Reg. Sci. Technol., 110, 223-230, 10.1016/j.coldregions.2014.11.009, 2015.

Redpath, T. A. N., Sirguey, P., and Cullen, N. J.: Repeat mapping of snow depth across an alpine catchment with RPAS photogrammetry, The Cryosphere, 12, 3477-3497, https://doi.org/10.5194/tc-12-3477-2018, 2018.

eBee RTK Accuracy Assessment: https://www.sensefly.com/app/uploads/2017/11/eBee_RTK_Accuracy_Assessment.pdf, access: 02.12.2019, 2017.

Schlatter, A., and Marti, U.: Höhentransformation zwischen LHN95 und den Gebrauchshöhen LN02, 103, 10.5169/seals-236251, 2005.

Schön, P., Prokop, A., Vionnet, V., Guyomarc'h, G., Naaim-Bouvet, F., and Heiser, M.: Improving a terrain-based parameter for the assessment of snow depths with TLS data in the Col du Lac Blanc area, Cold Reg. Sci. Technol., 114, 15-26, https://doi.org/10.1016/j.coldregions.2015.02.005, 2015.

Shaw, T. E., Gascoin, S., Mendoza, P. A., Pellicciotti, F., and McPhee, J.: Snow Depth Patterns in a High Mountain Andean Catchment from Satellite Optical Tristereoscopic Remote Sensing, Water Resour. Res., 56, https://doi.org/10.1029/2019WR024880, 2020.

Shean, D. E., Alexandrov, O., Moratto, Z. M., Smith, B. E., Joughin, I. R., Porter, C., and Morin, P.: An automated, open-source pipeline for mass production of digital elevation models (DEMs) from very-high-resolution commercial stereo satellite imagery, ISPRS J. Photogramm., 116, 101-117, 10.1016/j.isprsjprs.2016.03.012, 2016.

Sirguey, P., and Cullen, N.: A very high resolution DEM of Kilimanjaro via photogrammetry of GeoEye-1 images (KILISoSDEM2012), NZ Surveyor, 19-215, 2014.

Sirguey, P., and Lewis, C.: Topographic mapping of Franz Josef glacier region with Pléiades satellite imagery, University of Otago, Technical Report 17-004.002.R1.0, 2019.

Spandre, P., François, H., Thibert, E., Morin, S., and George-Marcelpoil, E.: Determination of snowmaking efficiency on a ski slope from observations and modelling of snowmaking events and seasonal snow accumulation, The Cryosphere, 11, 891-909, https://doi.org/10.5194/tc-11-891-2017, 2017.

Steiner, L., Meindl, M., Fierz, C., and Geiger, A.: An assessment of sub-snow GPS for quantification of snow water equivalent, The Cryosphere, 12, 3161-3175, https://doi.org/10.5194/tc-12-3161-2018, 2018.

Stumpf, A., Malet, J. P., Allemand, P., and Ulrich, P.: Surface reconstruction and landslide displacement measurements with Pléiades satellite images, ISPRS J. Photogramm., 95, 1-12, https://doi.org/10.1016/j.isprsjprs.2014.05.008, 2014.

Sturm, M., Derksen, C., Liston, G., Silis, A., Solie, D., Holmgren, J., and Huntington, H.: A Reconnaissance Snow Survey across Northwest Territories and Nunavut, Canada, April 2007, 80 pp., 2008.

Sturm, M., and Holmgren, J.: An Automatic Snow Depth Probe for Field Validation Campaigns, Water Resour. Res., 54, 9695-9701, https://doi.org/10.1029/2018WR023559, 2018.

Telling, J., Lyda, A., Hartzell, P., and Glennie, C.: Review of Earth science research using terrestrial laser scanning, Earth-Science Reviews, 169, 35-68, https://doi.org/10.1016/j.earscirev.2017.04.007, 2017.

Thibert, E., Bellot, H., Ravanat, X., Ousset, F., Pulfer, G., Naaim, M., Hagenmuller, P., Naaim-Bouvet, F., Faug, T., Nishimura, K., Ito, Y., Baroudi, D., Prokop, A., Schon, P., Soruco, A., Vincent, C., Limam, A., and Heno, R.: The full-scale avalanche test-site at Lautaret Pass (French Alps), Cold Reg. Sci. Technol., 115, 30-41, https://doi.org/10.1016/j.coldregions.2015.03.005, 2015.

Toth, C., and Jozkow, G.: Remote sensing platforms and sensors: A survey, ISPRS J. Photogramm., 115, 22-36, https://doi.org/10.1016/j.isprsjprs.2015.10.004, 2016.

Vallet, J., Gruber, U., and Dufour, F.: Photogrammetric avalanche volume measurements at Vallee de la Sionne, Switzerland, Ann. Glaciol., 32, 141-146, https://doi.org/10.1016/j.isprsjprs.2015.10.004, 2001.

Vallet, J., Turnbull, B., Joly, S., and Dufour, F.: Observations on powder snow avalanches using videogrammetry, Cold Reg. Sci. Technol., 39, 153-159, https://doi.org/10.1016/j.coldregions.2004.05.004, 2004.

Vander Jagt, B., Lucieer, A., Wallace, L., Turner, D., and Durand, M.: Snow Depth Retrieval with UAS Using Photogrammetric Techniques, Geosciences, 5, 264-285, https://doi.org/10.3390/geosciences5030264, 2015.

Walter, B., Huwald, H., Gehring, J., Bühler, Y., and Lehning, M.: Radar measurements of blowing snow off a mountain ridge, The Cryosphere, 14, 1779-1794, https://doi.org/10.5194/tc-14-1779-2020, 2020.

Westoby, M. J., Brasington, J., Glasser, N. F., Hambrey, M. J., and Reynolds, J. M.: 'Structure-from-Motion' photogrammetry: A low-cost, effective tool for geoscience applications, Geomorphology, 179, 300-314, https://doi.org/10.1016/j.geomorph.2012.08.021, 2012.

Formatiert: Englisch (Vereinigtes Königreich)
Formatiert: Englisch (Vereinigtes Königreich)
Feldfunktion geändert
Feldfunktion geändert
Formatiert: Englisch (Vereinigtes Königreich)
Formatiert: Englisch (Vereinigtes Königreich)
Formatiert: Englisch (Vereinigtes Königreich)
Formatiert: Englisch (Vereinigtes Königreich)
Feldfunktion geändert
Feldfunktion geändert
Formatiert: Englisch (Vereinigtes Königreich)
Formatiert: Englisch (Vereinigtes Königreich)
Feldfunktion geändert
Formatiert: Englisch (Vereinigtes Königreich)
Formatiert: Englisch (Vereinigtes Königreich)
Feldfunktion geändert
Formatiert: Englisch (Vereinigtes Königreich)
Formatiert: Englisch (Vereinigtes Königreich)
Feldfunktion geändert
Formatiert: Englisch (Vereinigtes Königreich)
Formatiert: Englisch (Vereinigtes Königreich)
Feldfunktion geändert
Formatiert: Englisch (Vereinigtes Königreich)
Formatiert: Englisch (Vereinigtes Königreich)
Feldfunktion geändert
Formatiert: Englisch (Vereinigtes Königreich)
Formatiert: Englisch (Vereinigtes Königreich)
Feldfunktion geändert
Formatiert: Englisch (Vereinigtes Königreich)
Formatiert: Englisch (Vereinigtes Königreich)
Formatiert: Englisch (Vereinigtes Königreich)
Formatiert: Englisch (Vereinigtes Königreich)
Feldfunktion geändert
Feldfunktion geändert
Formatiert: Englisch (Vereinigtes Königreich)
Formatiert: Englisch (Vereinigtes Königreich)
Feldfunktion geändert
Formatiert: Englisch (Vereinigtes Königreich)
Formatiert: Englisch (Vereinigtes Königreich)

Wipf, S., Stoeckli, V., and Bebi, P.: Winter climate change in alpine tundra: plant responses to changes in snow depth and snowmelt timing, Climatic Change, 94, 105-121, https://doi.org/10.1007/s10584-009-9546-x, 2009.

Feldfunktion geändert

Formatiert: Englisch (Vereinigtes Königreich)

Formatiert: Englisch (Vereinigtes Königreich)